Order Number 8917938

Hydrology and drainage of a thin colluvium hillside in Delhi Township, Ohio

Haneberg, William Christopher, Ph.D.

University of Cincinnati, 1989

U·M·I
300 N. Zeeb Rd.
Ann Arbor, MI 48106

HYDROLOGY AND DRAINAGE OF A THIN COLLUVIUM HILLSIDE IN DELHI TOWNSHIP, OHIO

A dissertation submitted to the
Division of Graduate Studies and Research
of the University of Cincinnati

in partial fulfillment of the
requirements of the degree of

DOCTOR OF PHILOSOPHY

in the Department of Geology
of the College of Arts and Sciences

1989

by

William C. Haneberg

B.S., Bowling Green State University, 1982
M.S., University of Cincinnati, 1985

UNIVERSITY OF CINCINNATI

February 20 19 89

I hereby recommend that the thesis prepared under my supervision by William C. Haneberg

entitled Hydrology and drainage of a thin colluvium hillside in Delhi Township, Ohio

be accepted as fulfilling this part of the requirements for the degree of Doctor of Philosophy

Approved by:

ABSTRACT

The hydrology of a thin colluvium hillside at the Delhi Pike landslide complex, approximately 15 km west of downtown Cincinnati, is controlled by infiltration and evapotranspiration. Pore water pressures approach -10 m H_2O during summer and autumn, but rise to -1 m H_2O or higher after several days of steady winter rains. This state of near saturation is maintained until large trees leaf out and pore pressures fall dramatically in late spring.

Short-term response to winter and spring rainstorms is characterized by simultaneous wetting and drying of the entire hillside, with localized zones of saturation and no wave-like downhill flow. This is consistent with models of both modified Dupuit hillside flow and vertical infiltration. The governing differential equations show that rapid water level fluctuations can occur only if the soil is nearly saturated before rainfall and that the occurrence of vertical, rather than slope-parallel, soil moisture flux after rainfall is controlled by evapotranspiration rates. During winter and early spring, vertical flux due to evapotranspiration will be greater than slope-parallel flux due to gravity drainage, but both will be low enough that no significant drying occurs. As large trees leaf out and evapotranspiration rates rise during late spring, vertical flux due to evapotranspiration predominates and the hillside becomes significantly drier.

Localized zones of saturation make it difficult to determine where drains should be placed to increase stability of thin colluvium hillsides, and if complete saturation of the hillside is assumed, drain installation would amount wholesale replacement of the natural hillside soil with free-draining material. However, if permanently saturated zones can be identified or extensive re-grading and destruction of natural hillsides is an acceptable consequence of development, then drain installation may be a realistic alternative.

ACKNOWLEDGEMENTS

This study was supported by a research grant from The Hillside Trust, a graduate teaching assistantship from the University of Cincinnati Department of Geology, and equipment loans and data from the U.S. Geological Survey Geologic Risk Assessment Branch. The Sisters of Charity kindly allowed me to conduct my field studies on their property in Delhi Township.

I am grateful to the members of my dissertation committee– Arvid Johnson, Robert Fleming, and David Nash– for their advice and guidance during the past two years. Many others, including Rex Baum, Robin Corathers, Kenneth Cruikshank, Evelyn Goebel, Andrea Haas, Thomas Lowell, Laurence Murdoch, Robert Olson, Wanda Osborne, and Mary Riestenberg helped with virtually every aspect of this project. In addition, Mark Truebe and the geotechnical staff of the Willamette National Forest provided valuable information on the use of drains for slope stabilization. Finally, I appreciate the support and friendship of Cheryl Clark, P.E. and Cassandra Liebe, A.K.C. throughout this project.

And yes, I used a Macintosh .

PREFACE

ORIGINS

This dissertation describes my work on the hydrology and drainage of a thin colluvium hillside along the Ohio River valley west of Cincinnati. Each of the three main chapters was written as a separate manuscript, and thus can be read independently of the others, but as a consequence there is some redundancy among the introductory sections. Moreover, the manuscripts are each intended to illustrate specific aspects of my work so the texts are short and to the point rather than encyclopedic. Supporting material such as field data, computer programs, and some mathematical derivations are included in seven appendices. In this preface I summarize the evolution of my research during the past two years and put each of the three main chapters into its proper historical context.

My research has its roots in work started nearly a decade ago when, during the late 1970s, Robert Fleming of the U.S. Geological Survey and Arvid Johnson of the University of Cincinnati began to investigate mechanisms of landsliding in the greater Cincinnati area. They decided to map and monitor part of a typical colluvium landslide complex along Delhi Pike, a two lane paved road along the Ohio River valley about 15 km west of downtown Cincinnati, that was closed in 1970 due to excessive landslide damage.

Fleming and Johnson installed porous stone piezometers in both thin (< 2 m) colluvium above Delhi Pike and thick (> 2 m) colluvium below Delhi Pike and Önder Gökce, a graduate student at the University of Cincinnati, began to measure water levels several times a month between 1979 and 1981 as part of his Ph.D. dissertation research. In addition, an automatic recorder was installed on two of the piezometers in thin colluvium, referred to as P-4 and P-6, and water levels were recorded at 15 minute intervals during spring 1980. Preliminary data suggested that water levels in thick colluvium changed slowly from season to season, whereas water levels in the usually unsaturated thin colluvium rose and fell quickly during and immediately after winter and spring storms, and these patterns were first described in the field trip guidebook for the 1981 Geological Society of America annual meeting held in Cincinnati.

Because the fortnightly sampling frequency was far too low to record the short-term water level fluctuation in the thin colluvium, most of the data collected by hand were impossible to analyze. The high-frequency data from P-4 and P-6 were nearly as puzzling because the notion of rapid water movement in dense, clayey colluvium runs counter to intuition. It was clear, however, that such rapidly changing water levels could be the key to understanding the sudden failure of thin colluvium hillsides in Cincinnati.

CHAPTER 1

I became interested in Önder Gökce's water level data during autumn 1986 while looking for a dissertation topic combining engineering geology and groundwater hydrology. The rapid water level fluctuations had been described, but not analyzed, in Gökce's dissertation, and Arvid Johnson suggested that I might continue this pursue this problem by investigating the effect of drains on the stability of thin colluvium hillsides.

Believing that the effects of drains could not be quantitatively evaluated until the hydrologic regime of the thin colluvium hillsides was understood, I began to work on a numerical model of hillside flow that would account for the 15 minute increment P-4 data from 14 storms during spring 1980. Soil profiles from trenches dug by Fleming showed a thin, highly inhomogeneous, layer of colluvium resting on top of a sloping contact with shale and limestone bedrock. Although colluvium thickness varied along the trench, it was about two orders of magnitude less than the head-to-toe length of the hillsides at Delhi Pike, and estimates of fillable porosity before all but one of the 1980 storms suggested that the colluvium was very near saturation, so I decided to approximate the hillside as a sloping, one-dimensional phreatic aquifer with rainfall represented as recharge to the water table.

Numerical solution of the modified Dupuit flow equations using rainfall and hydraulic conductivity values extracted from field data agreed very well with the observed water level fluctuations in piezometer P-4 only if fillable porosity was assumed to be no more than a few percent. Most importantly, the model, which grew from water level observations at a single point, predicted a distinct, testable pattern of water level changes along the entire length of the hillside. According to the governing differential equations, water level should increase uniformly along the entire hillside during rainfall. If evapotranspiration is negligible after the rainfall, water levels should fall gradually from head to toe in a wave-like pattern. If evapotranspiration is significant, however, water levels should fall uniformly along the entire hillside.

CHAPTER 2

While I was beginning work on my model, Larry Murdoch installed nests of tensiometers near piezometers P-4 and P-6 to investigate infiltration processes during December 1986 as part of his master's thesis research in the Department of Civil and Environmental Engineering at the University of Cincinnati. He observed a rapid transition from very dry to wet, but only occasionally saturated, colluvium during the first heavy rains of winter, and also illustrated the importance of monitoring unsaturated flow in the colluvium.

In order to test my model of hillside flow, I installed a series of tensiometers above and below P-4 and P-6. Pressure heads at the first three tensiometer groups, installed in late May 1987, approached -10 m a few days after installation, which was well below the range of my interest, so I disconnected the tensiometers for the summer. I re-connected the first three tensiometer groups and installed two more groups in late September 1987, only to find that pressure heads still ranged between -8 and -10 m. Pressure head changes in response to rainfall were erratic throughout the autumn months, and remained very low as temperatures began to fall below freezing in mid-December. I disconnected the tensiometers again in anticipation of freezing temperatures during the Christmas holiday, but returned to find that pressure heads throughout the hillside had increased to about -1 m during heavy rains the last two weeks of December 1987, much the same as described by Murdoch. Thereafter, pressure head remained at -1 m or more throughout spring 1988 until large trees were completely leafed out in early May and pressure heads decreased rapidly.

Shallow tensiometers characteristically showed much more pore pressure variation than deep tensiometers at the same station, and drying occurred uniformly along the hillside rather than by slope-parallel drainage during the period of record. So, in addition to showing that the high, but unsaturated, pore water pressures necessary for rapid water level increases could be maintained for several months with only occasional rainfall, this portion of my work emphasizes the importance of atmospherically- and biologically-controlled processes on the hydrology of a typical hillside.

CHAPTER 3

The final chapter describes the installation of two experimental drains at Delhi Pike. When I began working on this project, I assumed that widespread zones of saturation– perched water tables– would develop in the colluvium at Delhi Pike. This assumption further suggested that drains might be an effective and inexpensive means of stabilizing natural hillsides. Preliminary estimates suggested that the radii of influence of gravel-filled trench drains in colluvium would be on the order of about 1 m; so, although it did not appear economical to drain an entire hillside with closely spaced drains, I was optimistic that widely-spaced drains could increase stability by creating stable zones that would buttress the rest of the hillside.

In April 1987, I designed and installed two gravel-filled trench drains (A and B) approximately 1 m (wide) x 2 m (deep) x 10 m (long) with PVC discharge pipes in thin colluvium at Delhi Pike. Whereas drain A discharged water up to 1×10^{-4} m^3/s during storms, there was never any observed discharge from drain B, although water did seep from the colluvium and filled holes that I dug downslope from drain B. Subsequent excavations showed no sign of damage to the drain B discharge pipe, and the design itself seemed to work well enough in drain A, suggesting that the reason drain B did not discharge any water was that no water was flowing into it. Darcy's law and tensiometer data suggest that thin, rocky colluvium directly uphill from drain B served to deflect flow upward where it seeped out along the surface. Such results imply that drain location in locally saturated colluvium is critical, which would make drain design impractical unless surface seeps pinpointed frequently saturated areas. If the colluvium were completely saturated, then the extremely close drain spacing required to stabilize the hillside would essentially require replacement of the entire hillside with free-draining material, which would not be aesthetically acceptable in most cases. Thus, whereas drains may be a useful method of stabilizing thick colluvium hillsides that undergo predictable seasonal water level fluctuations, they do not appear to be a practical way to stabilize most thin colluvium hillsides.

TABLE OF CONTENTS

LIST OF FIGURES

LIST OF TABLES

CHAPTER 1

RAPID WATER LEVEL FLUCTUATIONS IN A THIN COLLUVIUM LANDSLIDE WEST OF CINCINNATI, OHIO[1]

INTRODUCTION

Nearly ten years ago, while examining dozens of landslides along the Ohio River and its tributaries near Cincinnati, Ohio, we began to to realize that in some landslides destabilizing pore water pressure is artesian whereas in others it is hydrostatic. We selected two study areas, one in glacial deposits and another in colluvium, for detailed observation and began to monitor movement and water levels in both places.

We began exploring the colluvium landslide complex in March, 1979 by drilling both deep boreholes on gentle slopes with a trailer-mounted auger rig and shallow boreholes on steeper slopes with a two-person portable auger, installing porous-stone piezometers, and measuring piezometric levels by hand at two week intervals. After realizing that piezometric levels in the shallow colluvium could change very rapidly in direct response to rainfall (Fleming and others, 1981), we installed instruments to record both rainfall and piezometric level in one piezometer at 15 minute intervals from late March through mid May, 1980. In this paper we describe details of these rainfall and piezometric level records, and then use a simple mathematical model of hillside groundwater flow to explain some important characteristics of piezometer water level records.

Previous Work

Iverson and Major (1987) describe both annual and short-term water level fluctuations in a long, thin northern California landslide, and note both that high frequency

[1] *to be published as a U.S. Geological Survey Bulletin with A.Ö. Gokce as co-author.*

fluctuations due to individual storms attenuate with depth and that the events of previous water years control annual water level increases. This is in line with the results of two separate field studies by Gillham (1984) and Novakowski and Gillham (1988), who concluded that high antecedent moisture content resulted in more rapid water table response to rainfall. Pyles and others (1987) observed asymmetric water level fluctuations similar to those described in this paper during their studies of thin landslides in western Oregon. Harr (1977) monitored both saturated and unsaturated flow in a steeply sloping forested hillside in the same western Oregon experimental forest used by Pyles and others (1987), and showed that flow was almost always unsaturated except near the foot of the hillside. He used measurements of stream and seepage face discharge to show that the lower reaches of the hillside remained saturated due to drainage of soil pores that had been filled during rainstorms. Upper reaches of the hillside became saturated at depth from time to time, but only after at least 0.003 m of rain fell within 12 hrs., and even then the saturation persisted less than 20 hrs. Harr attributed these intermittent zones of saturation to the accumulation of infiltrating water along the contact between soil, where hydraulic conductivity decreased an order of magnitude. Anderson and Burt (1977a) show longitudinal water table profiles from a natural hillside that show water accumulating in the lower portion of the hillside while water level falls in the upper portions, and in a related laboratory study (Anderson and Burt, 1977b) show that a sloping, sand-filled gutter drains from the top down and a small saturated wedge remains at the base throughout the experiment. Estimates of discharge from the laboratory setup agree closely with those predicted using the slope of the water table as the hydraulic gradient, but do not agree with those taking release of water from the unsaturated zone into account.

Geologic Setting

Landslides in the Delhi Pike area (Figure 1.1) occur in illitic, bouldery-silty-clayey colluvium formed along the northern wall of the Ohio River valley about 15 km west of downtown Cincinnati. Colluvium thickness ranges from less than a meter near hilltops to more than ten meters at river level, and basal slip surfaces generally run along the contact between colluvium and weathered bedrock. Flat lying, interstratified shales and limestones of the Upper Ordovician Kope Formation (approximately 80% shale and 20% limestone) and overlying Upper Ordovician Fairview Formation (approximately 60% shale and 40% limestone) comprise the local bedrock and are parent material for the overlying colluvium.

Landslide Morphology

For the most part, landslides in the Delhi Pike area are elongate parallel to topographic contours, but in some cases this pattern is broken by narrow, U-shaped landslides reaching farther uphill. The slide that we describe is one of these U-shaped fingers, as shown in a detailed plane table map (Figure 1.2). Topography is generally irregular, containing many small hummocks and scarps with a meter or so of relief, but overall surface slope angles range between 20° and 30° and the bedrock surface slopes approximately 30° across most of the hillside. The main slide mass is bounded by a left-lateral strike-slip zone along its entire eastern flank, a headscarp to the north, and a right-lateral strike-slip zone along the northern half its western flank. All of these boundaries are characterized by a topographic depression, in some places up to 1 m deep. The southern half of the western flank grades into several east-west scarps, and there is no distinct boundary. The northern half of the slide mass is broken into a number of smaller slides, each with a subsidiary, U-shaped headscarp reflecting the shape of the slide as a whole. Vertical offset along these scarps is generally 1 m or less. Subsidiary scarps in the

Figure 1.1 Index map showing location of Cincinnati, Hamilton County, the Ohio River, and the Delhi Pike study area.

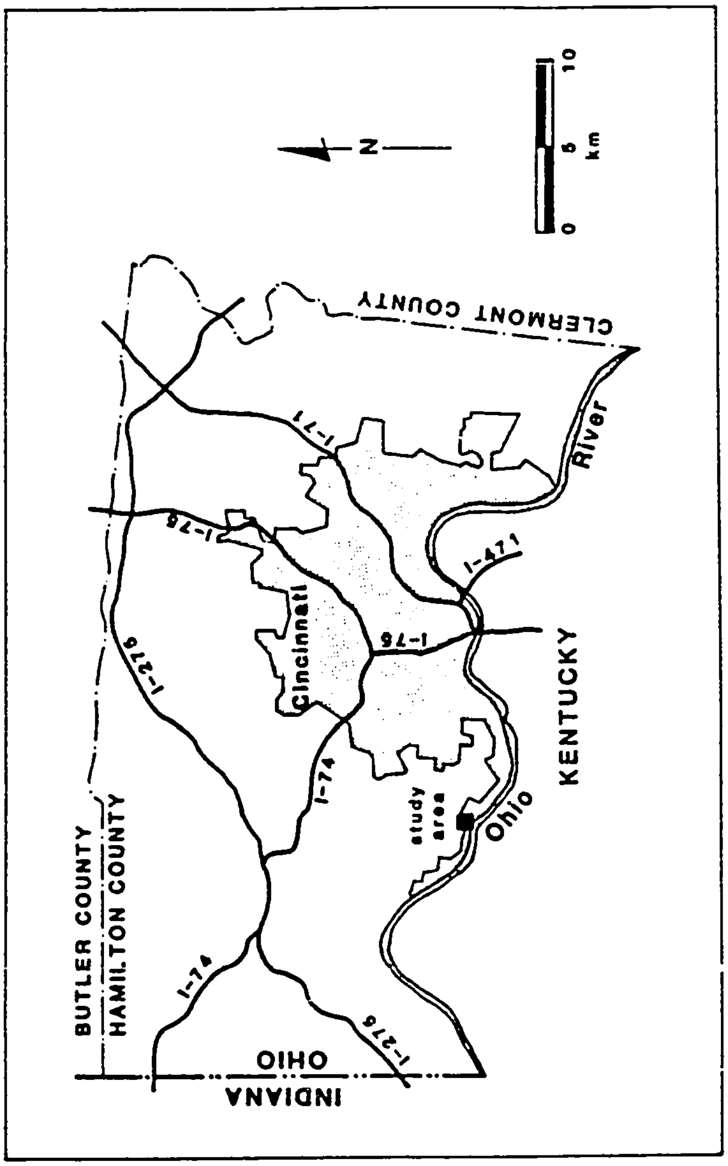
BUTLER COUNTY
HAMILTON COUNTY
CLERMONT COUNTY
INDIANA
OHIO
KENTUCKY
Ohio
River
Cincinnati
study area
I-74
I-275
I-75
I-71
I-471
N
0
5
10
km

Figure 1.2 Plane table geologic map of the portion of the Delhi Pike landslide complex studied in this chapter. All elevations are relative to an arbitrary station on Delhi Pike.

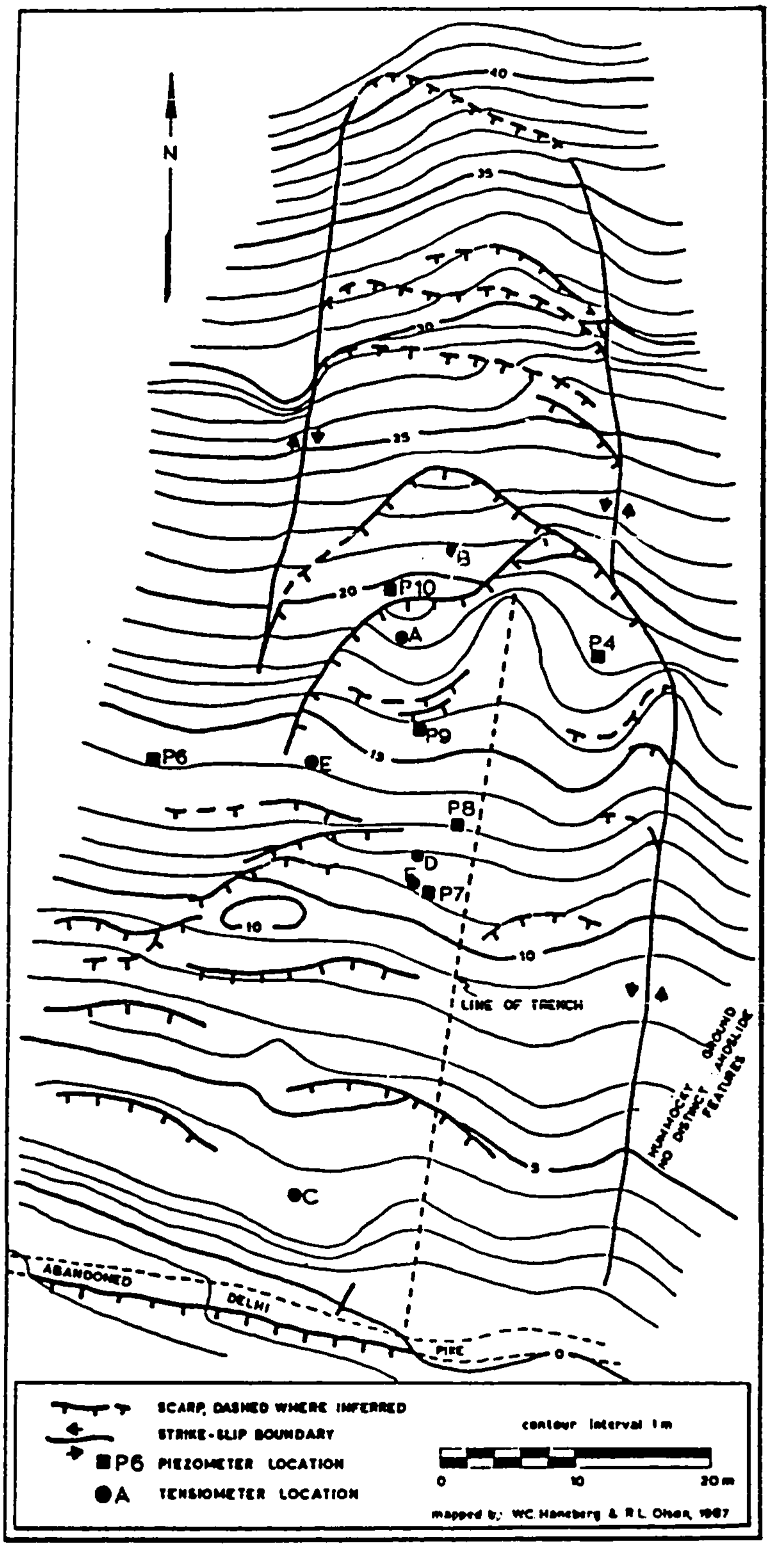
N
40
35
30
25
20
15
10
5
0
P10
P4
P9
P6
P8
P7
P
A
B
C
D
E
LINE OF TRENCH
HUMMOCKY GROUND AND NO DISTINCT LANDSLIDE FEATURES
ABANDONED
DELHI
PIPE
SCARP, DASHED WHERE INFERRED
STRIKE-SLIP BOUNDARY
P6 PIEZOMETER LOCATION
A TENSIOMETER LOCATION
contour interval 1 m
0
10
20 m
mapped by: W.C. Haneberg & R.L. Olsen, 1987

southern half of the slide, where the western boundary becomes indistinct, tend to be nearly linear and parallel to topographic contours. Locally, however, these parallel scarps branch and join to form an anastomosing network. The subtle increase in slope above the +30 m contour (all elevations are relative to an arbitrary control point on Delhi Pike) reflects the transition from Kope Formation to Fairview Formation bedrock.

Colluvium Stratigraphy and Physical Properties

The colluvium at Delhi Pike is mapped as Eden silty clay loam, a residual soil formed on moderate to steep slopes, in the Hamilton County Soil Survey (Lerch and others, 1982). It is described as well-drained, with slow permeability and very rapid runoff (cf. our field observations of very little during storms). The soil survey further states that excavations in lower parts of slopes commonly have seepage problems and recommends that drains be installed around foundations. We had five test trenches excavated using backhoes and larger tracked excavators, and found that within about 0.1 to 0.2 m of the surface the colluvium is grayish-brown and commonly breaks into peds, whereas colluvium about 0.2 m or more from the surface is yellowish and massive. In places, however, brown colluvium is found in isolated lenses within the yellow colluvium. Both types of colluvium are composed of roughly 70% silty-clayey matrix and 30% limestone slabs up to 0.3 m thick and 3 m long with no apparent preferred orientation. The distribution of brown colluvium, yellow colluvium, large limestone slabs, and slip surfaces exposed in a longitudinal trench is shown in Figure 1.3.

Laboratory falling head permeability tests were run on each of nine samples taken from different depths in a trench at Delhi Pike, and then the results were averaged to obtain a single value for each sample. These average values range from a high of 2.63×10^{-5} m/s to a low of 7.70×10^{-8} m/s with an arithmetic average of 1.31×10^{-5} m/s (Figure 1.4);

Figure 1.3 North-south longitudinal cross-section along the trench shown in Figure 2. Section shows distribution of brown colluvium, yellow colluvium, limestone slabs, slip surfaces, and the contact between colluvium and weathered bedrock. Profile courtesy of R.W. Fleming, U.S. Geological Survey.

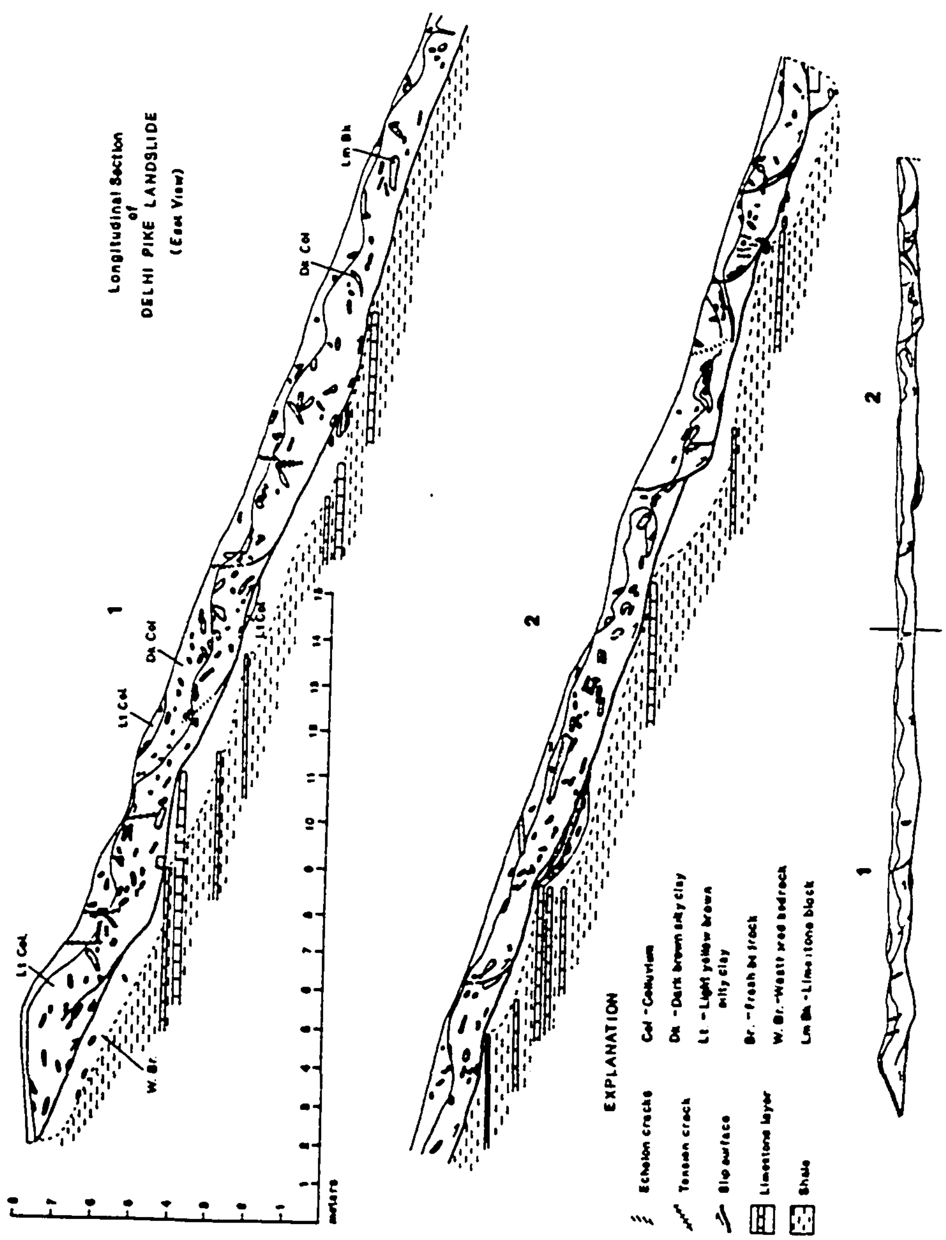
Longitudinal Section
of
DELHI PIKE LANDSLIDE
(East View)
1
2
Lt Col
Dk Col
W. Br.
Lm Bk
meters
EXPLANATION
Echelon cracks
Tension crack
Limestone layer
Shale
Col - Colluvium
Dk - Dark brown silty clay
Lt - Light yellow brown silty clay
W. Br. - Weathered bedrock

Figure 1.4 Variation of colluvium hydraulic conductivity with depth. Points labeled H and V are values for horizontal and vertical conductivity of closely spaced samples from a depth of 1.2 m. Data courtesy of R.W. Fleming, U.S. Geological Survey.

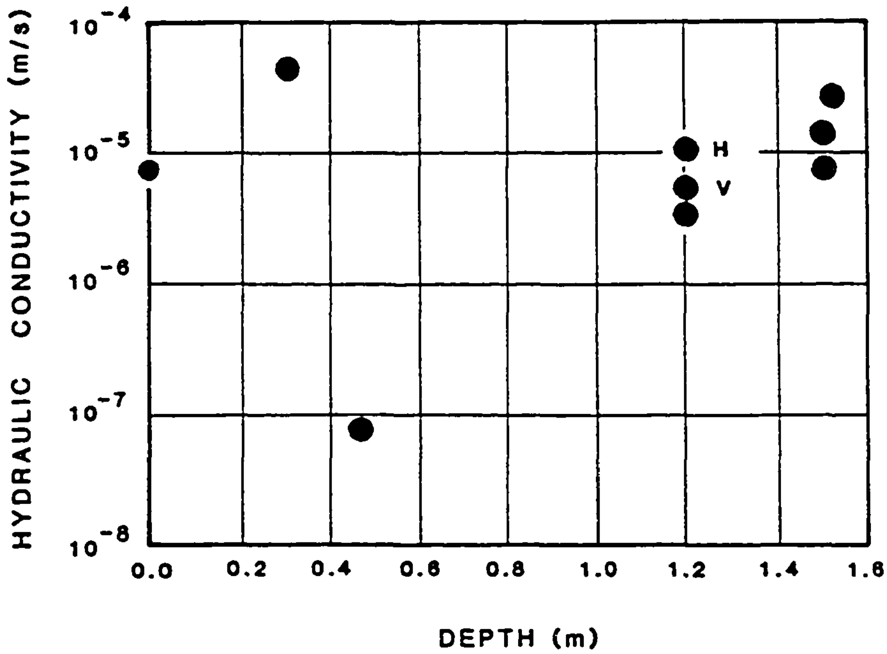
HYDRAULIC CONDUCTIVITY (m/s)
10^{-4}
10^{-5}
10^{-6}
10^{-7}
10^{-8}
H
V
0.0
0.2
0.4
0.6
0.8
1.0
1.2
1.4
1.6
DEPTH (m)

if the latter value is excluded, the lowest average value becomes 3.26×10^{-6} m/s and the mean becomes 1.47×10^{-5} m/s. With the exception of two errant values, hydraulic conductivity appears to be very nearly constant with depth. Both horizontal and vertical components of hydraulic conductivity were measured for one of the samples from 1.2 m deep, and the average vertical conductivity is 5.11×10^{-6} m/s whereas the average horizontal conductivity is 1.03×10^{-5} m/s. It is difficult to assess the significance of measurements on only one sample, but if accurate these results imply that the colluvium at Delhi Pike is weakly anisotropic.

Atterberg limits and clay mineralogy were determined using four samples taken from different depths in an auger hole, which is approximately 60 m southeast of piezometer P-4 but not shown in Figure 1.2. There is very little variation in grain size distribution, Atterberg limits, or clay mineralogy with depth in the borehole (Table 1.1). Both the colluvium and the weathered

Table 1.1 Colluvium grain size distribution, Atterberg limits, and clay type from a borehole at Delhi Pike (courtesy R.W. Fleming, U.S. Geological Survey).

depth	grain size (wt. %)				Atterberg limits		clay type
(m)	gravel	sand	silt	clay	LL	PL	
1.2	1	6	26	67	50	25	mixed layer, illite
2.1	4	7	29	60	48	24	mixed layer, illite
4.8	1	4	31	64	45	24	mixed layer, illite
6.8	5	9	31	55	41	21	illite, kaolinite

bedrock samples were composed primarily of clay-sized grains with lesser amounts of silt-sized grains. Gravel- and sand-sized grains comprised less than 15% of sample weight in all cases. Liquid limits average 46% and plastic limits average 24%, both decreasing slightly with depth.

WATER LEVEL FLUCTUATIONS

Our piezometers were cylindrical porous stones 0.050 m in diameter and 0.30 m long attached to 0.025 m diameter PVC pipe. Each piezometer hole was backfilled with quartz sand to a level approximately 0.20 m above the top of the porous stone and sealed with approximately 0.40 m of bentonite (Figure 1.5). We measured water levels in six piezometers at Delhi Pike by hand at least twice a month between March 1979 and August 1980. In addition, we installed an automatic recorder in one piezometer, referred to as P-4 (see Figure 1.2 for location), approximately halfway up the landslide to monitor piezometric levels at 15 minute intervals between late March and mid April, 1980. Our original intent was to use these short term data to estimate piezometer lag time, but they also provided the first evidence of rapid piezometric level fluctuations in the Delhi Pike landslide complex. During the past year we have found that P-4 often contains water when other piezometers are dry, and have limited data to suggest that this was also true during 1980, which will be considered in our Discussion.

General Characteristics of P-4 Water Level Records

We see several characteristics common to the water level records that we describe below, and which are typical of all our data from P-4. During the summer and early autumn the bottom of P-4 is dry (water level at least 1.20 m below the surface), whereas during the late winter and spring of 1980 the background water level stood about 0.8 to 0.9 m below the surface. This background water level is punctuated by distinct increases of several decimeters that correspond to individual rainstorms. Short, intense storms generally produced sharp peaks, whereas gentle and prolonged rainfall generally produced flat-

Figure 1.5 Change in water level *vs*. rainfall. With one exception, maximum effective porosity estimates range from 0.01 to 0.07, suggesting that the colluvium was nearly saturated before rapid water level increases.

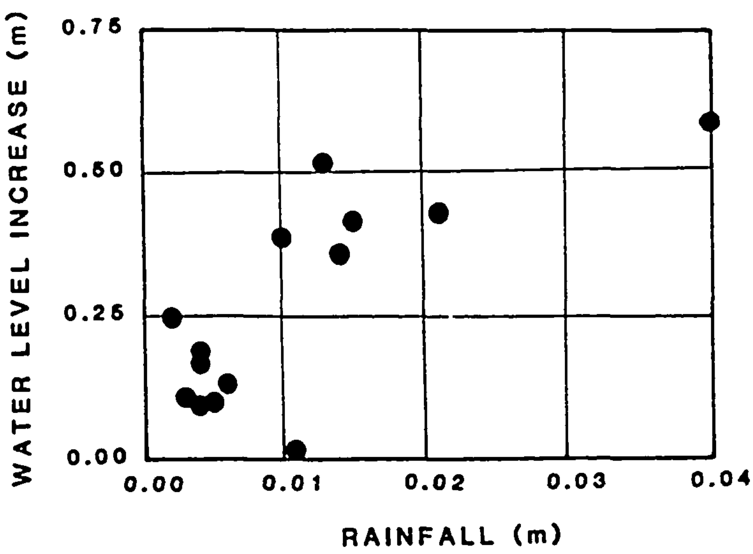
WATER LEVEL INCREASE (m)
0.75
0.50
0.25
0.00
0.00
0.01
0.02
0.03
0.04
RAINFALL (m)

Figure 1.6 Schematic drawing of a piezometer P-4 at Delhi Pike. See Figure 1.2 for location.

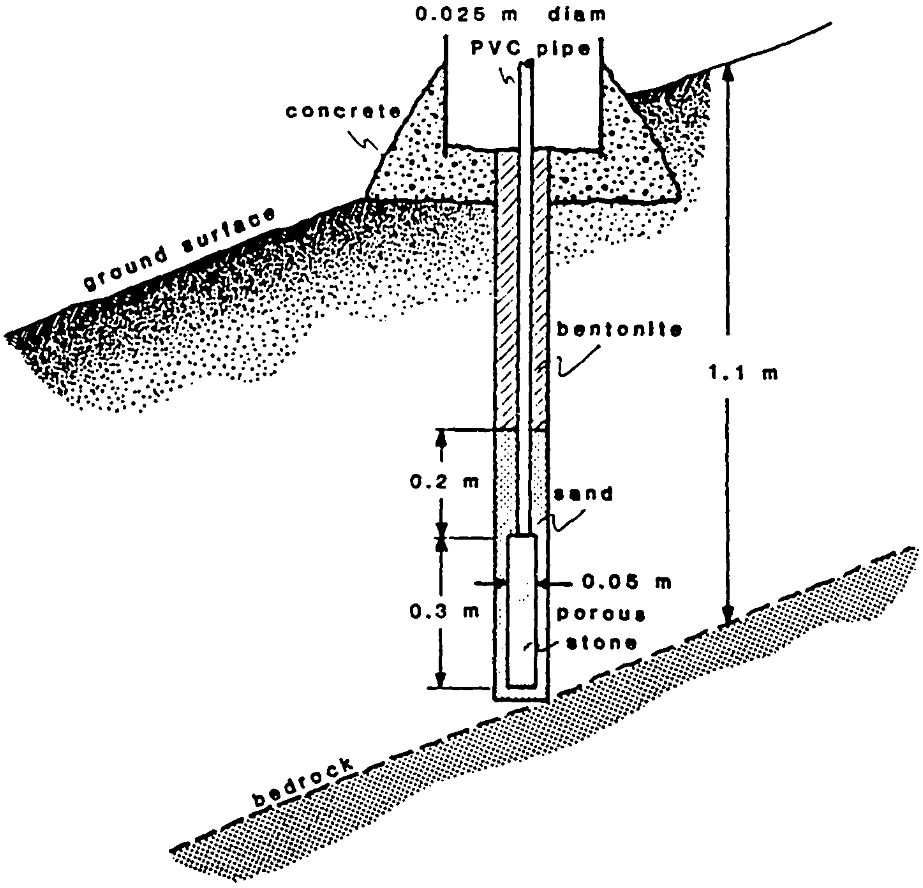
0.025 m diam
PVC pipe
concrete
ground surface
bentonite
1.1 m
0.2 m
sand
0.05 m
0.3 m
porous
stone
bedrock

topped peaks. Regardless of rainfall intensity and duration, the water level record peaks are asymmetric. In some cases piezometric level rose virtually instantaneously in response to rainfall and in other cases the rise in piezometric level was considerably slower, but piezometric levels always fell slower than they rose. After rainfall had stopped, piezometric levels characteristically fell slowly at first, then more rapidly, and then slowly again as the background piezometric level was approached to form a sigmoidal falling water level record that continued to fall very slowly for many tens of hours in the absence of additional rain. When more rain fell several hours after a storm, the fall of the water table slowed substantially. In some cases a small hump appears to be superimposed upon the overall slope of the falling water level record, but in other cases there is no sign of any hump. We use specific examples, in chronological order, to illustrate these generalities below.

Individual Storms

March 20 through March 22, 1980.- The first P-4 water level record that we describe, illustrated in Figure 1.7, is flat-topped and associated with a period of intermittent, relatively gentle rainfall distributed over about 17 hours. Base level was about 0.83 m beneath ground level both before and after the rainfall. Significant features of this water level record are a compound rising limb associated with two distinct storms on the evening of March 20, and a broad, gently sloping crest associated with gentle rainfall on the morning of March 21. As with all of our records, the falling limb of the water level record is, on the whole, much flatter than the rising limb and is sigmoidal in shape.

April 8 through April 18, 1980.- The P-4 water level record for this ten day period (Figure 1.8) contains a closely-spaced series of four storms and attendant water level increases. All of the water level record peaks during these ten days were much sharper than the water level record from March 20 through March 22, but the rates (i.e. slopes of the

Figure 1.7 Rainfall and piezometric level in piezometer P-4 for the period of March 19, 1980 through March 22, 1980. This is an example of a flat-topped water level record in which water levels remain high due to prolonged, gentle rain following an initial storm or storms.

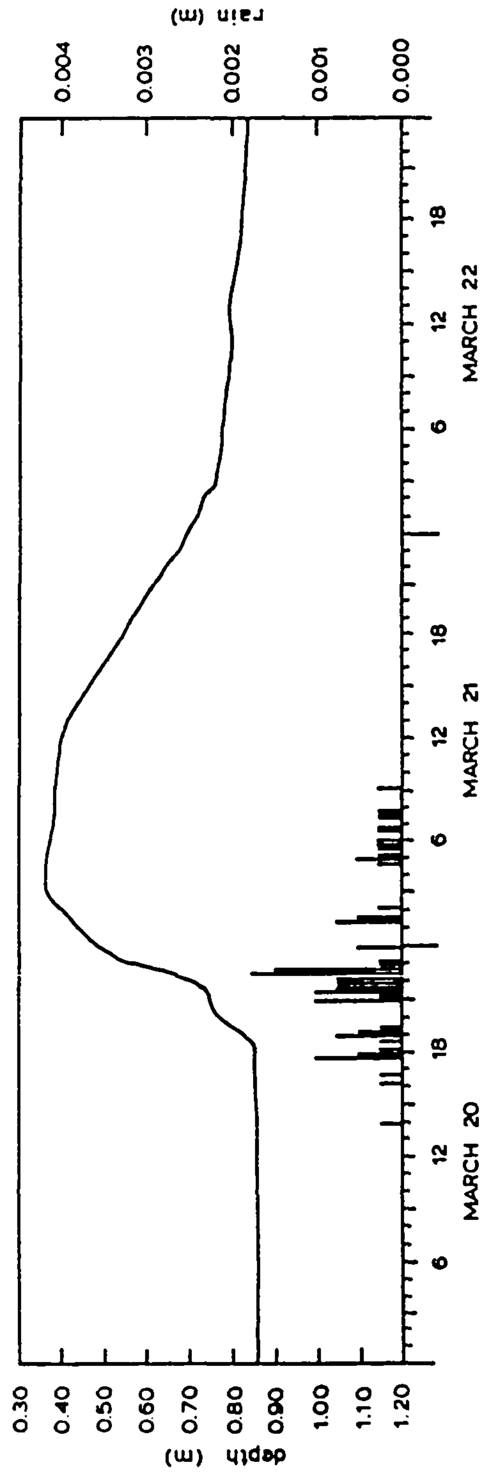
depth (m)
0.30
0.40
0.50
0.60
0.70
0.80
0.90
1.00
1.10
1.20
rain (m)
0.004
0.003
0.002
0.001
0.000
6
12
18
6
12
18
6
12
18
MARCH 20
MARCH 21
MARCH 22

Figure 1.8 Rainfall and piezometric level in piezometer P-4 for the period of April 8, 1980 through April 18, 1980. This is an example of a sharp-peakedwater level record in which water levels rise and fall rapidly following a short-lived, intense storm. In this record the slopes of the rising water level records have nearly the same absolute values as the maximum slopes of the falling water level records.

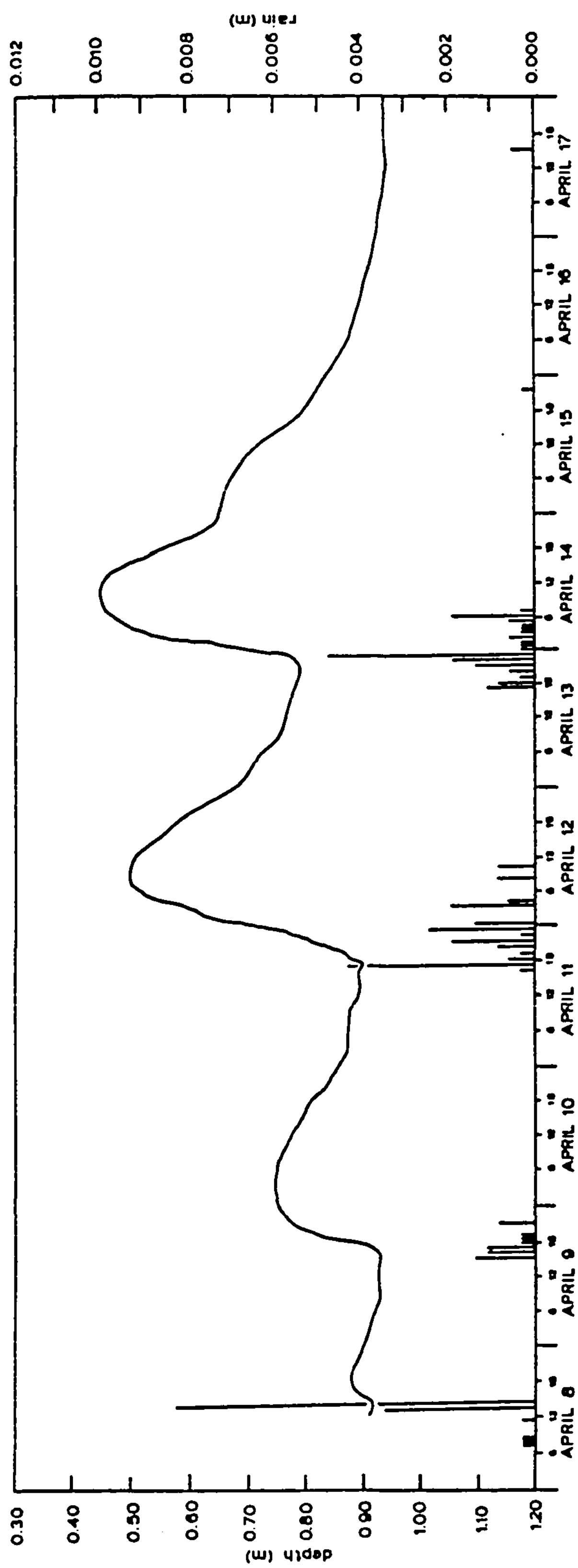
rain (m)
0.012
0.010
0.008
0.006
0.004
0.002
0.000
depth (m)
0.30
0.40
0.50
0.60
0.70
0.80
0.90
1.00
1.10
1.20
APRIL 8
APRIL 9
APRIL 10
APRIL 11
APRIL 12
APRIL 13
APRIL 14
APRIL 15
APRIL 16
APRIL 17

water level record limbs) of water level changes are similar. What appears to be missing is the prolonged, intermittent rainfall that occurred during March 20 through March 22. Base level before and after this series of storms was about 0.92 to 0.95 m below ground level. During the first storm, approximately 0.011 m of rain is associated with a water level increase of only 0.03 m, but in subsequent storms the water level increase is much greater. On April 9 a total of 0.004 m of rain was associated with a water level increase of 0.23 m, on April 11 a total of 0.015 m of rain was associated with a water level increase of 0.51 m, and on April 13 a total of 0.014 m of rain was associated with a water level increase of 0.54 m. All four of these water level records are distinctly asymmetric, as is typical of our data.

May 12 through 13, 1980.- We include this water level record in our descriptions because it contains both the most rapid piezometric level increase (0.54 m/s), the most rainfall in a single storm (0.04 m), and the highest piezometric levels (0.10 m below ground level) we recorded at Delhi Pike. As shown in Figure 1.9, the rising water level record limbs for both storms are very nearly vertical, suggesting a nearly instantaneous water level increase.

Effective porosity.- We estimated maximum effective porosity for each storm as total rainfall divided by total change in water level. In doing this, we assume that all rainfall entered the soil and contributed to water table rise, so our estimates represent maximum possible values. In all but one case we found maximum effective porosity ranged between 1% and 7% for all of the storms during our period of record (Figure 1.5), and in general that the magnitude of water level increase is proportional to the amount of rainfall. The lone exception, which occurred on 8 April 1980 when rainfall of 0.011 m produced a piezometric level increase of 0.025 m for a maximum effective porosity of 44%, will be addressed in the Discussion of this paper.

Figure 1.9 Rainfall and piezometric level in piezometer P-4 for the period of May 12, 1980 through May 13, 1980. This is an example of a sharp-peaked water level record in which water levels rise and fall rapidly following a short-lived, intense storm. In this record the slopes of the rising water level records are nearly vertical and much steeper than the falling water level record slopes.

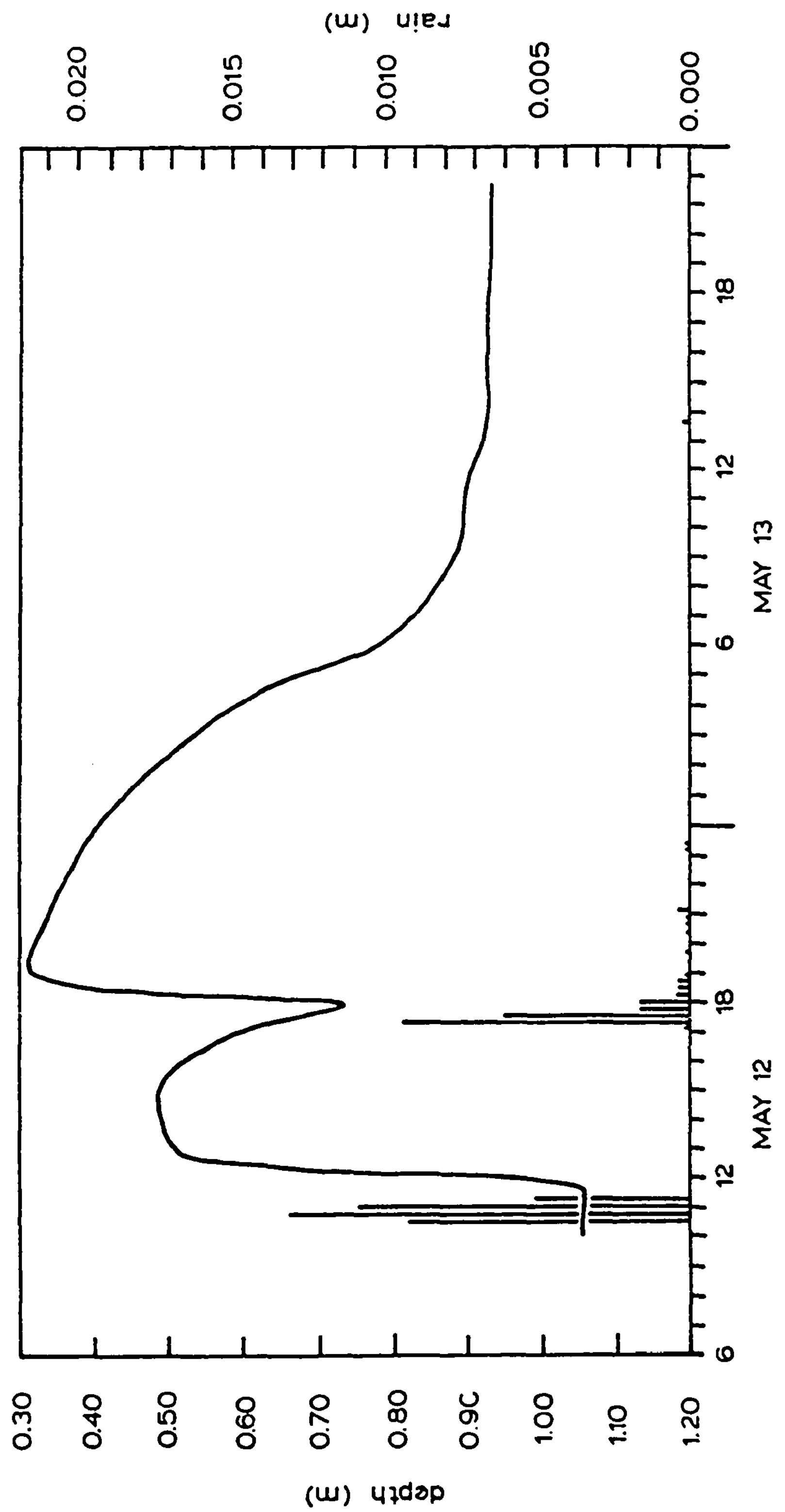

rain (m)
0.020
0.015
0.010
0.005
0.000
depth (m)
0.30
0.40
0.50
0.60
0.70
0.80
0.9C
1.00
1.10
1.20
6
12
18
6
12
18
MAY 12
MAY 13

A THEORETICAL MODEL OF HILLSIDE WATER LEVEL FLUCTUATIONS

Modified Dupuit Flow

The well-known approximation of groundwater flow through a phreatic aquifer developed by Dupuit in the middle of the 19th century incorporates the assumptions that flow is horizontal and equipotential lines are vertical, and is drawn from the observation that in most phreatic aquifers the water table slope is small (Bear, 1972, p. 361). Boussinesq (1904) extended the Dupuit model to account for unconfined flow above a sloping impervious substrate, but retained the assumption of horizontal flow, so the model works well only for very gentle slopes. Schmid and Luthin (1964) derived an analytic solution for the Boussinesq model for steady-state flow and fixed head boundaries, and Guitjens and Luthin (1965) used Hele-Shaw models to show that the solution is accurate for slopes up to about 30%. Departing from the Boussinesq assumption of horizontal flow, as opposed to slope-parallel flow, Klute and others (1965) solved the two-dimensional steady-state fully-saturated inclined flow problem and found that flow through slopes with length to thickness ratios greater than 10:1 could be accurately represented by a one-dimensional, slope-parallel flow model. Childs (1971) and Towner (1975) give analytic solutions to steady-state unconfined slope-parallel flow both with and without recharge, whereas Chauan and others (1968) as well as and Ram and Chauan (1987) present analytic solutions for the problem of transient slope-parallel flow between two trenches on a slope with constant recharge. Karadi and others (1968) solve the related problem of transient flow between drains resting on a shallow, impermeable substrate, and Wong (1977) has published nomographs for the problem of flow to drains in sandy leachate collection layers overlying clay landfill liners. Beven (1977) used a two-dimensional finite element model of saturated-unsaturated flow, and predicted that saturated zones, controlled by pre-existing pressure heads, would form by accumulation of water at the toes of hillsides. More recently, Beven (1981, 1982) and Hurley and Pantelis (1985) have used linearized one-dimensional approximations to successfully model some aspects of saturated and unsaturated hillside discharge. Hurley and Pantelis show that flow through a thin sloping aquifer is indeed one-dimensional to a first approximation, but they solve the unsaturated flow problem in terms of total soil moisture flux.

We approximate hillside flow, at least as we have observed it, as a fully-saturated, unconfined flow problem. Bear (1979, p.74-75) discusses limitations of the fully-saturated approach, particularly the error introduced by ignoring the capillary fringe, or zone of tension saturation, above the water table. As we will show, however, our model has the advantage of predicting water table height rather than total soil moisture flux, as would a more rigorous saturated-unsaturated model (e.g., Hurley and Pantelis, 1985), and can account for many important characteristics of our field data.

For a thin porous slab underlain by a sloping impervious substrate we define total hydraulic head, Φ, as

$$\Phi = h \cos \beta - \xi \sin \beta \tag{1.1}$$

(*cf.* Beven, 1981; Hurley and Pantelis, 1985) where ξ is the slope-parallel coordinate [L], h is height of the phreatic surface [L] measured perpendicular to the substrate (Figure 1.10), and β is slope angle. Combining equation (1.1) with Darcy's law, the governing equation for fully-saturated, incompressible one-dimensional flow through a homogeneous, unconfined aquifer

$$\frac{\partial h}{\partial t} = \frac{K}{p}\frac{\partial}{\partial \xi}\left(h \frac{\partial \Phi}{\partial \xi}\right) + \frac{R}{p} \tag{1.2}$$

Figure 1.10 Idealization of a thin slab of uniform thickness resting atop a sloping, impervious substrate and the representative element used to derive the governing equation for hillside flow through a homogeneous, isotropic, phreatic aquifer.

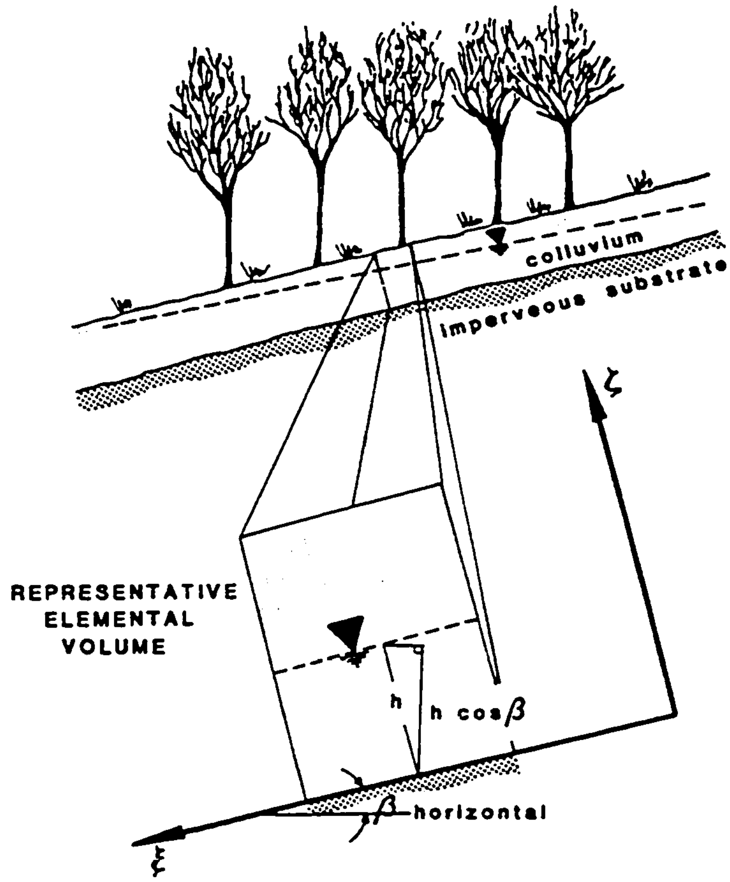
colluvium
imperveous substrate
ζ
REPRESENTATIVE
ELEMENTAL
VOLUME
h
h cosβ
β
horizontal
ξ

where p is effective porosity, K is saturated hydraulic conductivity [L/T], and R is net recharge ($R > 0$ for precipitation, $R < 0$ for evapotranspiration) to the water table [L/T]. Positive recharge is not necessarily the same as rainfall, so the two should not be used synonymousiy unless there is evidence to suggest that all rainfall reaches the water table. Because we have not observed any runoff at Delhi Pike except in areas where we have exposed colluvium at the surface we will assume that a large proportion of rain finds its way to the water table and that recharge is approximately equal to rainfall when weather is cloudy and cool during winter and spring storms. We also use effective porosity, p, in place of the more common specific yield on the assumption that the elastic storage component of thin hillside soil layers is negligible (Bear, 1972, p. 376). For the limiting case of $p = 0$, corresponding to a state of tension saturation, the temporal derivative in equation (1.2) goes to infinity and piezometric level should rise instantaneously in response to rainfall.

Differentiating equation (1.1) with respect to ξ and substituting the result into equation (1.2) we arrive at

$$\frac{\partial h}{\partial t} = \frac{K}{p}\frac{\partial}{\partial \xi}\left(\frac{\partial h}{\partial \xi} h \cos \beta - h \sin \beta\right) + \frac{R}{p} \tag{1.3}$$

or, equivalently,

$$\frac{\partial h}{\partial t} = \frac{K}{p}\left[\frac{\partial^2 h}{\partial \xi^2} h \cos \beta + \left(\frac{\partial h}{\partial \xi}\right)^2 \cos \beta - \frac{\partial h}{\partial \xi} \sin \beta\right] + \frac{R}{p} \tag{1.4}$$

both of which are nonlinear in h and have no known analytic solutions for time-variant recharge.

Dimensional Analysis of the Governing Equation

For a porous slab of length L and thickness D we introduce the dimensionless variables

$$H = h/D$$

$$X = \xi/L$$

$$T = t/t_r$$

$$t_r = D/K$$

as well as the scaling factor

$$\sigma = D/L$$

and then non-dimensionalize equation (1.4) to arrive at

$$p\frac{\partial H}{\partial T} = \left[\frac{\partial^2 H}{\partial X^2} H + \left(\frac{\partial H}{\partial X}\right)^2\right]\sigma^2 \cos\beta - \frac{\partial H}{\partial X}\sigma \sin\beta + \frac{R}{K} \tag{1.5}$$

We chose to use a characteristic time of $t_r = D/K$ because we are interested principally in short-term water level changes rather than the long term fluctuations that would occur on a scale of $t_r = L/K$; thus for a slab on the order of $D = 10^0$ m and $K = 10^{-5}$ m/s, characteristic of the hillsides at Delhi Pike, we will be looking at changes that occur on a time scale of order 10^5 s, or about one day. For long, thin slabs all terms containing σ will be negligible, hence integration to solve equation (1.5) for H yields

$$H = \int_{T_1}^{T_2} \frac{R}{pK} dT + H_0 \tag{1.6}$$

where H_0 is uniform water level along the slope at T_1. Equation (1.6) suggests that water levels will rise and fall uniformly along the entire slope, with no component of wave-like flow. Furthermore, effective porosity, p, will be different before each storm and prediction of rapid water level changes in response to rainfall, even using this simple model, requires detailed knowledge of pre-storm effective porosity, hydraulic conductivity, rainfall intensity, and rainfall duration.

One way to produce wave-like flow with the model is to redefine the characteristic time of the system as $t_r = L/K$, so that typical values of $L \approx 10^2$ m and $K \approx 10^{-5}$ m/s give a characteristic time on the order of 10^7 s, or about 100 days. Using this new definition, equation (1.4) can be written as a nonhomogeneous kinematic wave equation (Lighthill and Whitham, 1955; Miller, 1984)

$$\frac{\partial H}{\partial T} + \left(\frac{\sin \beta}{p}\right)\frac{\partial H}{\partial X} = \frac{R}{\sigma\ p\ K} \tag{1.7}$$

which will indeed produce wave-like flow, but on a time scale much longer than that of the rapid fluctuations observed at Delhi Pike. Another way to produce wave-like flow with the model is to return to our original definition of $t_r = D/K$, set $R = 0$, and assume that for a nearly-saturated hillside $\sigma \approx p$. To first order in σ, then, equation (1.4) can be re-written as a homogeneous kinematic wave equation

$$\frac{\partial H}{\partial T} + c\frac{\partial H}{\partial X} = 0 \tag{1.8}$$

where

$$c = \frac{\sigma \sin \beta}{p}$$

is the celerity of the traveling waveform. Thus net recharge, due to either infiltration or evapotranspiration, must be insignificant in order for wave-like flow to occur on the time scales observed at Delhi Pike. For a phreatic surface with periodic perturbations of arbitrary wavelength λ and amplitude A_0, a general solution to equation (1.8) is

$$H = A_0 \sin\left[\frac{2\pi}{\lambda}(X - cT)\right] \tag{1.9}$$

which can be verified by differentiating with respect to X and T, and then substituting the results into equation (1.8).

Finite Difference Formulation

We assume that spatial grid increments are uniform, solve for the second derivative, and linearize by letting coefficient h values lag one time increment behind (Anderson and others, 1984, p. 337). In order to minimize the error introduced by letting coefficients lag over large temporal increments, we use the alternate predictor-corrector method of Douglas and Jones (1963) with a fully-explicit predictor to estimate values of h at time t + (δt /2), which are then substituted into a Crank-Nicholson corrector to solve for values of h at time t + δt. For interior nodes the predictor form of equation (1.4) is

$$h_{i-1}^{j+1/2} - 2\left[1 + \frac{p\,(\delta\xi)^2}{K\,\delta t\,h_i^j \cos\beta}\right] h_i^{j+1/2} + h_{i+1}^{j+1/2} = \frac{-\,2p\,(\delta\xi)^2}{K\,\delta t \cos\beta}$$

$$- \frac{1}{4h_i^j}\left(h_{i+1}^j - h_{i-1}^j\right)^2 + \frac{\xi \tan\beta}{2h_i^j}\left(h_{i+1}^j - h_{i-1}^j\right) + \frac{R\,(\delta\xi)^2}{K\,h_i^j \cos\beta} \tag{1.10}$$

whereas for internal nodes the corrector form of equation (1.4) is

$$h_{i-1}^{j+1} - 2\left[1 + \frac{p\,(\delta\xi)^2}{K\,\delta t\,h_i^{j+1/2} \cos\beta}\right] h_i^{j+1} + h_{i+1}^{j+1} = \frac{-\,2p\,(\delta\xi)^2}{K\delta t\,h_i^{j+1/2} \cos\beta}$$

$$- \frac{1}{4h_i^{j+1/2}}\left(h_{i+1}^j - h_{i-1}^j\right)^2 + \frac{\xi \tan\beta}{2h_i^{j+1/2}}\left(h_{i+1}^j - h_{i-1}^j\right)$$

$$+ \frac{R(\delta\xi)^2}{K\,h_i^{j+1/2} \cos\beta} - h_{i-1}^j + 2h_i^j - h_{i+1}^j \tag{1.11}$$

Note that because the predictor, equation (1.10), is fully explicit it uses a forward difference temporal derivative and is only first order accurate in time, but because the Crank-Nicholson corrector, equation (1.11), is half explicit and half implicit it uses a central difference temporal derivative and is second order accurate in time. Both the predictor and the corrector are second order accurate in space, so the combined accuracy over one entire time increment is accurate to order $[(\delta\xi)^2,(\delta t)^{3/2}]$ (Douglas and Jones, 1963).

Boundary and Initial Conditions

We chose to fix water table height at both the uphill and downhill ends of our numerical model both to account for the steady baseflow, represented by relatively constant water levels in P-4 between storms, that we observed at Delhi Pike and also to insure that water levels near the lower boundary did not exceed soil thickness. As shown in the perturbation analysis above, though, boundary effects act only over small portions of the problem domain so that choice of a specific set of boundary conditions will not greatly affect the behavior of the model. For a fixed piezometric level at spatial node 1 the boundary form of the predictor, equation (1.10), expanded around neighboring spatial node 2 is

$$-2\left[1+\frac{p\,(\delta\xi)^2}{K\delta t\, h_2^j \cos\beta}\right]h_2^{j+1/2}+h_3^{j+1/2}=\frac{-2\,p\,(\delta\xi)^2}{K\,\delta t\cos\beta}-\frac{1}{4h_2^j}\left(h_3^j-h_1^j\right)^2$$

$$+\frac{\xi\tan\beta}{2h_2^j}\left(h_3^j-h_1^j\right)+\frac{R\,(\delta\xi)^2}{K\,h_2^j\cos\beta}-h_1^{fixed} \qquad (1.12)$$

and the accompanying form of the corrector, equation (1.11), is

$$-2\left[1+\frac{p\,(\delta\xi)^2}{K\,\delta t\,h_2^{j+1/2}\cos\beta}\right]h_2^{j+1}+h_3^{j+1}=\frac{-2\,p\,h_2^{j}(\delta\xi)^2}{K\,\delta t\,h_2^{j+1/2}\cos\beta}$$

$$-\frac{1}{4h_2^{j+1/2}}\left(h_3^{j}-h_1^{j}\right)^2+\frac{\xi\tan\beta}{2\,h_2^{j+1/2}}\left(h_3^{j}-h_1^{j}\right)+\frac{R\,(\delta\xi)^2}{Kh_2^{j+1/2}\cos\beta}$$

$$-2h_1^{\text{fixed}}+2h_2^{j}-h_3^{j} \qquad (1.13)$$

Both the predictor and the corrector for the downhill boundary expanded around the (n - 1)th node are similar in form to equations (1.12) and (1.13).

To solve the model, we used the standard Thomas algorithm (e.g. Press and others, 1986; Anderson and others, 1984) for tridiagonal linear systems to solve finite-difference approximations of the forms given in equations (1.10) and (1.11) with boundary approximations of the forms given by equations (1.12) and (1.13), and verified our algorithm with an analytical steady-state perturbation solution of equation (1.4). The complete computer program is listed in Appendix C, and the analytical solution is derived and compared to numerical results in Appendix E.

NUMERICAL RESULTS

On the basis of our theoretical analyses and field observations we chose representative values for all of the constants in equation (1.2), and then experimented with the numerical model in order to produce synthetic water level records similar to those we recorded at Delhi Pike. First we attempted to match actual water level records with synthetic water level records from our model. Then, after we were satisfied that the model could account for our field observations, we experimented with different combinations of rainfall intensity and duration to see what effect changes in these variables would have on water level record shapes. In order to better understand the effects of rainfall patterns on water level record shape, we decided to use relatively simple rainfall distributions rather than the more complex patterns we recorded at Delhi Pike.

Simulation of P-4 Water Level Records

By trial and error we found that field water level records with very abrupt changes or multiple storms, such as we have described for May 12 through May 13, 1980 (Figure 1.9) are difficult to model. However, we were able to obtain good results for simple, single storms with gradually changing water level records.

In general we found that, as predicted by our first order analysis, the model is very sensitive to changes in effective porosity, p, hydraulic conductivity, K, and recharge, R. For example, Figure 1.11 compares actual and calculated water level records for the storm of April 11 and 12, 1980. We used values of $p = 0.025$, $K = 1.3 \times 10^{-5}$ m/s, $\delta t = 3600$ s, $\delta\xi = 5$ m, $\beta = 22^{\circ}$, upslope head fixed at 0.1 m, downslope head fixed at 1.2 m, and recharge, R, equal to measured rainfall. Except for effective porosity, p, we selected these representative values from our field observations. Calculated maximum effective porosity for this storm, which assumes that all of the rain contributes to the measured water level increase, was $p = 0.035$, but our model runs showed that $p = 0.025$ gave better results. The necessity of such an adjustment, however, is not surprising because the field estimates were obtained by solving the equivalent of equation (1.7) for p, which does not include high order terms for downhill flow, whereas the computer model solves an approximation of equation (1.4), in which the water is being lowered due to the higher order terms at the same time it is being raised due to the lower order terms; thus the lack of higher order terms causes equation (1.7) to underestimate effective porosity.

The shapes of falling hydrograph limbs in our simulations were also controlled by location along the slope, but this is an artifact of our incomplete knowledge of the

Figure 1.11 Comparison of actual and synthetic water level records from P-4 on April 11 and 12, 1980. Effective porosity in the numerical model was lowered from the actual maximum effective porosity of 0.035 to 0.025, and recharge to the model water table was set equal to actual rainfall.

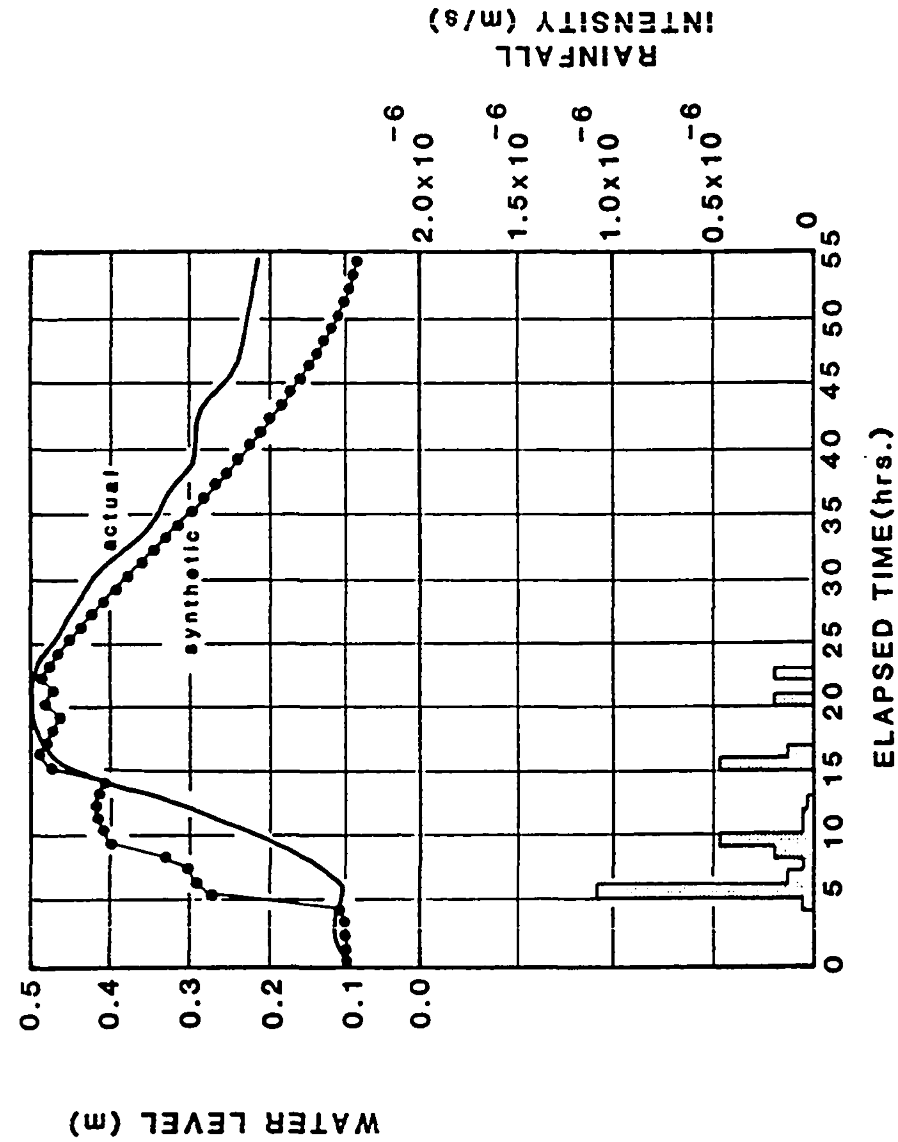
WATER LEVEL (m)
RAINFALL INTENSITY (m/s)
ELAPSED TIME(hrs.)
actual
synthetic
0.0
0.1
0.2
0.3
0.4
0.5
0
0.5x10^{-6}
1.0x10^{-6}
1.5x10^{-6}
2.0x10^{-6}
0
5
10
15
20
25
30
35
40
45
50
55

necessary variables. While attempting to reproduce P-4 hydrographs we assumed that both K and R = $f(t)$ were known with some confidence and then adjusted our estimate of p until the simulations agreed with our rainfall data. Rapid increases, governed by equation (1.7), occur uniformly along the entire slope so the shape of rising hydrograph limbs is independent of position; however, when rainfall ceases and R = 0 in the numerical model drainage occurs from the head to the toe of the slope, so the steepness of simulated falling hydrograph limbs will be a function of position along the slope. By trial and error we found that synthetic hydrographs from the finite difference node at ξ = 15 m (measured from the top of the slope) gave the best match with field data from P-4, which is not unreasonable because the colluvium mantle thins and becomes more rocky above the contact between Kope and Fairview Formations some 15 to 20 m upslope from P-4.

The synthetic water level record for P-4 during the storms of March 11 and 12 (Figure 1.11) begins to rise steeply as soon as rainfall begins, whereas the actual field water level record begins to rise slowly 2 hours after rainfall begins. Furthermore, the synthetic water level record is very sensitive to changes in rainfall intensity, producing an irregular curve, whereas the actual water level record is smooth and does not reflect variations in rainfall intensity. Both water level records peak at about 0.50 m and 22 hours elapsed time. (Note that we give model results in water table height above the impermeable substrate and elapsed time, as compared to water depth beneath the surface and time of day for our field data). The synthetic water level record falls more rapidly to its fixed head boundary base level of 0.10 m, whereas the actual water level record falls to about 0.20 m before leveling off and shows several small perturbations on its falling limb.

Simulation of short, intense rainfall.- Our numerical experiments with short, intense rainfall produced distinctly asymmetric water level records with very steep rising limbs. Figures 1.12 and 1.13 show that for one simulation of this type water level began to rise

Figure 1.12 Model results for drainage of a fully saturated, thin homogeneous aquifer of uniform thickness resting atop a sloping impervious substrate. Water level rises almost uniformly along the entire slope, but drains from head to the toe of the hillside. Variables used were $p = 0.01$, $K = 1.3\times10^{-5}$ m/s, $\beta = 22^{\circ}$, $h = 2$ m, and slope length = 100 m. Rainfall intensity was 1×10^{-7} m/s for the first hour, 5×10^{-7} m/s for the second and third hours, 1×10^{-7} m/s for the fourth hour, and zero thereafter.

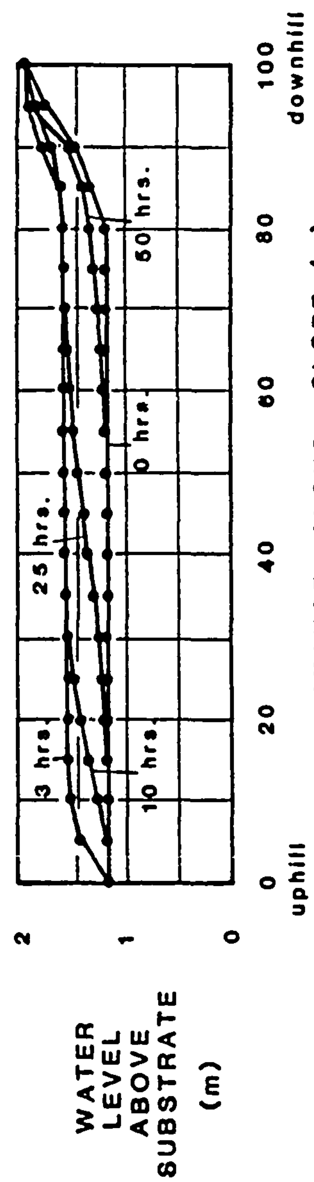
WATER LEVEL ABOVE SUBSTRATE (m)
0
1
2
DISTANCE ALONG SLOPE (m)
0
uphill
20
40
60
80
100
downhill
3 hrs.
10 hrs.
25 hrs.
50 hrs.

Figure 1.13 Synthetic water level records in response to a short, intense rainstorm providing 0.004 m of net recharge to the water table. Curves are for finite difference nodes located 25 and 50 m from the top of the hillside.

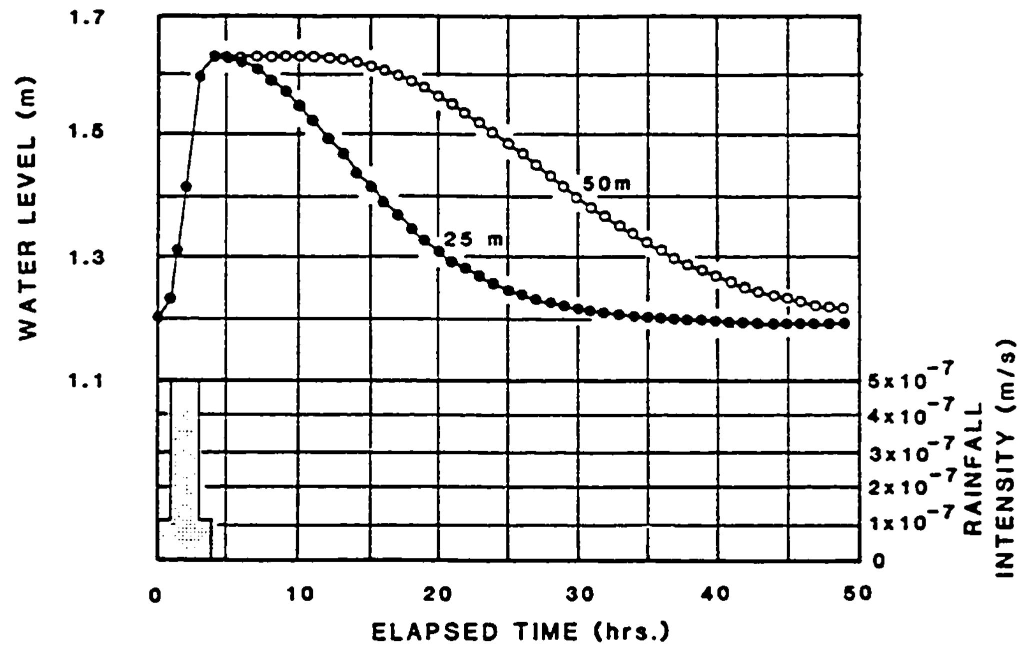
1.7
1.5
1.3
1.1
WATER LEVEL (m)
50m
25 m
5x10^-7
4x10^-7
3x10^-7
2x10^-7
1x10^-7
0
RAINFALL INTENSITY (m/s)
0
10
20
30
40
50
ELAPSED TIME (hrs.)

almost immediately after rainfall began, and peaked shortly after it stopped. Although water level rose uniformly at all of the interior finite-difference nodes, it fell much more rapidly near the top of the hillside than at its midpoint, and the water level record from $\xi = 50$ m is much flatter than the water level record from $\xi = 25$ m. Total recharge for the simulation shown in Figure 1.13 was 0.004 m.

Simulation of prolonged, gentle rainfall.- Next, we simulated the effects of a prolonged, gentle rainfall providing the same amount of recharge as the short, intense rainfall simulation that we describe above (0.004 m). Figure 1.14 shows that the $\xi = 25$ m water level record peaked slightly below and before the $\xi = 50$ m water level record. Except for this offset of peaks, the falling limbs are virtually identical to those in Figure 1.13. The rising limb, however, is much flatter, and is no steeper than the steepest portion of the falling limb.

Simulation of intense followed by gentle rainfall.- We observed that in some cases, for example the water level record of 19-22 March, a small amount of rain distributed over several hours seemed to maintain the water table at a high level until the rain stopped. So, we modeled such a situation using an initial short, intense storm identical to that in Figure 1.13 followed by followed by seven hours of very light but continuous rain (5×10^{-8} m/s). The results of our simulation (Figure 1.15) show that water level first peaked at the same level and time as in Figure 1.13, and then began to fall slowly when the rain stopped. Before the water level could fall very much, though, the light rain began and slope of the falling limb for $\xi = 25$ m remained constant until the rain stopped and then increased markedly. The $\xi = 50$ m water level record, however, fell only until the second round of rain began, and then rose to peak at about 1.75 m while the $\xi = 25$ m water level record was falling. Thus the effect of a small secondary storm is differs along the length of the hillside.

Figure 1.14 Synthetic water level records in response to gentle rainfall providing 0.004 m of net recharge to the water table, the same as in Figure 12. Curves are for finite difference nodes located 25 and 50 m from the top of the hillside. Note differences between synthetic water level records in Figures 13 and 14 produced net recharge of equal magnitude but different intensity and duration.

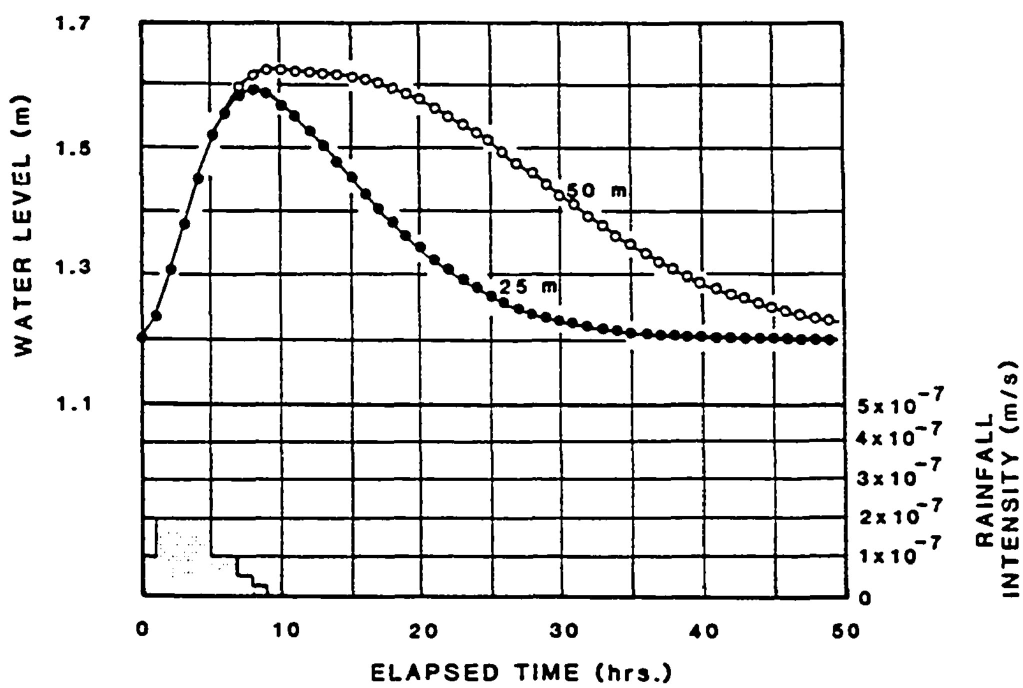

WATER LEVEL (m)
1.7
1.5
1.3
1.1
50 m
25 m
5x10^{-7}
4x10^{-7}
3x10^{-7}
2x10^{-7}
1x10^{-7}
0
RAINFALL INTENSITY (m/s)
0
10
20
30
40
50
ELAPSED TIME (hrs.)

Figure 1.15 Synthetic water level records in response to a short, intense storm followed by several hours of gentle rainfall. Curves are for finite difference nodes located 25 and 50 m from the top of the hillside. The initial storm provided 0.004 m of net recharge, the same as in Figures 12 and 13, but the additional recharge was able to significantly decrease the rate at which the water table fell after the storm.

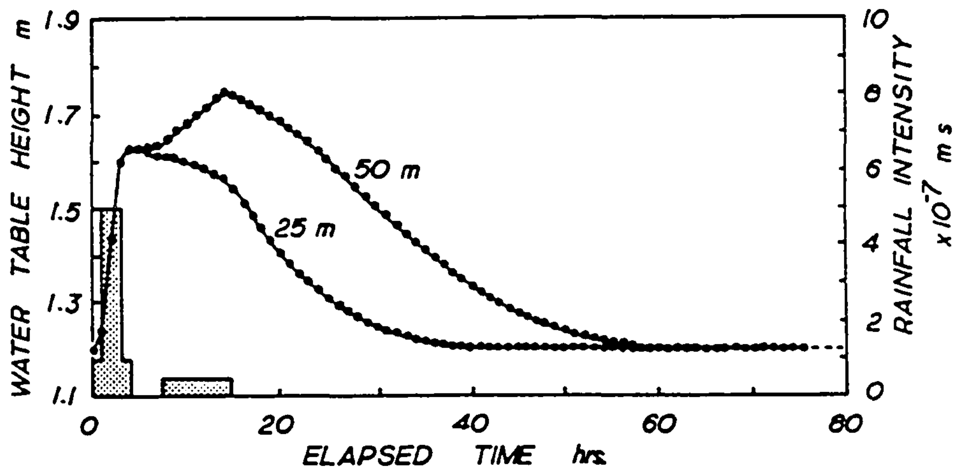
WATER TABLE HEIGHT m
1.9
1.7
1.5
1.3
1.1
50 m
25 m
RAINFALL INTENSITY x10^-7 m s
10
8
6
4
2
0
0
20
40
60
80
ELAPSED TIME hrs.

DISCUSSION

Our simple theoretical model accounts for the shapes and amplitudes of asymmetric, short-term piezometer hydrographs from Delhi Pike surprisingly well if we assume that pre-storm effective porosity was on the order of a few percent when our field data were collected. Most importantly, we have shown that rapid water level fluctuations should occur uniformly along the entire slope during periods of significant rainfall or evapotranspiration and that wave-like downhill flow, as predicted by other mathematical and laboratory models, is controlled by higher order terms in the governing equation that are significant only when rainfall or evapotranspiration are negligible.

Although we have developed a conceptually simple model, we stress that it is also extremely sensitive to variations in all four of the values needed to predict rapid water level fluctuations: rainfall intensity, rainfall duration, hydraulic conductivity, and pre-storm effective porosity. Because these critical values are also extremely difficult to assess in complex natural hillsides, we are wary of the many recent attempts to predict sudden hillside failures during rainstorms by correlating so-called threshold rainfall with slope instability, particularly when such predictions may have a bearing on human life and limb (e.g. Keefer and others, 1987). We recommend that instead of relying solely on statistical correlations, any future slope instability warning system include monitoring of pre-storm soil moisture conditions in areas where sudden failure would have significant economic or social consequences.

Numerical solutions of our model using reasonable values for the hillside at Delhi Pike agree in both shape and magnitude with our field data but, like the first order analytical model, are also sensitive to variations in rainfall, conductivity, and porosity estimates. Differences between actual and synthetic water level records produced using the model

(Figure 1.11) give us some insight into the hillside hydrologic system. The first major difference, a noticeable time lag between the onset of rainfall and piezometer response, can be attributed largely to the time required for rainwater to infiltrate through the unsaturated zone. For example, if we assume that R was constant with time and $p = 0.03$ before the storm of April 11, 1980, we can solve equation (1.7) for $R \approx 5\times10^{-6}$ m/s using the observed 7200 s time lag, suggesting that the water table is being recharged at a rate of about K/2. Examination of Murdoch's (1987) laboratory data for colluvium from Delhi Pike show that unsaturated hydraulic conductivity for $p \approx 0.03$ is about two-thirds to one-half of saturated hydraulic conductivity, so a 7200 s time lag for a piezometer tip about 1 m deep in slightly unsaturated colluvium is not unreasonable. Because the hydraulic conductivity of unsaturated soils is a highly nonlinear function of pressure head, both the time lag and the slope of the rising hydrograph will vary exponentially with pre-storm fillable porosity, which is also a function of pressure head. Once the soil does become saturated, however, water can flow into the piezometer tube and Hvorslev's (1951) method predicts a response time for P-4 of about one minute, so the effect of the piezometer tube itself on response time should be negligible.

The differences between actual and synthetic falling water level record limbs in Figure 1.11 suggest to us that water is being introduced from a source not considered in the model, perhaps bedrock seeps. Localized seepage from fractured limestone layers in the bedrock would also explain the steady baseflow observed in P-4 between storms, and are consistent with observations of weakly artesian bedrock springs throughout the Cincinnati area (Baum, 1983).

There are not enough high frequency water level data uphill and downhill from P-4 frequently enough to tell us how well our model or any other model applies to the entire hillside, but the data do tell us that sampling frequencies of several days or weeks can be too low to resolve the effects of single storms at Delhi Pike. The Hamilton County Soil Survey (Lerch and others, 1982) does describe common seepage problems along only the lower portions of Eden silty clay loam slopes, though, so there is some evidence for slope-parallel drainage in hillsides such as those at Delhi Pike, and similar results have been reported elsewhere.

CHAPTER 2
SEASONAL AND SHORT-TERM HYDROLOGY OF A THIN COLLUVIUM HILLSIDE NEAR CINCINNATI, OHIO[1]

INTRODUCTION

Studies of hillside flow, particularly those dealing with storm discharge hydrographs, are common in the hydrologic literature, but studies of pressure head variations in natural hillsides are rare. This paper describes the hydrology of a thin, predominantly unsaturated colluvium hillside near Cincinnati, Ohio between October 1987 and May 1988, and shows that field observations can be explained largely in terms of infiltration and evapotranspiration, with only secondary contributions from bedrock seeps. Goals of the research, which grew out of previous work on local landsliding problems, were: 1) to determine whether nearly-saturated conditions conducive to rapid water level increases could be maintained between storms during winter and spring months, 2) to assess the relative contributions of rainfall and bedrock seepage to the hillside hydrologic regime, and 3) to test the applicability of published wave-like hillside flow models.

Geologic Setting

The Delhi Pike landslide complex, located in Holocene colluvium along the Ohio River valley about 15 km west of downtown Cincinnati, Ohio (Figure 2.1) is typical of thin colluvium landslides throughout the Cincinnati area, where annual <u>per capita</u> landslide damage costs are among the highest in the United States (Fleming and Taylor, 1980). Physiographically, the Cincinnati area consists of flat uplands dissected by valleys of the modern day Ohio River and its predecessors (Teller, 1973; Durrell, 1961), with relief on the order of 100 m or more. Valley walls are lined with clayey to rocky colluvium resting

---

[1] *in review for Journal of Hydrology.*

Figure 2.1 Index map showing location of the study area in relation to major geographic features near Cincinnati.

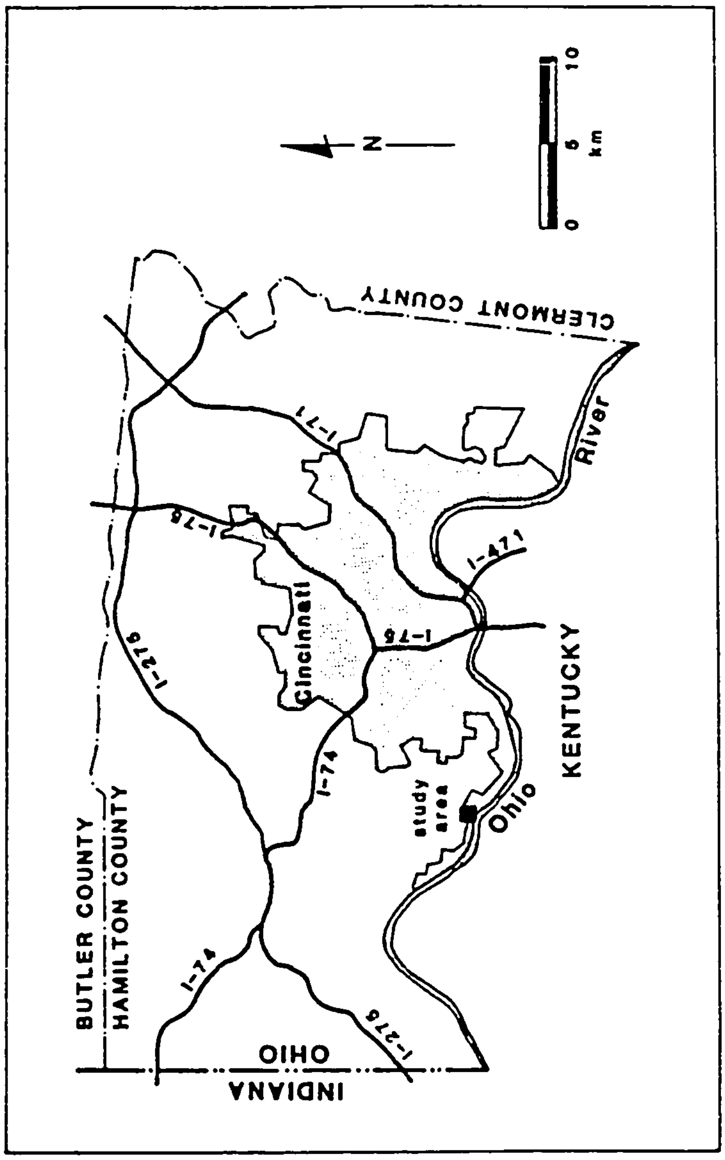
N
0
5
10
km
CLERMONT COUNTY
BUTLER COUNTY
HAMILTON COUNTY
INDIANA
OHIO
KENTUCKY
Cincinnati
study area
Ohio
River
I-71
I-75
I-75
I-471
I-74
I-74
I-275
I-275

on top of the flat-lying Upper Ordovician shale and limestone bedrock, and are covered by 0.10 to 0.15 m of organic soil and forest litter. The colluvium, which ranges in thickness from zero near hilltops to 10 m or more near river level, consists of about 70% silty to clayey matrix derived from local illitc shale bedrock that slakes to its constituent grains, and about 30% tabular limestone clasts ranging from a few centimetres to metres in length. It is mapped as Eden silty clay loam, a well-drained residual soil with low permeability formed on moderate to steep slopes, in the Hamilton County, Ohio soil survey (Lerch and others, 1982).

Both weathered and fresh head scarps and strike-slip lateral boundaries delineate individual landslide blocks in the study area, but in some areas the topography is hummocky and landslide features cannot be identified (Figure 2.2). Colluvium thickness ranges up to 1.5 m thick in this portion of the complex, but thins to a decimetre or two at the base of large scarps. A longitudinal trench through part of the landslide complex (Figure 2.3) shows that the bedrock surface is nearly parallel to the ground surface but contains many small undulations, particularly over limestone layers, and erratically distributed limestone blocks.

Previous Work

The Delhi Pike landslide complex has been the site of several research projects, some concerned with hydrologic problems, during the past decade. Fleming and others (1981) first described rapid water level fluctuations in thin (< 2 m) colluvium as well as an association between water levels and landslide movement; they also noted that water level fluctuations in thick colluvium at Delhi Pike, in contrast to rapid fluctuations in the thin colluvium, were seasonal. In a preliminary study, Murdoch (1987) found that extremely dry colluvium, with pressure heads approaching -10 m H_2O, could be wetted during late winter rains and remain moist through the following spring. Using a numerical model of

Figure 2.2 Surficial geologic map of part of the Delhi Pike landslide complex showing landslide morphology and instrument locations. All elevations relative to an arbitrary datum on Delhi Pike.

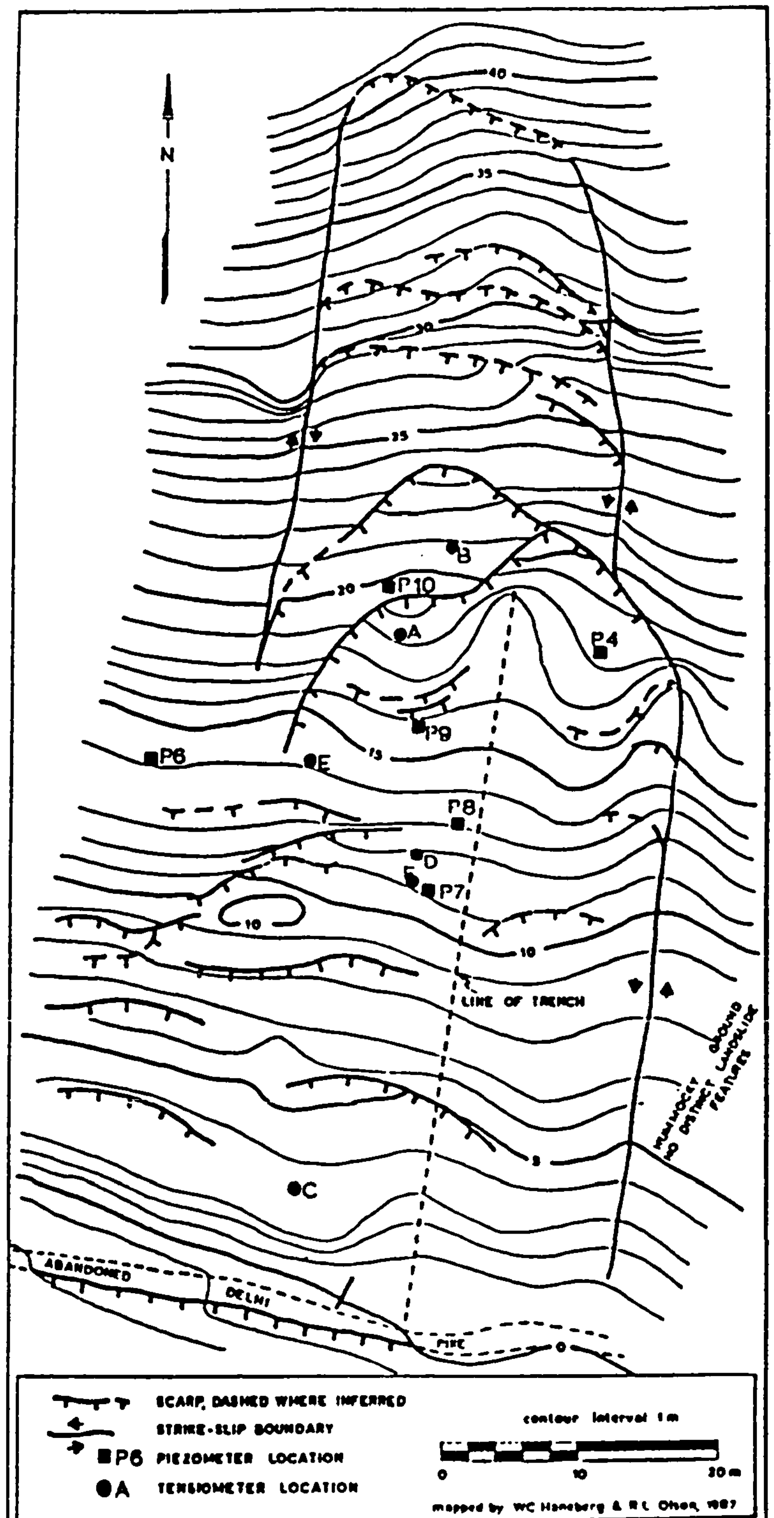
N
40
35
30
25
20
15
10
5
0
P10
P4
P9
P6
P8
P7
A
B
C
D
E
LINE OF TRENCH
HUMMOCKY GROUND
NO DISTINCT LANDSLIDE
FEATURES
ABANDONED
DELHI
PIKE
SCARP, DASHED WHERE INFERRED
STRIKE-SLIP BOUNDARY
P6 PIEZOMETER LOCATION
A TENSIOMETER LOCATION
contour interval 1 m
0
10
20 m
mapped by WC Haneberg & R L Olson, 1987

Figure 2.3 Longitudinal trench profile showing distribution of soil types, landslide features, and bedrock clasts (see Figure 2 for trench location). Trenching operations destroyed hummocky surface topography.

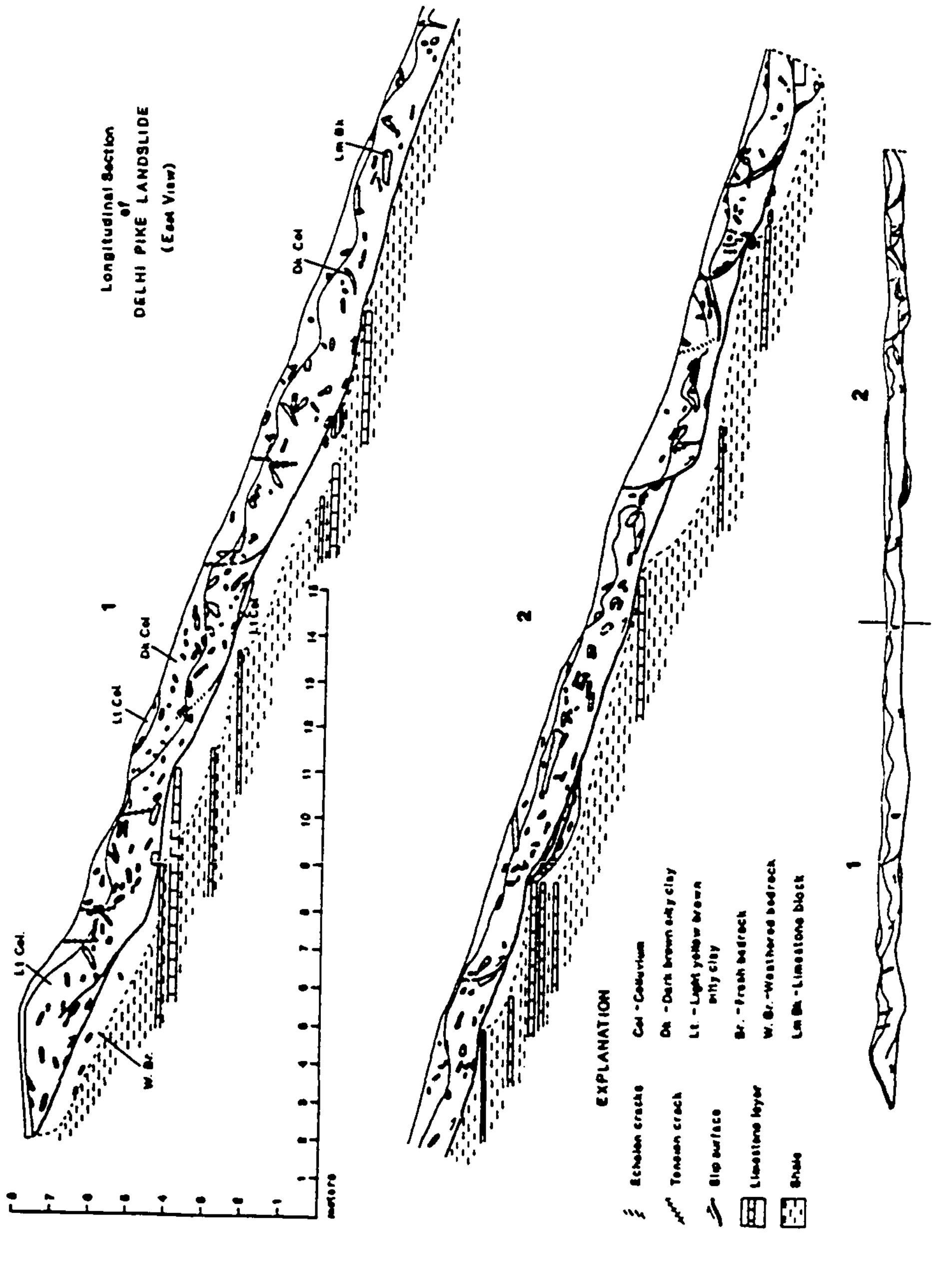
Longitudinal Section
of
DELHI PIKE LANDSLIDE
(East View)
1
2
Lt Col.
W. Br.
Lt Col
Dk Col
Lt Col
Dk Col
Lm Bk
metere
1 2 3 4 5 6 7 8 9 10 11 12 13 14 15
1 2 3 4 5 6 7 8
EXPLANATION
Echelon cracks
Tension crack
Slip surface
Limestone layer
Shale
Col - Colluvium
Dk - Dark brown silty clay
Lt - Light yellow brown silty clay
Br. - Fresh bedrock
W. Br. - Weathered bedrock
Lm Bk - Limestone block

infiltration into an infinite half-space to interpret his field data, Murdoch concluded that seepage was predominantly vertical during storms or periods of high evapotranspiration and predominantly slope-parallel between storms. Using the theoretical model developed in Chapter 1, analysis of piezometer data recorded between 1979 and 1981 shows that fillable porosity must have been low (≈ 0.02) before rapid water level increases during winter and spring 1980 storms at Delhi Pike. When evapotranspiration is insignificant, the Chapter 1 model predicts wave-like downhill flow in which water levels rise uniformly along the entire slope during storms and then gradually fall from top to bottom as water flows downhill, much the same as predicted by linear kinematic wave (Beven, 1981, 1982; Hurley and Pantelis, 1985), two-dimensional finite element (Beven, 1977), and laboratory sandbox (Anderson and Burt, 1977b) models of hillside flow. When evapotranspiration is significant, however, the Chapter 1 model predicts a uniform reduction of water levels along the entire hillside.

FIELD OBSERVATIONS

Instrumentation

Both mercury manometer tensiometers and porous stone piezometers were chosen to measure pressure heads at Delhi Pike because of their low cost and simplicity, and daily measurable precipitation data (Figure 2.6) were obtained from the National Weather Service office at the Greater Cincinnati International Airport, about 5 km south of the study area. The practical lower limit of the manometer tensiometers is -0.7 m of Hg (Croney and others, 1952), or about -9.5 m of H_2O, which coincides with the lowest pressure heads recorded in this study.

A total of six tensiometer groups, each consisting of three or four instruments at different depths, were installed in thin colluvium at Delhi Pike using a hand auger (see Figure 2.2 for locations). Groups A, B, and C were installed in late May 1987, but were then disconnected until late September 1987 because of extremely low pressure heads. Groups D and E were installed in late September 1987, and group F was installed in April 1988. Piezometers P-4 and P-6 are the same instruments described in Fleming and others (1981) and Haneberg and Gökce (in press), and piezometers P-7 through P-10 were installed in February 1988 using a two-person power auger. Large roots and rocks made installation difficult, and controlled locations and depths of the instruments. Pressure heads were measured by hand at intervals ranging from once or twice a week during dry periods to several times a day during winter and spring rains, with the exception of several gaps when the tensiometers were disconnected in anticipation of freezing temperatures. The data presented here are not comprehensive, but rather were chosen to illustrate processes observed during the study period; Appendices A and B contain complete sets of field data as well as details of tensiometer design and calibration.

Seasonal Variations

Precipitation before and during the period of record was substantially below normal. Typically, snow and rain are uniformly distributed throughout the year in the Cincinnati area (Figure 2.4), but a cumulative plot of actual monthly precipitation between January 1987 and May 1988 shows a cumulative deficit of about -0.2 m during this period. The precipitation shortfall between July 1987 and January 1988 was particularly severe, accounting for nearly half to the total deficit during the period of record, and normal rainfall levels during spring 1988 could not compensate for drought conditions during the previous summer and autumn.

Pressure head data from Delhi Pike show extremely strong seasonal variations during the study period, and except for brief transitional periods the soil was either uniformly dry or uniformly moist (Figure 2.5). For example, between October and December 1987, pressure heads in group E tensiometers ranged between -8 m and -10 m,

Figure 2.4 Cumulative total monthly precipitation, average monthly precipitation, and departure from monthly average precipitation at Greater Cincinnati International Airport, about 5 km south of the study area. Data from National Oceanic and Atmospheric Administration (1987, 1988).

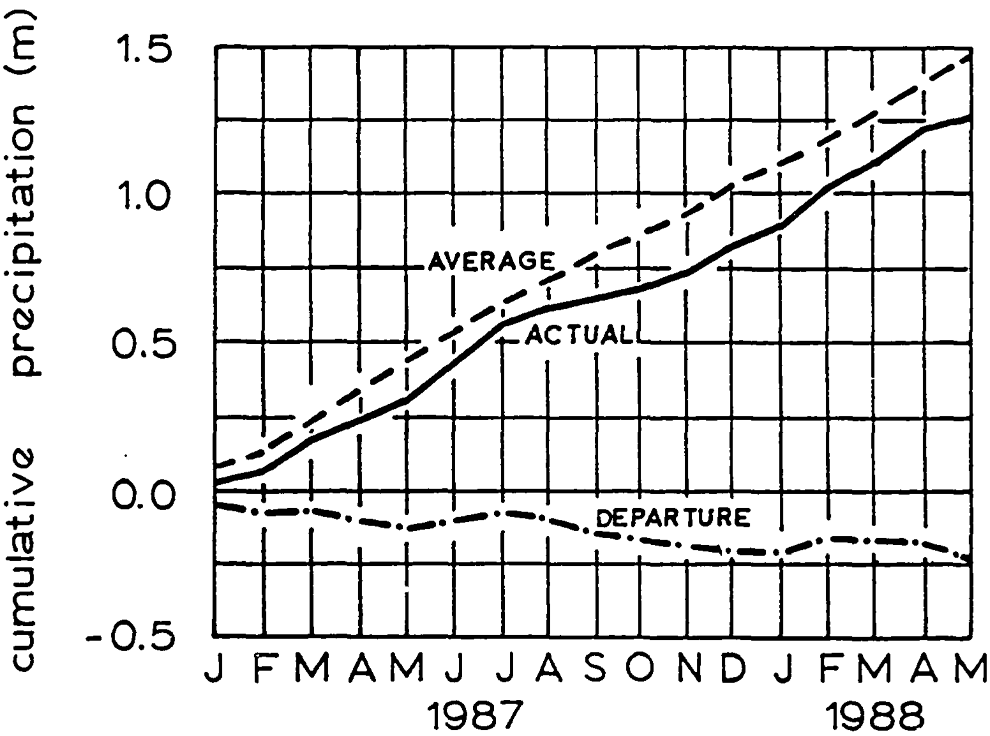
cumulative precipitation (m)
1.5
1.0
0.5
0.0
-0.5
AVERAGE
ACTUAL
DEPARTURE
J F M A M J J A S O N D J F M A M
1987
1988

Figure 2.5 Tensiometer group E pressure heads, October 1987 through May 1988. Lower limit of mercury manometer tensiometers is approximately -9.5 m H_20.

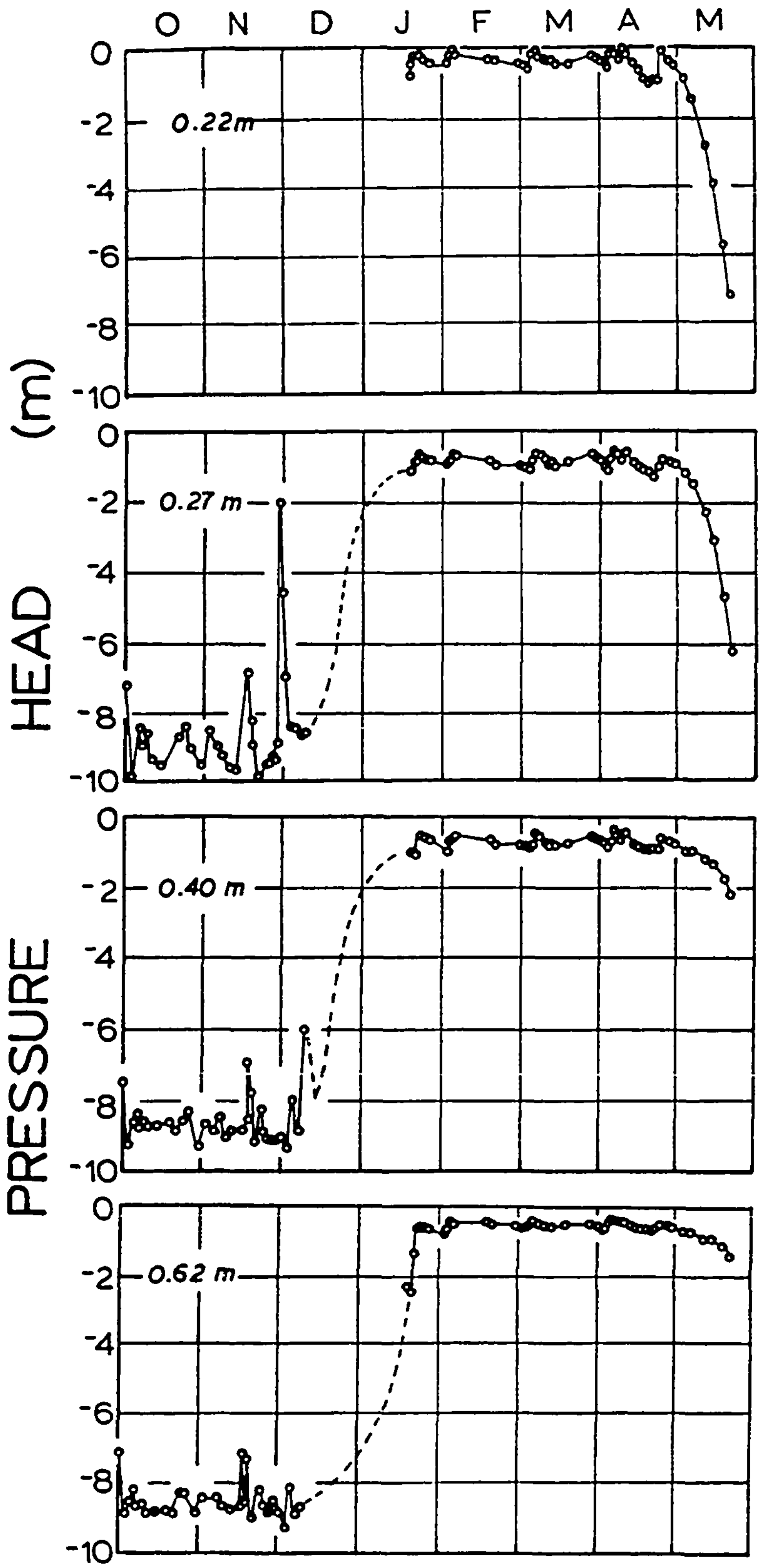
O N D J F M A M
0
-2
-4
-6
-8
-10
0.22m
0.27 m
0.40 m
0.62 m
PRESSURE HEAD (m)

and fluctuated erratically from day to day to produce a jagged sawtooth pattern. After steady winter rains in late December 1987 (Figure 2.6), however, pressure heads abruptly increased to about -1 m or greater, and were maintained at this level throughout the following months with only occasional precipitation. Pressure head plots for spring 1988 are much flatter than those from autumn 1987, but increases in response to significant rainfall stand out clearly (compare Figures 2.5 and 2.6). In general, shallower tensiometers characteristically showed higher amplitude fluctuations than deeper tensiometers during both dry and wet periods, especially during autumn 1987.

Piezometers P-4 and P-6 were dry throughout autumn 1987, and held water only during and immediately after storms during spring 1988 (Figure 2.7). Although both piezometers responded to rainfall, P-4 commonly rose higher and maintained high water levels longer than P-6; in particular, water level in P-4 remained about 0.9 m below the ground between rainfalls during spring 1988, whereas P-6 characteristically held no water between rainfall.

Other piezometers installed in spring 1988 responded erratically; some never contained water, whereas others almost always held several centimetres of water. During spring 1988, water trickled from cracks in an asphalt road downhill from the study area and from nearly vertical cuts in bedrock approximately 1000 m west of the study area. In both places, seeps continued for several days after rainfall, and stood in sharp contrast to the surrounding dry asphalt and bedrock. The bedrock seeps occurred in only a few places, rather than along the entire exposed lengths of limestone layers, and could not be traced to any fractures, voids, or other irregularities in the bedrock.

Transitional Periods

Tensiometer data for much of the late December 1987 dry to wet transition are unavailable. However, temperatures were well below freezing during early January 1988,

Figure 2.6 Daily measurable precipitation at Greater Cincinnati International Airport, approximately 5 km south of the Delhi Pike landslide complex, between October 1987 and May 1988.

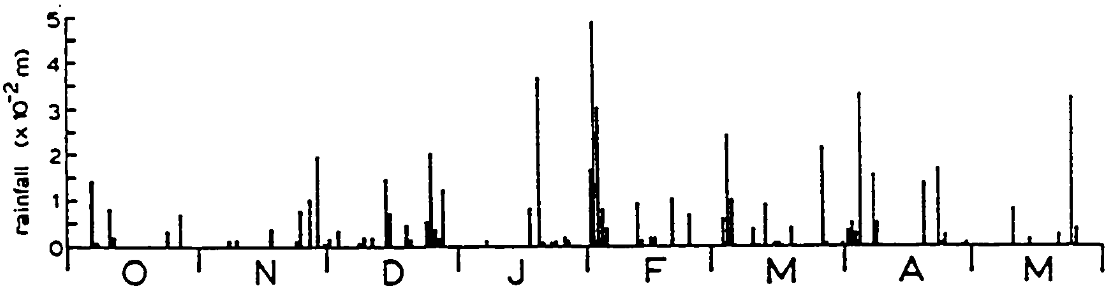
rainfall (x 10^{-2} m)
5
4
3
2
1
0
O
N
D
J
F
M
A
M

Figure 2.7 Water levels in piezometers P-4 and P-6 between January and May 1988. Water levels rose and fell rapidly in response to rainfall, but the consistent water level in P-4 between storms suggests that localized bedrock seeps may occur. Neither P-4 nor P-6 held water during autumn 1987.

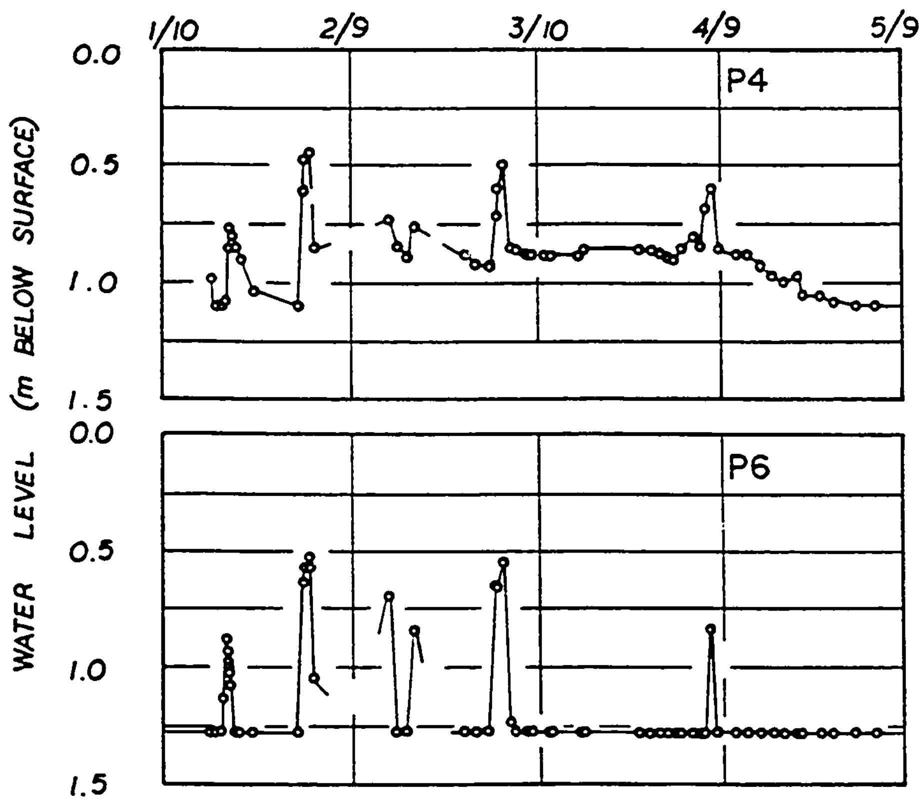

1/10
2/9
3/10
4/9
5/9
P4
P6
0.0
0.5
1.0
1.5
WATER LEVEL (m BELOW SURFACE)

so the transition must have occurred as a result of heavy rains during the last ten days of December 1987. Test excavations during late November and early December, when even the shallowest tensiometers did not approach saturation during steady rainfall (Appendix A), showed that moisture moved slowly downward through the soil behind a distinct wetting front that advanced only a few centimetres per day. For example, after approximately 0.02 m of light rain during the previous three days, on the morning of November 27 colluvium was moist and plastic to a depth of approximately 0.05 m and became gradually less plastic between 0.05 and 0.10 m deep. Below a depth of about 0.10 m, however, the colluvium remained dry and could be crumbled between the fingers, so the wetting front moved downward at a velocity on the order of 10^{-7} m s^{-1} and, assuming that all of the rain infiltrated into the soil, pre-storm fillable porosity was approximately 0.27. Neither P-4 nor P-6 held water during this time.

Small shrubs began to leaf out in late March 1988, but pressure heads did not begin to fall precipitously until May 1988, when large trees leafed out completely during warm, sunny weather. When significant drying began, it was from the surface downward (Figures 2.5 and 2.8) and as drying progressed, vertical pressure head gradients increased beyond unity, which would be the equilibrium gradient if drainage were due to gravity alone (Day and Luthin, 1956). As drying proceeded, the ground surface became cracked, dusty, and desiccated while deeper colluvium remained moist and plastic.

Short Term Effects of Rainfall

Tensiometer response to rainfall during the dry months of October through early December 1987 is erratic and short-lived, as illustrated by daily rainfall and pressure heads at tensiometer group E during November 1987 (Figure 2.9). For example, approximately 0.004 m of rainfall on November 17 produced a pressure head increase of nearly 1 m, whereas greater amounts of rainfall between November 23 and 27 produced much smaller

Figure 2.8 Tensiometer group E vertical pressure head profiles, May 1988. Pressure heads decreased downward, and the ground surface became cracked and dusty during this period of warm, sunny days and low rainfall.

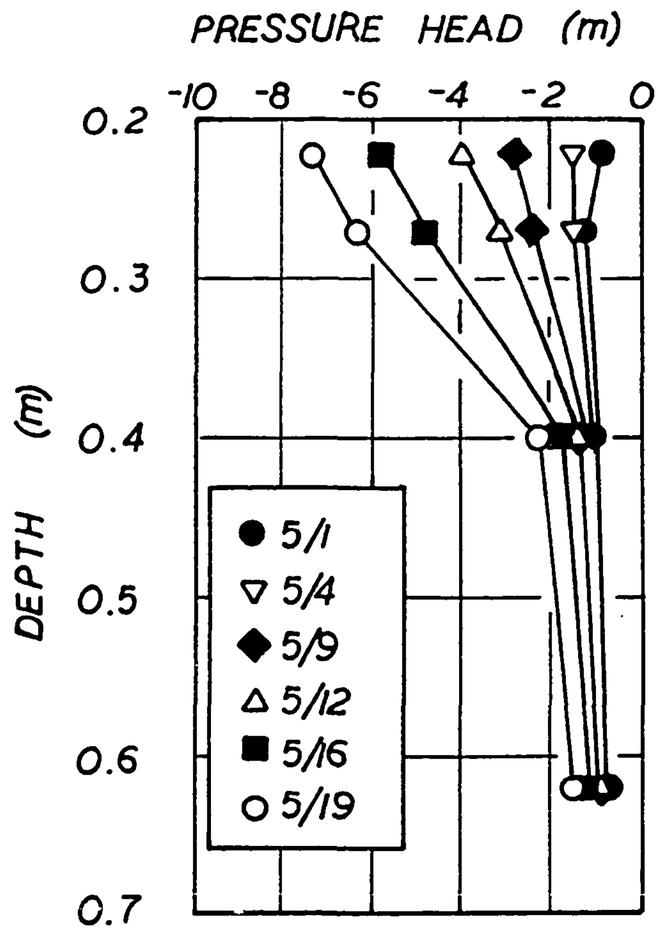
PRESSURE HEAD (m)
-10 -8 -6 -4 -2 0
DEPTH (m)
0.2
0.3
0.4
0.5
0.6
0.7
5/1
5/4
5/9
5/12
5/16
5/19

Figure 2.9 Tensiometer group E pressure heads, November 1987. High amplitude, short duration response to rainfall is characteristic of dry season behavior, particularly in shallower instruments.

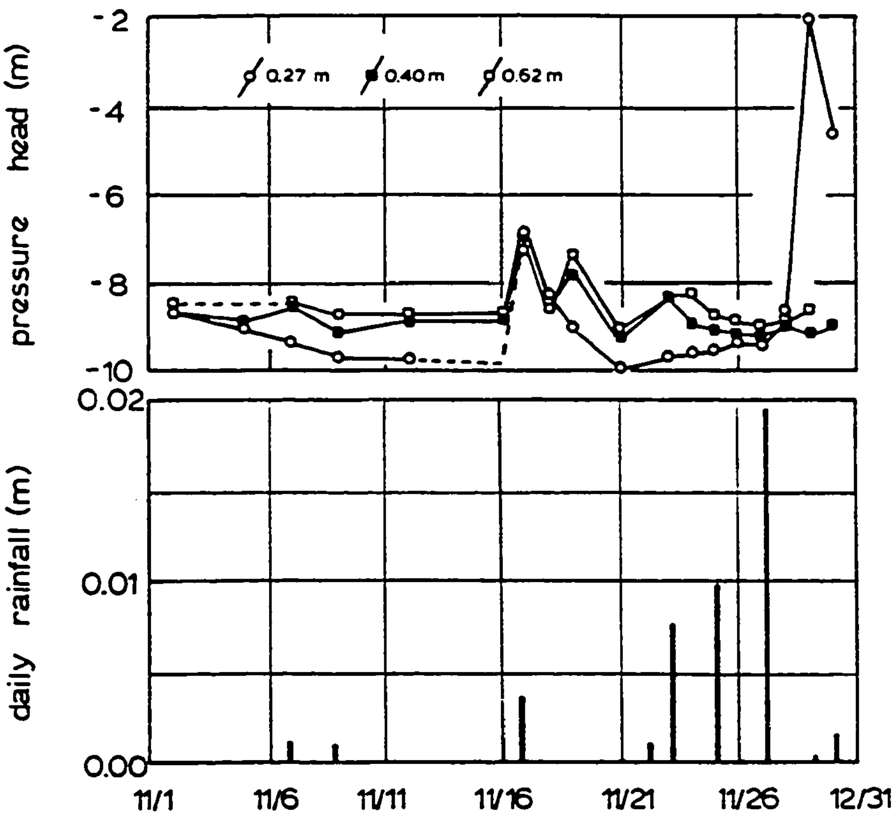
0.27 m
0.40 m
0.62 m
-2
-4
-6
-8
-10
pressure head (m)
0.02
0.01
0.00
daily rainfall (m)
11/1
11/6
11/11
11/16
11/21
11/26
12/31

pressure head increases. Such erratic pressure head fluctuations of up to 1 m are typical of dry season behavior in all of the tensiometer groups, and stands in contrast to the wet season behavior described below.

Field data from mid January through early May 1988, after the colluvium had been moistened by late December rains, are characterized by smaller amplitude fluctuations and higher overall pressure heads (see Figure 2.5). Pressure heads measured with group E tensiometers during the first few days of February 1988, the wettest period observed, are shown in Figure 2.10a. Pressure head in the shallowest tensiometer, 0.22 m below ground surface, increases to nearly atmospheric on February 2 and then falls to its pre-storm level by February 3. The middle two tensiometers may record the passing of a wetting front that crests at a depth of 0.27 m on February 2 and a depth of 0.40 m on February 3. If both crests do indeed represent the same wetting front, downward velocity of the front was on the order of 10^{-6} m/s, an order of magnitude greater than the wetting front velocity estimated during the previous autumn. The deepest tensiometer, 0.62 m deep, also peaks on February 2 and falls somewhat by February 3, but at a pressure head higher than those recorded by the two tensiometers directly above it. A similar plot of total head versus depth (Figure 2.10a) over the same three days shows that the vertical hydraulic gradient decreases with depth, suggesting that some slope-parallel flow must occur at depth in order to maintain continuity. During this time water levels rose from more than 1 m beneath the surface to less than 0.5 m beneath the surface in piezometers P-4 and P-6, which are located at about the same elevation on the hillside as tensiometer group E.

Data from tensiometers located up and down the longitudinal axis of the landslide mass, positioned to document any wave-like downhill flow, show that pressure heads peaked at approximately the same time during rainy periods, and lacked any consistent evidence of head to toe hillside drainage. As an example, during late January and early February 1988, when the greatest rainfall of the study period occurred, pressure heads

Figure 2.10 A) Tensiometer group E total head profiles during early February 1988. B) Tensiometer group E total head and pressure head profiles during early February 1988. In both cases head decreases with depth, requiring that seepage vectors change from vertical to inclined downward.

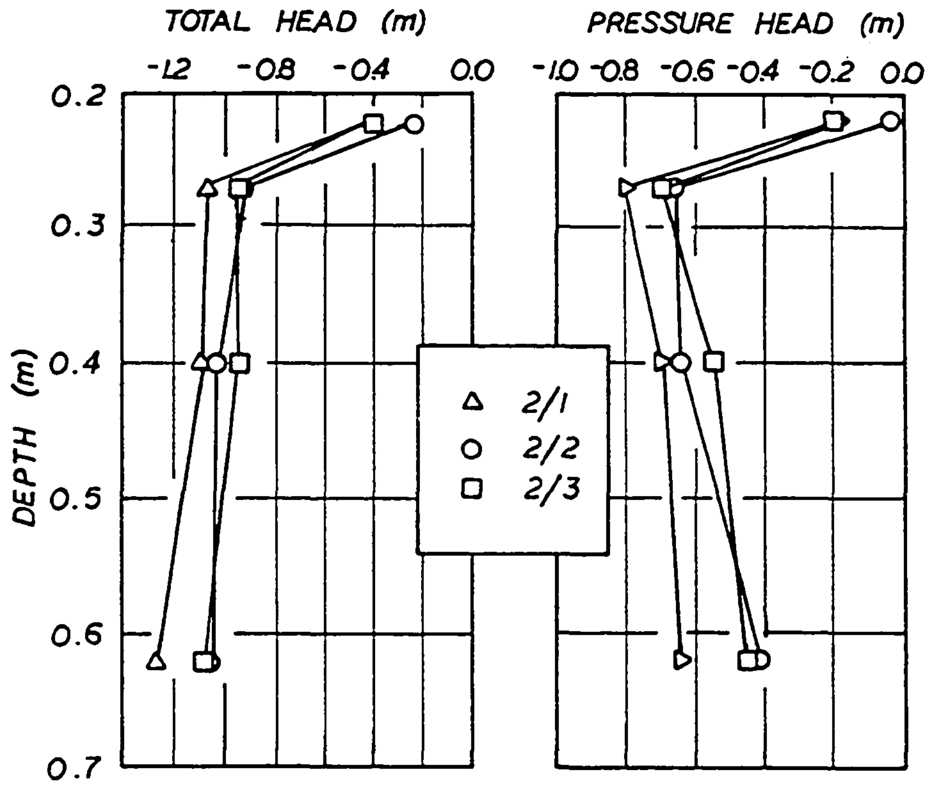
TOTAL HEAD (m)
-1.2
-0.8
-0.4
0.0
PRESSURE HEAD (m)
-1.0
-0.8
-0.6
-0.4
-0.2
0.0
DEPTH (m)
0.2
0.3
0.4
0.5
0.6
0.7
2/1
2/2
2/3

A.

B.

peaked at group B, the highest on the hillside, one day before pressure heads at groups A, C, and E. However, pressure heads at group C, the lowest on the hillside, rose and fell much more suddenly than those in groups A and E, located mid-way up the hillside (Figure 2.11).

DISCUSSION

Field observations described in this chapter suggest that rainfall and evapotranspiration control seasonal hydrologic fluctuations in thin colluvium at the Delhi Pike landslide complex. When temperatures are high and trees are leafed out in late spring through autumn, pressure heads are near the lower limit of mercury manometer tensiometers. Tensiometric response to rainfall is short lived during this time, and only the upper few inches of topsoil and colluvium become moistened during rainfall. After trees lose their leaves, however, several days of steady winter rains are sufficient to thoroughly wet the thin colluvium by infiltration, although not necessarily to saturate it. The same kind of abrupt dry-to-wet transition was also observed by Murdoch (1987) at Delhi Pike in December 1986, so this phenomenon is apparently an annual occurrence. Relatively high, but unsaturated, pressure heads can then be maintained throughout the spring months with only occasional rainfall. Late spring drying of the colluvium occurs only when temperatures rise and large trees are completely leafed out, and proceeds from the ground surface downward. Vertical pressure head gradients are much greater than unity during drying, and must be due to evapotranspiration rather than gravity drainage alone. This dry-wet seasonal dichotomy stands in contrast to the continuously saturated conditions observed in large, persistently active landslide complexes in Oregon (Pyles and others, 1987) and northern California (Iverson and Major, 1987).

Maintenance of relatively high, but unsaturated, pressure heads for days or weeks between spring rainstorms can be explained by a combination of low soil drainage and

Figure 2.11 Longitudinal pressure head variation among tensiometer groups A, B, C, and E during late January and early February 1988. Data are from one tensiometer per group, at a depth of 0.3 to 0.4 m. The pattern of pressure head fluctuations shown is not consistent with the notion of wave-like downhill flow, as discussed in the text.

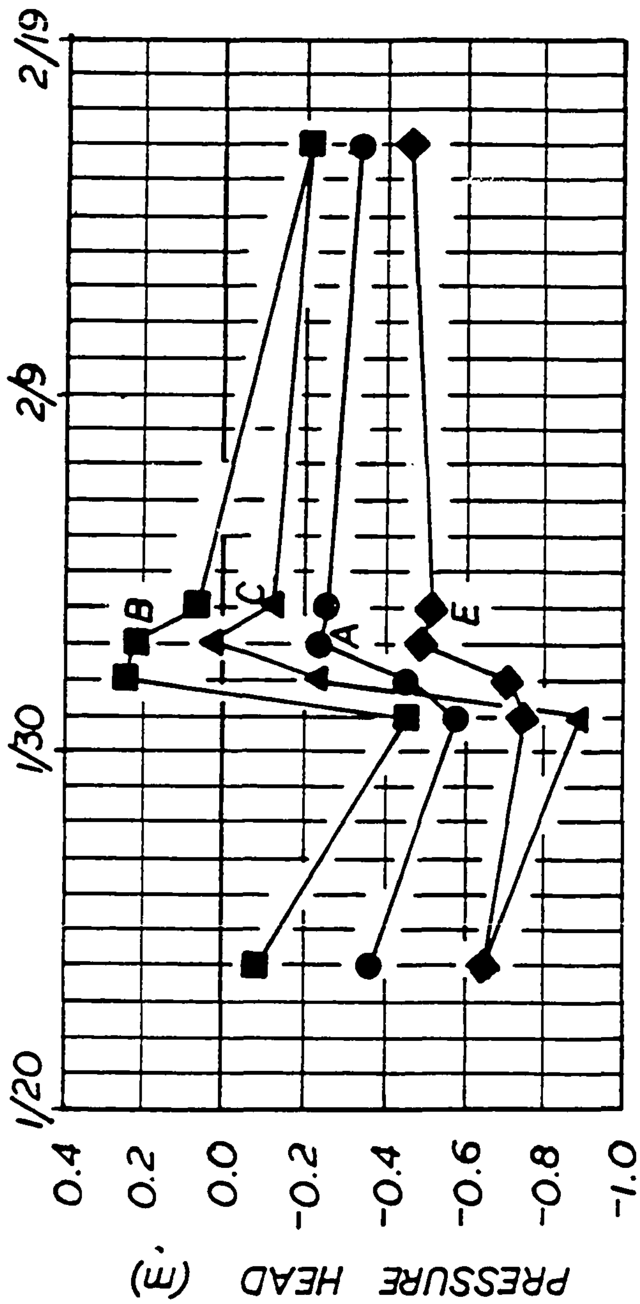

1/20
1/30
2/9
2/19
0.4
0.2
0.0
-0.2
-0.4
-0.6
-0.8
-1.0
PRESSURE HEAD (m)
A
B
C
E

evaporation rates. Hydraulic conductivity of Delhi Pike colluvium at -1 m H_2O pressure head is approximately two orders of magnitude less than saturated hydraulic conductivity (Murdoch, 1987), or about 10^{-7} m s^{-1}, so Darcy's law predicts that slope-parallel flux through a 1 m thick soil layer with uniform pressure head of -1 m H_2O on a 22° hillside should be on the order of 4×10^{-8} m^3 s^{-1}. An order of magnitude estimate of evaporation using the Priestly-Taylor method (Chow and others, 1988, p. 90) shows that losses from an open pan of water on a 25°C day will be about 10^{-7} m^3 s^{-1} m^{-2}. If this rate is integrated over the surface area of a hillside, typically on the order of 10^3 m^2, losses due to evaporation will greatly exceed losses due to gravity drainage (10^{-4} m^3 s^{-1} $\times$ 12 hr. $day^{-1} \approx 4 \times 10^0$ m^3 *vs.* 4×10^{-8} $m^3 s^{-1}$ for 24 hr. $day^{-1} \approx 3 \times 10^{-3}$ m^3).

When evaporation is significant compared to the slope-parallel hydraulic gradient, as discussed in the previous paragraph, the theoretical model developed in Chapter 1 predicts that wave-like downhill flow should not occur. Although this prediction is consistent with the field observations described in this chapter, it is inconsistent with other theoretical (Beven, 1977, 1981, 1982; Hurley and Pantelis, 1985) and laboratory (Anderson and Burt, 1979b) models of hillside flow that do not take evapotranspiration into account. The unsaturated flow model developed by Murdoch (1987) for colluvium at Delhi Pike, however, predicts that post-storm evaporation can redirect near-surface seepage vectors upward although it does not address the problem of wave-like downhill flow.

Even at the rate of evaporation estimated above, however, barely 1% of the saturated water content in a soil with 50% porosity would be removed per day, and neither evaporation nor gravity drainage alone appears capable of significantly drying the hillsides at Delhi Pike, particularly during cool, cloudy weather. It is only when trees become fully leafed out during warm, late spring weather that evapotranspiration increases markedly and pressure heads plunge, which agrees with both experimental and field data data (e.g., Vznuzdaev, 1968; Remson and Randolph, 1958) showing that evapotranspiration can significantly decrease pressure head. Clearly, then, the importance of biological factors on hillside hydrologic budgets can be significant.

The short-term effects of rainfall at Delhi Pike depend on antecedent pressure heads, which has been observed in other field studies (Novakowski and Gillham, 1988; Iverson and Major, 1987; Gillham, 1984) and is also predicted by theoretical models of unsaturated flow (e.g. Philip, 1957; Freeze, 1969). Field observations also show that perched water tables develop only when antecedent pressure heads are greater than -1 m, which provides the low fillable porosity required for rapid water level fluctuations (Chapter 1). Similar behavior was described by Harr (1977), who found that unsaturated pressure heads predominated in a steep, forested slope in western Oregon, but that during storms short-lived saturated zones could develop on top of a low permeability zone at depth.

Perched water tables were localized without any apparent pattern, as in early February 1988. There are at least two possible explanations for this localization. First, consistently saturated areas might be fed by bedrock seeps, as suggested by the consistent baseflow recorded in P-4 between storms and seepage from nearby outcrops. Second, inhomogeneities in the colluvium, particularly large roots and limestone blocks, might control the development of localized perched water tables. Nearby bedrock seeps are only slow trickles, so it seems unlikely that seeps near piezometers would have the artesian head necessary to form perched water tables, but otherwise, there is no compelling evidence to favor one explanation over the other.

The effects of antecedent pressure heads on wetting front shape and velocity, as well as the accumulation of perched water tables, can be illustrated with numerical simulations of the infiltration process using hydraulic parameters typical of Delhi Pike colluvium (see Appendix D). The wetting front shown in Figure 2.12a, with initial uniform pressure head of -5 m H_2O, is very sharp and piston-like. Pressure head near the upper

Figure 2.12 A) Numerical simulation of infiltration/evaporation cycle in typical Delhi Pike colluvium with uniform initial pressure head of -5.0 m. Note distinct wetting front and lack of water table on imperveous lower boundary. B) Numerical simulation of infiltration/evaporation cycle in typical Delhi Pike colluvium with uniform initial pressure head of -0.5 m. Wetting front is much more diffuse than in dry colluvium, and a perched water table accumulates on top of the imperveous boundary.

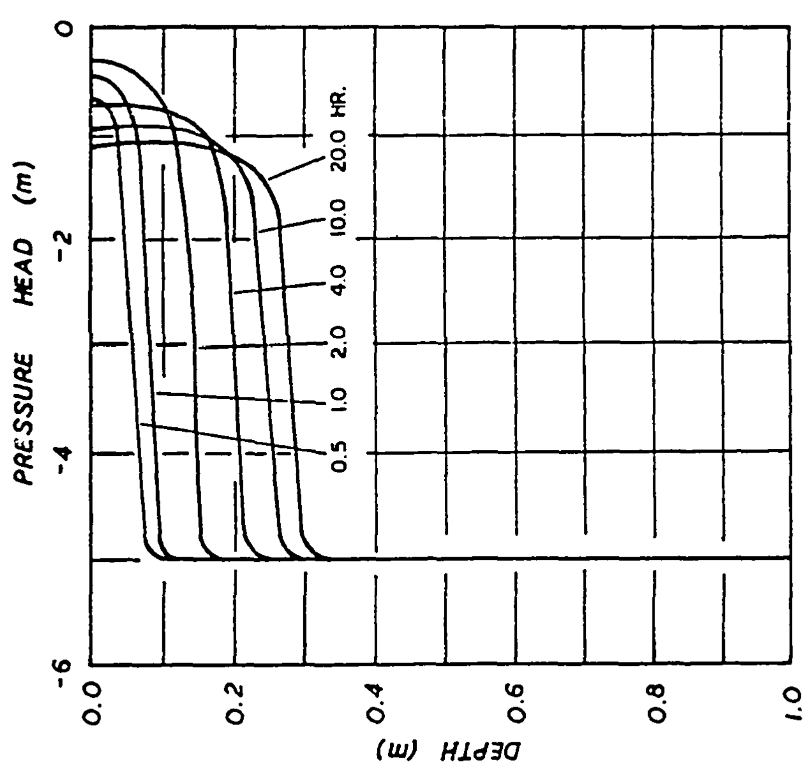
PRESSURE HEAD (m)
DEPTH (m)
-6
-4
-2
0
0.0
0.2
0.4
0.6
0.8
1.0
0.5
1.0
2.0
4.0
10.0
20.0 HR.

A.

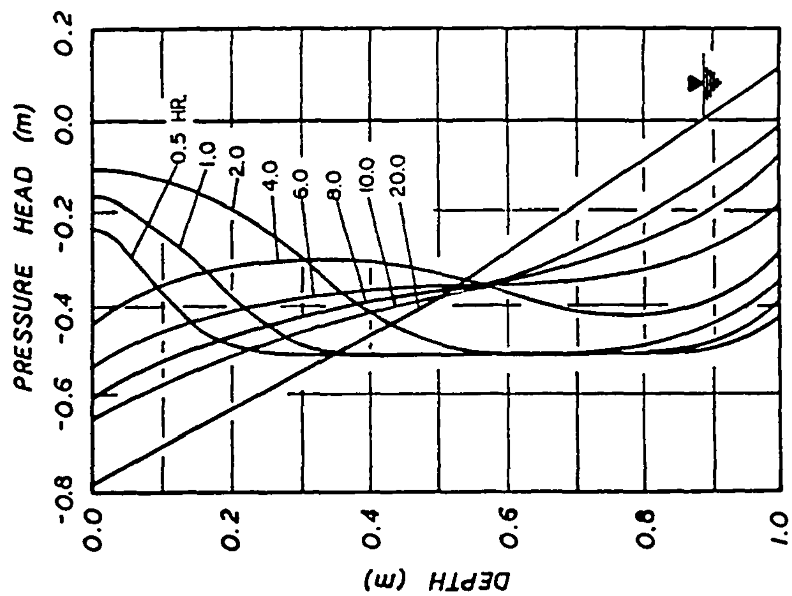
PRESSURE HEAD (m)
DEPTH (m)
-0.8
-0.6
-0.4
-0.2
0.0
0.2
0.0
0.2
0.4
0.6
0.8
1.0
0.5 HR.
1.0
2.0
4.0
6.0
8.0
10.0
20.0

B.

boundary increases while rain is falling, but decreases when the rain has stopped. In contrast, the wetting front in Figure 2.12b, with initial uniform pressure head of -0.5 m H_2O, is diffuse and moves much more rapidly than in dry soil. Most importantly, pressure heads and hydraulic conductivity in the bottleneck beneath the wetting front are high enough to permit downward soil moisture flux and the accumulation of a perched water table even though the upper boundary is unsaturated. The water table is further fed by gravity drainage after the rainfall stops and the pressure head gradient approaches unity. Vertical pressure head gradients that change with depth (Figures 2.9b and 2.10b), along with the development of locally-saturated zones at depth, require curved equipotential lines much the same as in the numerical models of Murdoch (1987) and Beven (1977). Accordingly, there must then be some slope-parallel unsaturated soil moisture flux although, as demonstrated above, low unsaturated hydraulic conductivity makes the magnitude of slope-parallel mass flux negligible.

CHAPTER 3
INSTALLLATION AND EVALUATION OF EXPERIMENTAL DRAINS IN THIN COLLUVIUM AT THE DELHI PIKE LANDSLIDE COMPLEX

INTRODUCTION

The relation between groundwater and landslides in both natural and man-made earth slopes has been known for more than half a century (Terzaghi, 1936) and installation of drains has long been recommended as a generic remedy for landsliding (Terzaghi, 1950). Despite the fact that annual per capita landslide damage costs in the greater Cincinnati area are among the highest in the nation (Bernknopf and others, 1988; Johnson and others, 1987; Fleming and Taylor, 1980), little attention has been given to the use of drains to stabilize landslides in the region. Instead, drilled pier walls (Nethero, 1982) are the preferred method of stabilization for natural hillsides. Therefore, one of the goals of my research was to install drains in a thin colluvium landslide and evaluate their effects on slope stability. In this chapter I describe the design and installation of two experimental drains, and discuss problems that arose when attempting to determine the effectiveness of drains as a method of stabilizing thin colluvium hillsides throughout the area.

ENGINEERED DRAINAGE SYSTEMS

Examples of Drain Installation

Lau (1983) tabulates examples of drilled horizontal drains, vertical drains, drain galleries, and trench drains used for landslide stabilization throughout the world. Of these, drilled horizontal drains are by far the most commonly described method in the engineering literature, and have been used successfully in California (Gedney and Weaver, 1978), Ontario (Lau and Kenney, 1983), British Columbia (Thomson and Mekechuk, 1982), western Oregon (Long, 1985), Tennessee (Moore, 1986; Royster, 1977), eastern Europe (Zaruba and Mencl, 1982), and many other locations (Lau, 1983). LaRochelle and others (1977) describe a combination of drilled horizontal drains and a toe drainage trench used to stabilize a large landslide in Quebec. Other drainage solutions mentioned in the literature include interceptor trench drains, sand or gravel blanket drains, integrated drain and retaining wall systems, and vertical wells with gravity drains (Cedergren, 1975; Veder, 1981).

Despite the widespread and successful use of drains to stabilize slopes throughout the world, there are no published accounts of their use in the Cincinnati area. However, an unpublished City of Cincinnati Department of Public Works report (Montgomery and McGavren, 1953) describes the installation of a drainage gallery in a thick colluvium landslide along the western side of the Mill Creek valley, an area with chronic landslide problems (Johnson and others, 1987). Because the report is neither well-known nor generally available, it is summarized below.

In 1949 colluvium was excavated and reinforced concrete walls, with drained porous backfill, were installed during construction of the Warsaw Avenue entrance ramp for the Sixth Street viaduct extension just west of downtown Cincinnati, Ohio. Offsets of up to 0.02 m between wall panels were observed in June 1950, about ten months after the wall was completed. Montgomery and McGavren write that by March 1951 sidewalks and pavement were buckled and curbs sheared both along Warsaw Avenue and the entrance ramp. Maximum offset of wall panels was about 0.12 m in March 1951 and 0.15 m in June 1951. The report further states that:

> *Throughout this period, the walls had remained substantially plumb, indicating a rather deep-seated earth movement, so that the walls were being shifted laterally without tendency to overturn (Montgomery and McGavren, 1953, p. 4).*

Following a geotechnical investigation that revealed a 100 m long tension crack on the wooded hillside above Maryland Avenue, a trench was constructed to intercept surface water, but the slide continued to move. By March 1953 maximum offset between wall panels had reached approximately 0.18 m. Further exploratory drilling and trenching were undertaken, and slope stability analyses suggested that groundwater seepage through the modified hillside was the cause of instability. Remedial measures considered at the time included reinforcement of the toe, removal of earth at the head of the slide, and installation of drains. Of the three proposed solutions, only drainage was economically feasible due to the great size of the slide. Between October 1952 and March 1953 a 3 m diameter shaft was driven to colluvium-bedrock contact and a 61 m long, 1.5 m diameter tunnel driven along the beneath the west curb line of Maryland Avenue in order to explore the possible effectiveness of drainage. Water levels in observation wells near the tunnel fell 2.4 to 3.1 m immediately after construction was completed, whereas water levels in more distant boreholes remained constant, suggesting that drainage could be an effective means of thick colluvium slope stabilization. Pumping was stopped and water levels allowed to rise after the tunnel was completed on March 1, 1953 and by March 23 water level stood at 1.9 m above the base of the tunnel. Montgomery and McGavren further proposed that a series of vertical sand drains be drilled to feed the horizontal tunnel, and also that an electric sump pump be installed to lift water from the tunnel, but apparently this work was never undertaken.

The Design Process

One approach to drain design is to select a solution and tailor it to individual sites using standardized design procedures, as described by Schmid and Luthin (1964), Kenney and others (1977), Prellwitz (1979), Ram and Chauhan (1986), Stanic (1985). However, this approach requires that conditions in the field agree closely with those assumed in a particular method. For example, all of the references cited immediately above assume that a steady state water table exists. This method of standardized procedure may be effective for man-made slopes and embankments, in which soil composition and geometry are largely a matter of choice, but can cause problems in more complex natural systems.

A second approach to design, the observational method (e.g. Peck, 1969), appears throughout the work of Karl Terzaghi and his followers. First, the seat of the problem is deduced by exploration and measurement. In my study, the problem is destabilizing groundwater. Second, one attempts to characterize the problem. For example, how much water infiltrates from the surface downward and how much seeps from bedrock, and what paths does it follow? Third, a solution is designed on the basis of necessarily incomplete data and continually modified as problems arise during construction. Finally, performance of the design is monitored to detect any problems that may arise during its useful life.

EXPERIMENTAL DRAINS AT DELHI PIKE

The general geology and hydrology of the Delhi Pike landslide complex are summarized in previous chapters of this dissertation, and will not be reiterated here. Only a few piezometer water level records (Fleming and others, 1981) from Delhi Pike were available when this study began in late 1986, but preliminary estimates using 1) infinite slope stability analyses to calculate critical water table height at failure (Appendices F and G), and 2) the method of Schmid and Luthin (1964) to calculate drain spacing necessary to maintain steady-state water level beneath the critical height, suggested that gravel-filled trench drains would have to be spaced on centers of about 1 m in order to stabilize the hillsides at Delhi Pike by lowering water levels throughout the entire slope. If these calculations were correct it would not have been practical to lower water levels throughout the entire hillside. Another possibility was that carefully-located drains might be used to stabilize hillsides by creating localized stable zones that would buttress the rest of the hillside. However, the rapid water level fluctuations described elsewhere (Fleming and others, 1981; Chapter 1 of this dissertation) suggested that conditions in the field might be substantially different from the steady-state conditions assumed in the preliminary calculations, and plans were made to install experimental drains in order to compare field data with theoretical predictions.

Installation

Two gravel-filled trench drains were installed at the Delhi Pike landslide complex in April 1987. Each drain was approximately 10 m long by 1 m wide by 2 m deep, and penetrated weathered bedrock to insure that all seepage would be intercepted. The first drain (drain A) was constructed approximately 80 m WSW of the most intensively-studied portion of the landslide complex to make sure that the drains could be built as designed and, once the construction technique had been tested, the second drain (drain B) was installed in the previously-studied landslide mass (Figure 3.1). Trees and brush were cleared with a tracked front-end loader and trenches excavated with a backhoe. An outlet trench was excavated perpendicular to each drain trench. After the stratigraphy of each trench was recorded, 9.1 m of 0.15 m diameter perforated PVC drain pipe was laid in each trench and connected to 6.10 m of 0.15 m diameter non-perforated discharge pipe. Then, each drain trench was filled with 0.02 m diameter pit-run gravel and sealed along the top and end with colluvium backfill. Some rough regrading was done, but a flat bench and short access drive from abandoned Delhi Pike was left at each of the drain locations, which were later fertilized and seeded to reduce surface erosion. As described in Chapter 2, a series of tensiometers and piezometers were installed around drain B, which was intended to be the primary drain because of the supporting geologic and hydrologic information available (Fleming and others, 1981; Murdoch, 1987; Chapter 1 of this dissertation). Stratigraphy, topography, and drain design at each of the sites, shown in Figure 3.2, is similar with the exception that colluvium at the drain B site seemed more plastic than that at the drain A site and at the time of construction there did not appear to be any geologic

Figure 3.1 Topographic map of the Delhi Pike-Hillside Avenue area showing locations of the two experimental drains described in this Chapter as well as major landslide features. Some landslide features from Fleming and others (1981).

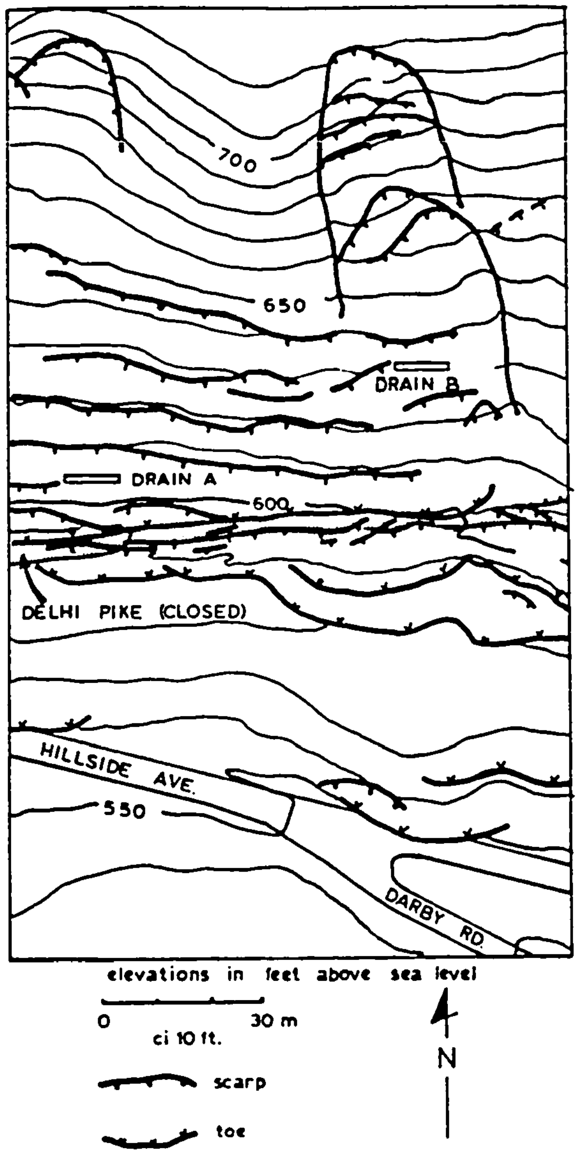
700
650
DRAIN B
DRAIN A
600
DELHI PIKE (CLOSED)
HILLSIDE AVE.
550
DARBY RD.
elevations in feet above sea level
0
30 m
ci 10 ft.
N
scarp
toe

Figure 3.2 Cross-section showing topography, stratigraphy, and drain design at locations A and B.

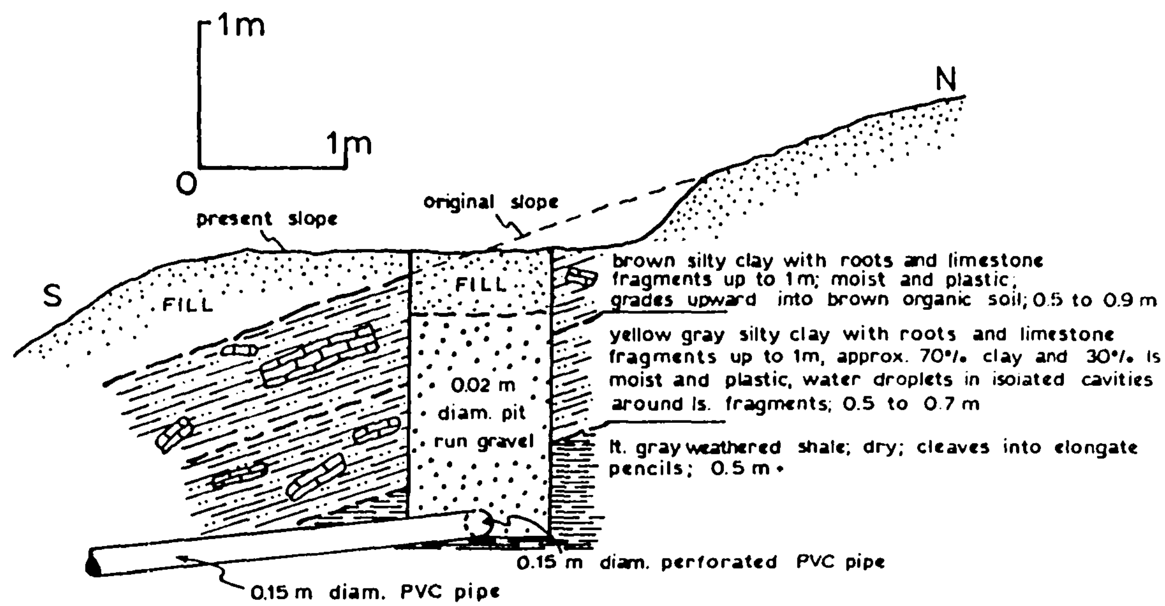
1m
1m
0
N
S
present slope
original slope
FILL
FILL
brown silty clay with roots and limestone fragments up to 1m; moist and plastic; grades upward into brown organic soil; 0.5 to 0.9 m
yellow gray silty clay with roots and limestone fragments up to 1m, approx. 70% clay and 30% ls; moist and plastic, water droplets in isolated cavities around ls. fragments; 0.5 to 0.7 m
lt. gray weathered shale; dry; cleaves into elongate pencils; 0.5 m +
0.02 m diam. pit run gravel
0.15 m diam. perforated PVC pipe
0.15 m diam. PVC pipe

reason why either of the drains might function differently than the other. Each drain took approximately one working day to complete using two equipment operators and myself as a supervisor, and cost approximately $1000.

Results

No discharge from either drain was observed during late spring, summer, or autumn 1987, when tensiometer and piezometer measurements showed the colluvium to be extremely dry and precipitation in the Cincinnati area was well below normal, as described in Chapter 2. The first observed drain discharge occurred during heavy rains the first week of February 1988, when discharge from drain A peaked at about 5×10^{-5} m^3/s. Drain A continued to discharge water during and immediately after storms throughout spring 1988 (Figure 3.3), and discharge volume was generally proportional to rainfall although many small storms produced no discharge and rainfall of at least 0.02 m/day was required to produce discharge greater than a slow trickle. When it became apparent that drain A was discharging water while drain B was not, two piezometers were installed in drain A (P-11) and in undisturbed colluvium approximately 5 m uphill from drain A (P-12) in late March 1988. Both of these piezometers remained dry except during heavy rains, when water level in P-12 rose to 0.55 to 0.66 m beneath ground level (Appendix A).

In contrast to drain A, the outlet pipe from drain B did not discharge any water during the period of record, but water seeped freely from colluvium just downhill from the outlet and quickly filled small holes dug with a spade. Subsequent excavation showed that the outlet pipe was not blocked and contained no sediment, suggesting that it had never carried water. Moreover, the excavations showed that there was no water leaking from or flowing along the outside of the drain B outlet pipe while seepage was occurring downhill.

Piezometer P-7, located in the gravel trench of drain B, never contained water whereas piezometer P-8, approximately 5 m directly uphill from drain B, consistently had a

Figure 3.3 Daily precipitation and discharge from drain A, January through May 1988. No discharge from drain B was recorded during this period.

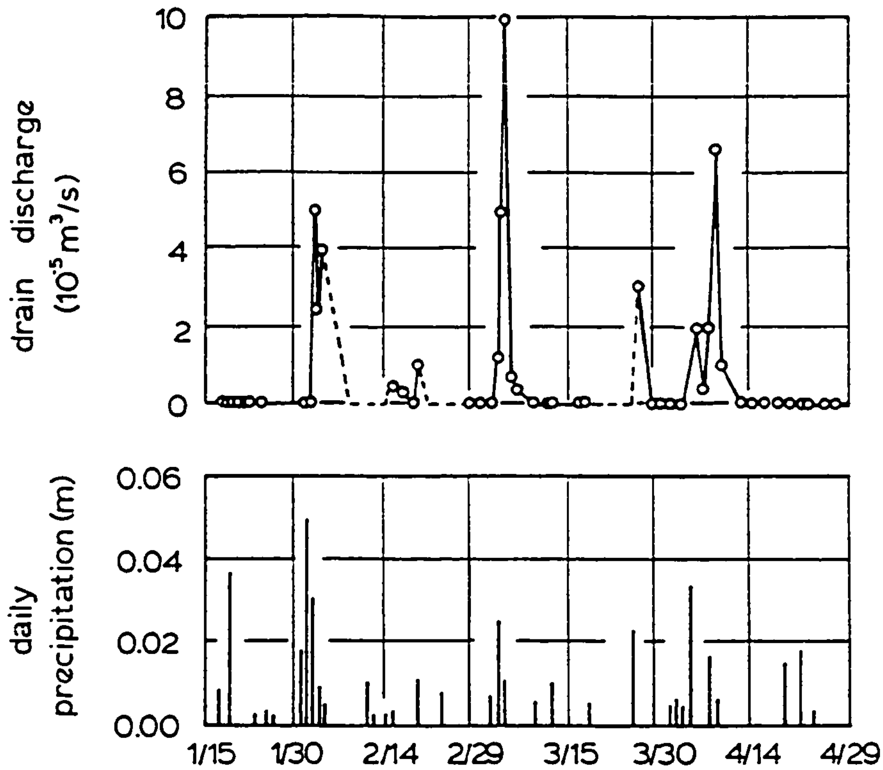
drain discharge
(10^{-5} m^3/s)
10
8
6
4
2
0
daily
precipitation (m)
0.06
0.04
0.02
0.00
1/15
1/30
2/14
2/29
3/15
3/30
4/14
4/29

water level 0.60 to 0.70 m beneath the ground surface, so there was clearly water in the colluvium uphill from the drain (see Figure 3.4 for instrument locations and cross-section, and Appendix A for piezometer and tensiometer data).

Data from tensiometer group D, located about 3 m uphill from drain B, however, suggested that seepage vectors were commonly directed upwards. Another set of tensiometers, group F, was installed between group D and drain B in mid-April 1988 and also showed that seepage vectors immediately uphill from drain B were directed upwards and out of the hillside.

During heavy rains there was some surface runoff from areas of bare colluvium, which were the result of drain construction, but it was impossible to tell whether the runoff was due to rainfall or seepage from the colluvium. Further excavations about 10 m west of tensiometer group D showed that colluvium is only about 0.1 to 0.2 m thick and underlain by limestone slabs up to 0.25 m^2 beneath a landslide scarp. The slabs were all flat-lying and opposite sides of fragments could be easily matched, suggesting that the limestone had not moved far and probably marks the top of weathered bedrock.

DISCUSSION

In light of the field data presented in Chapter 2, it is not surprising that drain performance was erratic and difficult to evaluate. The slope-wide rise and fall of a water table predicted on the basis of preliminary field and and numerical modeling (Chapter 1) was never observed; rather, zones of saturation were highly localized and short-lived. Although rainfall was below normal before and during the early parts of this study, which spanned a period of drought in much of the eastern United States, rainfall levels were normal or above normal during most of spring 1988 (Chapter 2). It is impossible, though, to say how drains would have responded had precipitation been greater during the early phases of this work. Field data from this and other field studies at Delhi Pike during the

Figure 3.4 Cross-section showing topography, instrumentation, and inferred slip surface near drain B. Note that colluvium thins immediately uphill from drain B due to both a natural landslide scarp and excavation during drain construction, causing upward-directed seepage at tensiometer groups D and F.

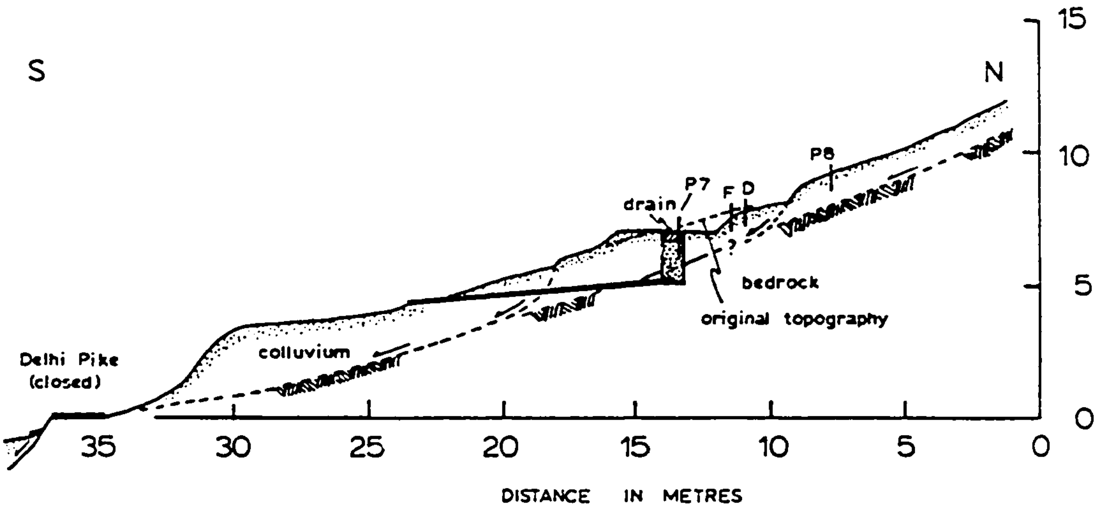
S
N
15
10
5
0
P8
P7
drain
F
D
?
bedrock
original topography
colluvium
Delhi Pike
(closed)
35
30
25
20
15
10
5
0
DISTANCE IN METRES

periods 1979-1981 (A.Ö. Gökce, personal communication) and 1987 (Murdoch, 1987) do combine to show that the hillside has been largely unsaturated for five of the past ten springs, however, so it is safe to say that the occurrence of widespread saturated zones in colluvium at Delhi Pike is not a common occurrence, and the use of drain design formulae based on the requirement of steady-state water tables (e.g. Schmid and Luthin, 1964; Kenney and others, 1977; Prellwitz, 1979; Ram and Chauhan, 1986; Stanic, 1985) under the conditions observed at Delhi Pike is thus inappropriate.

The lack of discharge from drain B poses an interesting problem: Design and construction of drain B was superficially identical to that of drain A. Inspection of the trenches during construction did not find evidence of any significant geological differences between the two drain locations. There were no signs that drain B had become blocked in any way. In short, if there was water flowing into drain B there is no apparent reason why it should not have flowed out of the discharge pipe.

Now the question becomes, why was there no water flowing into drain B?

The most plausible explanation is that surface and subsurface hillside geometry caused water to flow away from drain B. Apparently, the colluvium is thin and rocky near the landslide scarp about 5 m uphill from drain B, as well as beneath the uphill side of the bench cut during drain construction. Examination of Darcy's law

$$Q = -\ K\, \delta H \text{ grad } \Phi \tag{3.1}$$

(where Q is volumetric flux per unit width of soil, Φ is total hydraulic head, and δH is saturated soil thickness) shows that decreasing soil thickness has the same effect as decreasing hydraulic conductivity. In effect, the form of (3.1) dictates that a zone of thin colluvium would deflect flow towards the nearest free surface, where pressure head is atmospheric, in the same way that a zone of low permeability would deflect flow, which explains the upward-directed seepage vectors at tensiometer groups D and F, just uphill from drain B. This can be easily illustrated using the flow net in Figure 3.5, which shows a sloping soil layer with its thickness reduced by one-half across a scarp and underlain by an impermeable substrate. Mass flux across any boundary of a flow net can be calculated using the well-known variation of Darcy's law

$$Q = -K \frac{N_f}{N_d} \delta\Phi \qquad (3.2)$$

where N_f is the number of flow channels (or, one less than the number of streamlines), N_d is the number of equipotential drops along the flow path, and $\delta\Phi$ is the total head decrease along the flow path. Using Q_{in} to represent mass flux into the problem domain above the scarp and Q_{out} to represent mass flux out of the problem domain below the scarp, and assuming the soil to be homogeneous, it follows that

$$\frac{Q_{in}}{Q_{out}} \approx 6$$

because all terms except N_f will cancel. Thus, reduction of colluvium thickness by one-half across a scarp reduces flow by five-sixths and seepage from scarps can be a significant factor in hillside hydrologic budgets.

Drains can remove water from the clayey colluvium at Delhi Pike, which means that they necessarily increase slope stability. But are they an **effective** solution to landslide problems in thin colluvium? In most cases probably not, for two major reasons:

A) Drain location is critical to success when a hillside is not completely saturated. However, soil inhomogeneity, irregular soil thickness, and isolated bedrock seeps (Chapters 1 and 2) make it impractical to predict where drains should be located unless surface seeps or permanently saturated areas can be found. When the soil is not saturated, drains can

Figure 3.5 Steady-state flow net showing deflection of stream lines due to reduction in thickness of a homogeneous, sloping porous layer. Boundary conditions are no flow across the lower impermeable substrate, total head equal to elevation head along the upper boundary, and constant flux Q_{in} and Q_{out} across each end of the problem domain.

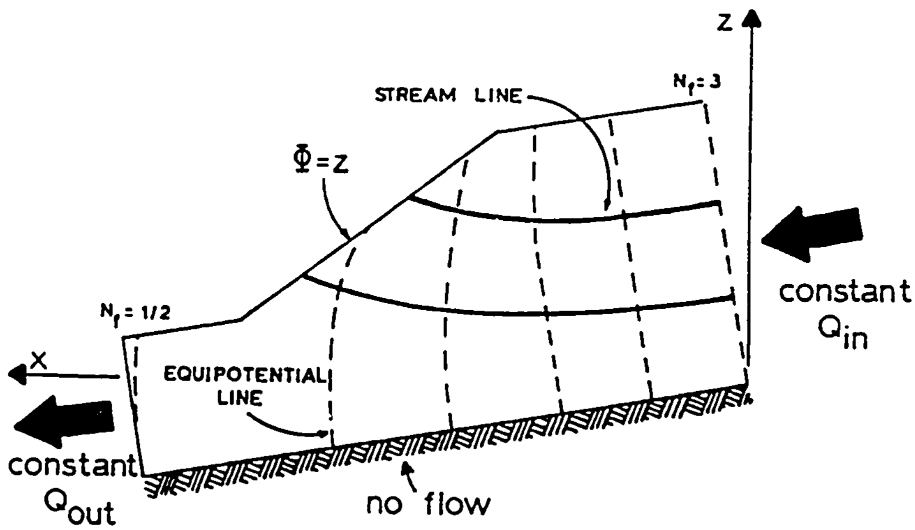
Z
STREAM LINE
$N_f = 3$
$\Phi = z$
constant Q_{in}
$N_f = 1/2$
x
EQUIPOTENTIAL LINE
constant Q_{out}
no flow

actually impede drainage if pressure head in the finer-grained soil is lower than can be supported by the coarser-grained drain material (Bear, 1979, p. 198; Clothier and others, 1977; Hanks and Bowers, 1962), so drains would be useless for stabilizing unsaturated soil.

B) Drain spacing would have to be unacceptably close. There is so much uncertainty about the hydrologic behavior of the thin colluvium hillsides at Delhi Pike that any drain installation would have to be designed under the conservative assumption of complete saturation. In essence, this would require that the entire hillside be excavated and replaced with free-draining material. Such an alternative would both destroy the aesthetic value of natural hillsides and be extremely expensive; while this may be acceptable for large construction projects where extensive re-grading is necessary, it would be unacceptable for most projects.

In conclusion, then, the data described in this chapter suggest that generalized drain design criteria should not be applied to thin colluvium hillsides in the Cincinnati area, and the hydrologic unpredictability of these hillsides makes it impractical to design customized solutions. Although the possible existence of the steady-state water table commonly required by generalized methods cannot be denied, it is clearly not a common occurrence and at this point it is impossible to say how often water levels in hillsides at Delhi Pike are high enough to cause instability. As such, drains do not appear to be an effective means of reducing **thin** colluvium landslide damage costs in the Cincinnati area. However, drainage may still be a viable, though largely untested, alternative for **thick** colluvium landslides in which hydrologic behavior is more predictable.

REFERENCES

Anderson, D.A., Tannehill, J.C., and Pletcher, R.H., 1984, Computational Fluid Mechanics and Heat Transfer: Hemisphere Publ., 599 p.

Anderson, M.G. and Burt, T.P., 1977a, Automatic monitoring of soil moisture conditions in a hillslope spur and hollow: Journal of Hydrology, v. 33, p. 27-36.

Anderson, M.G. and Burt, T.P., 1977b, A laboratory model to investigate the soil moisture conditions on a draining slope: Journal of Hydrology, v. 33, p. 383-390.

Baum, R.L., 1983, Engineering geology and relative slope stability in the area of the Fay Apartments and in part of Mount Airy Forest, Cincinnati, Ohio: unpublished M.S. thesis, Department of Geology, University of Cincinnati, 74 p.

Bear, J., 1972, Dynamics of Fluids in Porous Media: American Elsevier, 764 p.

Bear, J., 1979, Hydraulics of Groundwater: McGraw-Hill, 569 p.

Bernknopf, R.L, Campbell, R.H., Brookshire, D.S., and Shapiro, C.D., 1988, A probabilistic approach to landslide hazard mapping in Cincinnati, Ohio with applications for economic evaluation: Bulletin of the Association of Engineering Geologists, v. 25, p. 39-56.

Beven, K., 1977, Hillslope hydrographs by the finite element method: Earth Surface Processes, v. 2, p. 13-29.

Beven, K., 1981, Kinematic subsurface stormflow: Water Resources Research, v. 17, p. 1419-1424.

Beven, K., 1982, On subsurface stormflow: Predictions with simple kinematic theory for saturated and unsaturated flows: Water Resources Research, v. 18, p. 1627-1633.

Boussinesq, J., 1904, Recherches theoretiques sur l'ecoulement des nappes d'eau infiltrees dans le sol et sur le debit les soures: J. Math. Pures Appl., v. 5, p. 5-78.

Bouwer, H., 1978, Groundwater Hydrology: McGraw-Hill, 480 p.

Boyce, W.E. and DiPrima, R.C., 1977, Elementary Differential Equations and Boundary Value Problems (3rd edition): Wiley, 582 p.

Cedergren, H.R., 1975, Drainage and dewatering, IN H.F. Winterkorn and H.-Y. Fang, editors, Foundation Engineering Handbook: Van Nostrand Rheinhold, p. 221-243.

Chauan, H.S., Schwab, G.O., and Hamdy, M.Y., 1968, Analytical and computer solutions of transient water tables in drainage of sloping lands: Water Resources Research, v. 4, p. 573-579.

Childs, E.C., 1971, Drainage of groundwater resting on a sloping bed: Water Resources Research, v. 7, p. 1256-1263.

Chow, V.T., Maidment, D.R., and Mays, L.W., 1988, Applied Hydrology: McGraw-Hill, 572 p.

Clothier, B.E., Scotter, D.R., and Kerr, J.P., 1977, Water retention in soil underlain by a coarse-textured layer: Theory and a field application: Soil Science, v. 123, p. 392-399.

Croney, D., Coleman, J.D., and Bridge, P.M., 1952, The suction of moisture held in soil and other porous materials: London, HMSO, Road Research Technical Paper No. 24, 42 p.

Day, P.R. and Luthin, J.N., 1956, A numerical solution of the differential equation of flow for a vertical drainage problem: Soil Science Society of America Proceedings, v. 20, p. 443-447.

Douglas, J., Jr., and Jones, B.F., 1963, On predictor-corrector methods for nonlinear parabolic differential equations: Journal of the Society for Industrial and Applied Mathematics (SIAM), v. 11, p. 195-204.

Durrell, R.H., 1961, Geomorphology of the Cincinnati area: Geological Society of America, Guidebook for Field Trips, Cincinnati, p. 219-223.

Ferziger, J.H., 1981, Numerical Methods for Engineering Application: Wiley, 270 p.

Fleming, R.W. and Taylor, F.A., 1980, Estimating the costs of landslide damage in the United States: U.S. Geological Survey Circular 832, 21 p.

Fleming, R.W., Johnson, A.M., and Hough, J.E., 1981, Engineering geology of the Cincinnati area: American Geological Institute, Geological Society of America Cincinnati Field Trip Guidebook, p. 543-570.

Fredlund, D.G., 1977, Slope stability analysis incorporating the effect of soil suction, IN Anderson, M.G. and Richards, K.S., editors, Slope Stability: Wiley & Sons, p. 113-144.

Freeze, R.A., 1969, The mechanism fo natural ground-water recharge and discharge, 1. One-dimensional, vertical, unsteady, unsaturated flow above a recharging or discharging ground-water flow system: Water Resources Research, v. 5, p. 153-171.

Gedney, D.S. and Weber, W.G., Jr., 1978, Design and construction of soil slopes, IN R.L. Schuster and R.J. Krizek, editors, Landslides: Analysis and Control: National Academy of Sciences, p. 172-192.

Gillham, R.W., 1984, The capillary fringe and its effect upon water-table response: Journal of Hydrology, v. 67, p. 307-324.

Guitjens, J.C. and Luthin, J.N., 1965, Viscous model study of drain spacing on sloping land and comparison with mathematical solution: Water Resources Research, v. 1, p. 523-530.

Hanks, R.J. and Bowers, S.A., 1962, Numerical solution of the moisture flow equation for infiltration into layered soils: Soil Science Society of America Proceedings, v. 26, p. 530-534.

Harr, R.D., 1977, Water flux in soil and subsoil on a steep forested slope: Journal of Hydrology, v. 33, p. 37-58.

Havercamp, R. and Vauclin, M., 1981, A comparative study of three forms of the Richards equation used for predicting one-dimensional infiltration in unsaturated soil: Soil Science Society of America Journal, v. 45, p. 13-20.

Havercamp, R., Vauclin, M., Touma, J., Wierenga, P.J., and Vachaud, G., 1977, A comparison of numerical simulation models for one-dimensional infiltration: Soil Science Society of America Journal, v. 41, p. 285-293.

Hurley, D.G. and Pantelis, G., 1985, Unsaturated and saturated flow through a thin porous layer on a hillslope: Water Resources Research, v. 21, p. 821-824.

Hvorslev, M.J., 1951, Time lag and soil permeability in groundwater observations: Vicksburg, Mississippi, United States Army Corps of Engineers Waterways Experiment Station Bulletin 36, 48 p.

Iverson, R.M. and Major, J.J., 1987, Rainfall, ground-water flow, and seasonal movement at Minor Creek landslide, northwestern California: Physical interpretation of empirical relations: Geological Society of America Bulletin, v. 99, p. 579-594.

Janbu, N., 1973, Slope stability computations, IN R.C. Hirschfeld and S.J. Poulos, editors, Embankment-Dam Engineering (Casagrande Volume): Wiley-Interscience, p. 47-86.

Johnson, A., Lowell, T., Nash, D., Cruikshank, K., Haneberg, W., Reistenberg, M., Neavel, K., Harrar, W., Olson, R., Savage, K., Rosemeyer, D., and Spurling, W., 1987, Report and recommendations on maintenance and repair of deteriorating retaining walls and streets damaged by landslides, City of Cincinnati: unpublished report, Infrastructure Commission, City of Cincinnati, 48 p.

Karadi, G., Krizek, R.J., and Elnaggar, H., 1968, Unsteady seepage flow between fully penetrating trenches. Journal of Hydrology, v. 6, p. 417-430.

Keefer, D.K., Wilson, R.C., Mark, R.K., Brabb, E.E., Brown, W.M., Ellen, S.D., Harp, E.L., Wieczorek, G.F., Alger, C.S., and Zatkin, R.S., 1987, Real-time landslide warning during heavy rainfall: Science, v. 238, p. 921-925.

Kenney, T.C., Pazin, M. and Choi, W.S., 1977, Design of horizontal drains for soil slopes: Journal of the Geotechnical Engineering Division, American Society of Civil Engineers, v. 103, p. 1311-1323.

Klute, A., Scott, E.J., and Whisler, F.D., 1965, Steady state water flow in a saturated inclined soil slab: Water Resources Research, v. 1, p. 287-294.

LaRochelle, P., Lefebvre, G., and Bilodeau, P.M., 1977, The stabilization of a slide in Saint-Jerome, Lac Saint-Jean: Canadian Geotechnical Journal, v. 14, p. 340-356.

Lau, K.C. and Kenney, T.C., 1984, Horizontal drains to stabilize clay slopes: Canadian Geotechnical Journal, v. 21, p. 241-249.

Lau, K.C., 1983, Horizontal drains in clay slopes: unpublished Ph.D. dissertation, University of Toronto, 340 p.

Lerch, N.K., Hale, W.F., and Lemaster, D.D., 1982, Soil Survey of Hamilton County, Ohio: U.S. Department of Agriculture, Soil Conservation Service, 219 p. + maps.

Lighthill, M.J. and Whitham, G.B., 1955, On kinematic waves. I. Flood movement in long rivers: Proceedings of the Royal Society, Series A, v. 229, p. 281-316.

Long, M.T., 1985, Camp Five slide-- exploration, design, and construction of a horizontal drain solution: unpublished report, U.S. Department of Agriculture, Willamette National Forest, Geotechnical Group, 20 p.

McTigue, D.F., Wilson, R.K., and Nunziato, J.W., 1983, An effective stress principle for partially saturated granular media, IN J.T. Jenkins and M. Satake, editors, Mechanics of Granular Materials: New Models and Constitutive Relations: Elsevier Science Publishers B.V., p. 195-210.

Miller, J.E., 1984, Basic Concepts of Kinematic Wave Models: U.S. Geological Survey Professional Paper 1302, 29 p.

Mls, J., 1987, A numerical solution of infiltration: Transport in Porous Media, v. 2, p. 19-30.

Montgomery, T.J. and McGavren, S.A., 1953, Sixth Street viaduct extension: Report on history and present status of incipient slide above Warsaw Avenue inbound ramp: unpublished report, City of Cincinnati, Department of Public works, Division of Engineering, 9 p + figures.

Moore, H.L, 1986, Wedge failures along Tennessee highways in the Appalachian region: Their occurrence and correction: Bulletin of the Association of Engineering Geologists, v. 23, p. 441-460.

Murdoch, L.C., III, 1987, Pore-water pressures and unsaturated flow during infiltration in colluvial soils at the Delhi Pike landslide, Cincinnati, Ohio: unpublished M.S. thesis, Department of Civil and Environmental Engineering, University of Cincinnati, 133 p.

National Oceanic and Atmospheric Administration, 1987, Monthly Climatic Data for the World: v. 40.

National Oceanic and Atmospheric Administration, 1988, Monthly Climatic Data for the World: v. 41.

Nethero, M.F., 1982, Slide control by drilled pier walls: Proceedings of Conference on Application of Walls to Landslide Control Problems, Las Vegas, Nevada, American Society of Civil Engineers, p. 61-76.

Novakowski, K.S. and Gillham, R.W., 1988, Field investigations of the nature of water-table response to precipiation in shallow water-table environments: Journal of Hydrology, v. 97, p. 23-32.

O'Neil, P.V., 1983, Advanced Engineering Mathematics: Wadsworth, 1108 p.

Peck, R.L, 1969, Advantages and limitations of the observational method: Geotechnique, v. 19, p. 171-187.

Philip, J.R., 1957, The theory of infiltration, 3: Soil Science, v. 84, p. 163-178.

Prellwitz, R.W., 1979, Analysis of parallel drains for highway cut-slope stabilization: Subdrainage and Soil Moisture, National Academy of Sciences Transportation Research Record 705, p. 1-7.

Press, W.H., Flannery, B.P., Teukolsky, S.A., and Vetterling, W.T., 1986, Numerical Recipes: Cambridge, 818 p.

Pyles, M.R., Mills, K., and Saunders, G., 1987, Mechanics and stability of the Lookout Creek earth flow: Bulletin of the Association of Engineering Geologists, v. 24, p. 267-280.

Ram, S. and Chauan, H.S., 1987, Drainage of sloping lands with constant replenishment: Journal of Irrigation and Drainage Engineering, American Society of Civil Engineers, v. 113, p. 213-223.

Remson, I. and Randolph, J.R., 1958, Root growth near tensiometer cups as a cause of diurnal fluctuations of readings: Soil Science, v. 85, p. 167-171.

Remson, I., Hornberger, G.M., and Molz, F.J., 1971, Numerical Methods in Subsurface Hydrology: Wiley-Interscience, 389 p.

Royster, D.L, 1977, Some observations on the use of horizontal drains in the correction and prevention of landslides: 28th Annual Highway Geology Symposium, Sioux City, South Dakota, 56 p.

Schmid, P. and Luthin, J., 1964, The drainage of sloping lands: Journal of Geophysical Research, v. 69, p. 1525-1529.

Skempton, A.W., 1964, Long-term stability of clay slopes: Geotechnique, v. 14, p. 77-102.

Skempton, A.W., 1985, Residual strength of clays in landslides, folded strata, and the laboratory: Geotechnique, v. 35, p. 3-18.

Stanic, B., 1985, Influence of drainage trenches on slope stability: Journal of the Geotechnical Engineering Division, American Society of Civil Engineers, v. 110, p. 1624-1636.

Teller, J.T., 1973, Preglacial (Teays) and early glacial drainage in the Cincinnati area, Ohio, Kentucky, and Indiana: Geological Society of America Bulletin, v. 84, p. 3677-3688.

Terzaghi, K., 1923, Die Berechnung der Durchlassigkeitziffer des Tones aus dem Verlauf der hydrodynamischen Spannungserscheinungen: Akademie der Wissenschaften Wien, Sitzubungsberichte, Mathematisch-naturwissenschaftklasse, Abt. IIA, 132 Bd., s. 125-138.

Terzaghi, K., 1936, Stability of slopes on natural clay: Proceedings 1st International Conference on Soil Mechanics and Foundation Engineering, Cambridge, Massachusetts, v. 1, p. 161-165.

Terzaghi, K., 1950, Mechanics of landslides, IN S. Paige, chairman, Application of Geology to Engineering Practice (Berkey Volume): Geological Society of America, p. 83-123.

Thomson, S. and Mekechuk, J., 1982, A landslide in glacial lake clays in central British Columbia: Canadian Geotechnical Journal, v. 19. p. 296-306.

Towner, G.D., 1975, Drainage of groundwater resting on a sloping bed with uniform rainfall: Water Resources Research, v. 11, p. 144-147.

USDA Forest Service, 1987, An Introduction to Probabilistic Analysis for Geotechnical Engineering Applications and Decision Making: unpublished notes from Geotechnical Engineering Training Session, 10-11 March 1987, Moscow, Idaho.

Veder, C., 1981, Landslides and Their Stabilization (translated by E. Jahn): Springer-Verlag, p. 73-180.

Vznuzdaev, N.A., 1968, Consumption of water by plants depending on the negative pressure of the soil water: 9th International Congress of Soil Science Transactions, v. 1, p. 109-116.

Wang, H.F. and Anderson, M.P., 1982, Introduction to Groundwater Modeling: Freeman, 237 p.

Wong, J., 1977, The design of a system for collecting leachate from a lined landfill site: Water Resources Research, v. 13, p. 404-410.

Zaruba, Q. and Mencl, V., 1982, Landslides and Their Control (2nd edition): Elsevier, 324 p.

APPENDIX A

TENSIOMETER, PIEZOMETER, DRAIN DISCHARGE, AND RAINFALL DATA

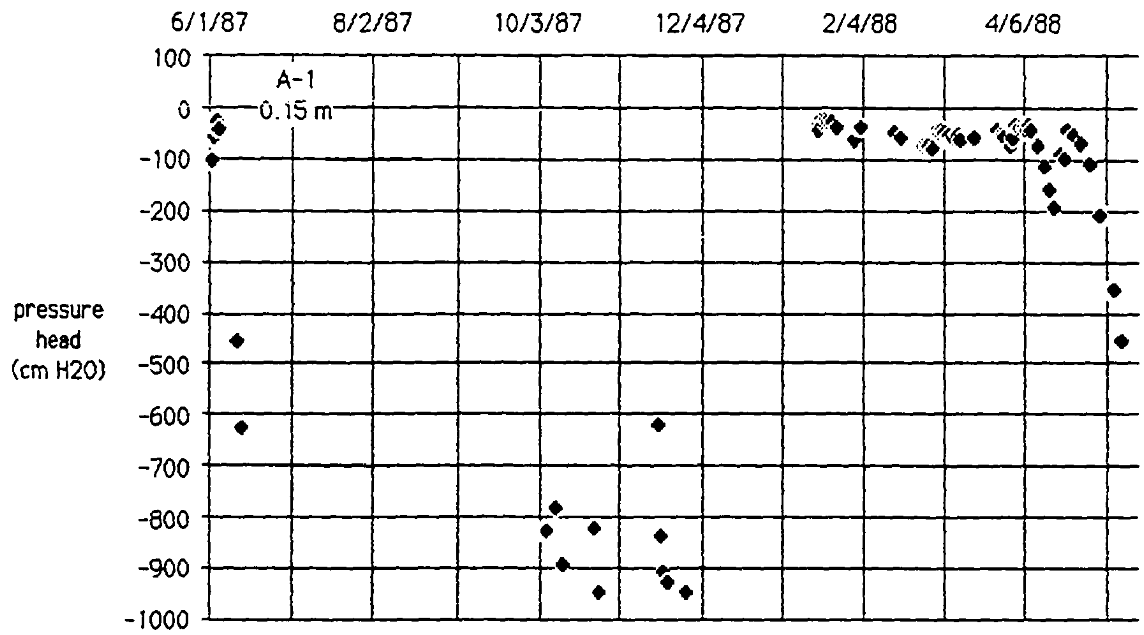
6/1/87
8/2/87
10/3/87
12/4/87
2/4/88
4/6/88
A-1
0.15 m
100
0
-100
-200
-300
-400
-500
-600
-700
-800
-900
-1000
pressure
head
(cm H2O)

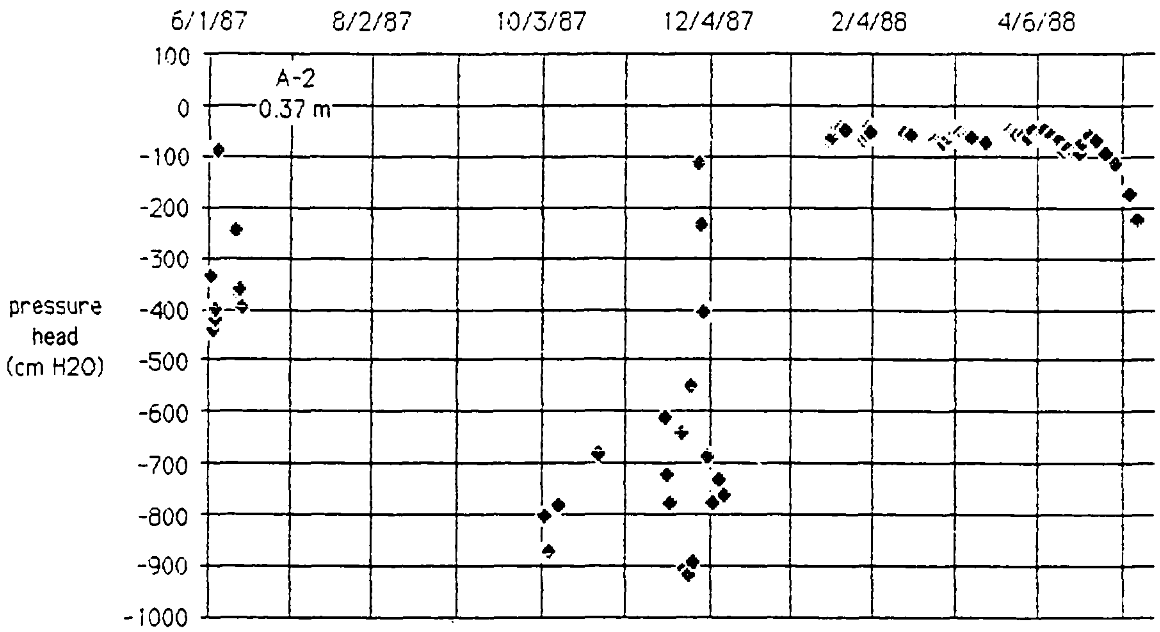

6/1/87
8/2/87
10/3/87
12/4/87
2/4/88
4/6/88
100
0
-100
-200
-300
-400
-500
-600
-700
-800
-900
-1000
A-2
0.37 m
pressure
head
(cm H2O)

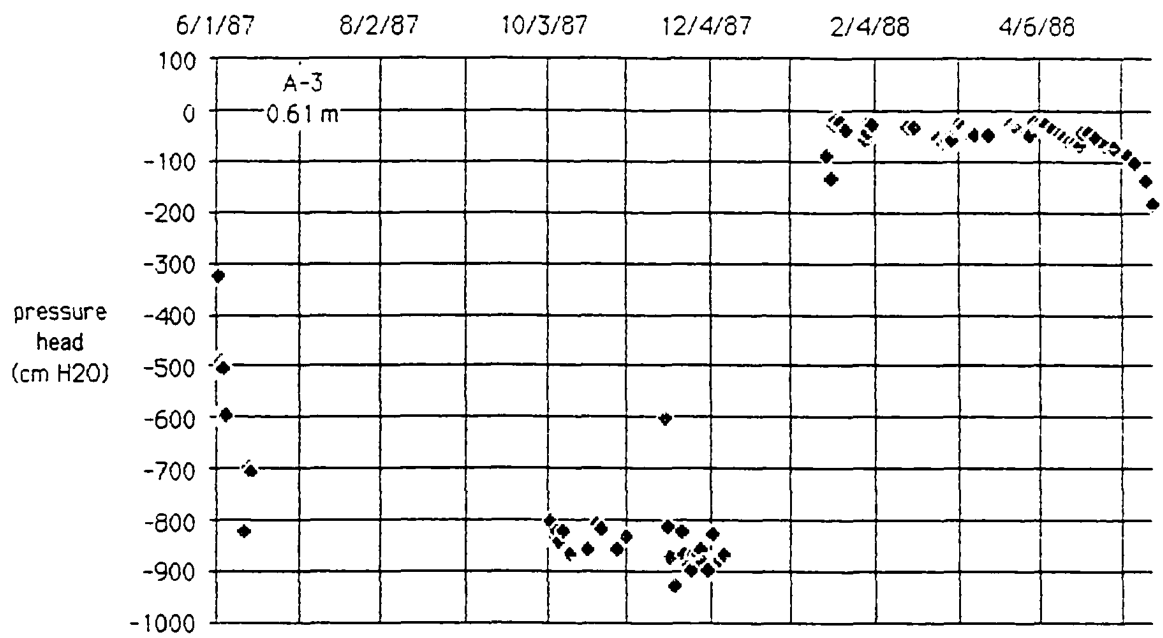
6/1/87
8/2/87
10/3/87
12/4/87
2/4/88
4/6/88
A-3
0.61 m
pressure
head
(cm H20)
100
0
-100
-200
-300
-400
-500
-600
-700
-800
-900
-1000

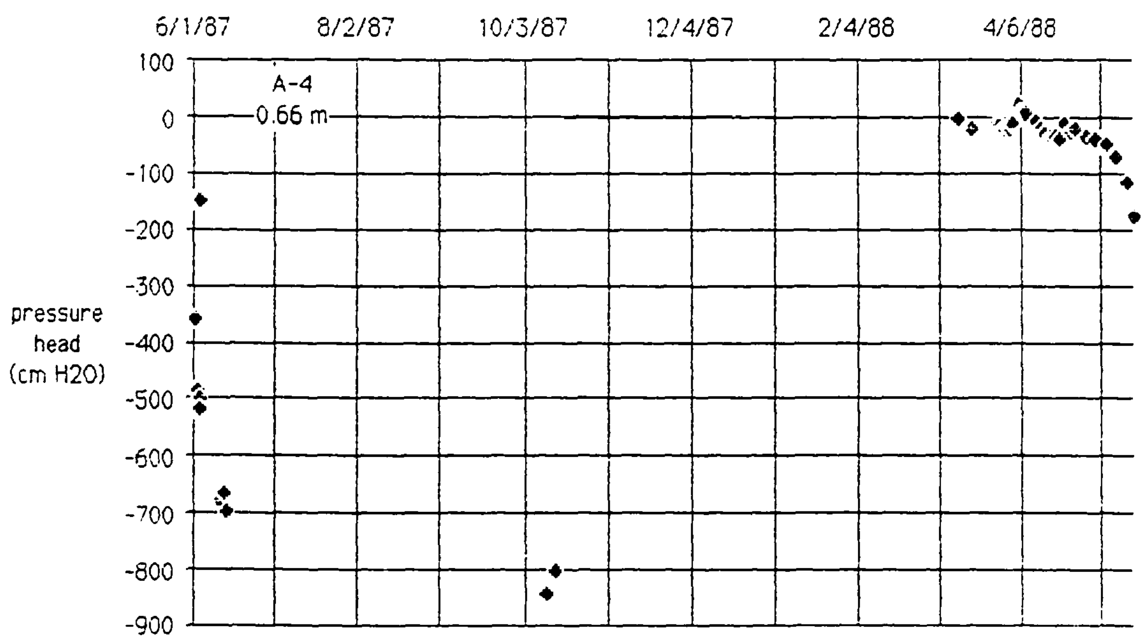
6/1/87
8/2/87
10/3/87
12/4/87
2/4/88
4/6/88
100
0
-100
-200
-300
-400
-500
-600
-700
-800
-900
A-4
0.66 m
pressure
head
(cm H2O)

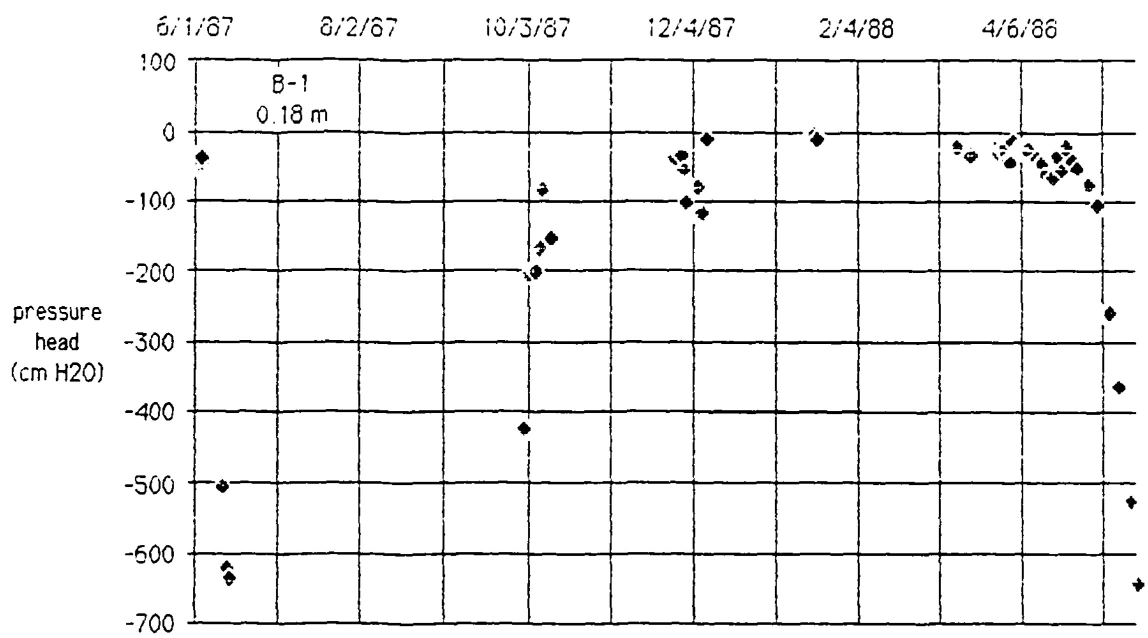
6/1/87
8/2/87
10/3/87
12/4/87
2/4/88
4/6/88
B-1
0.18 m
pressure
head
(cm H2O)
100
0
-100
-200
-300
-400
-500
-600
-700

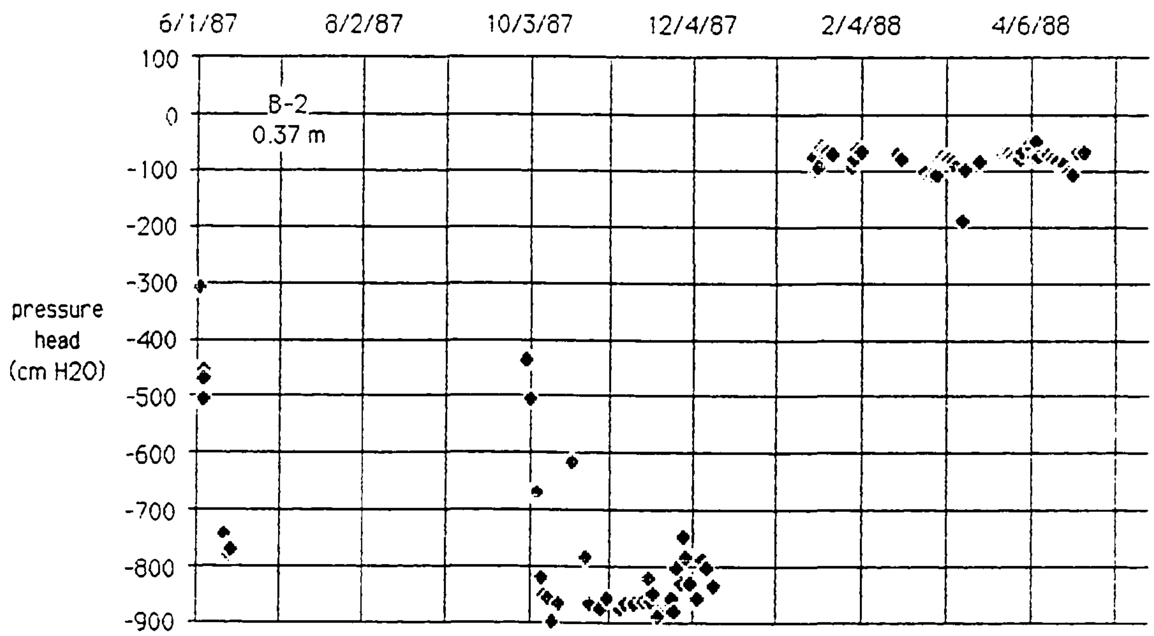

6/1/87
8/2/87
10/3/87
12/4/87
2/4/88
4/6/88
100
0
-100
-200
-300
-400
-500
-600
-700
-800
-900
pressure head (cm H2O)
B-2
0.37 m

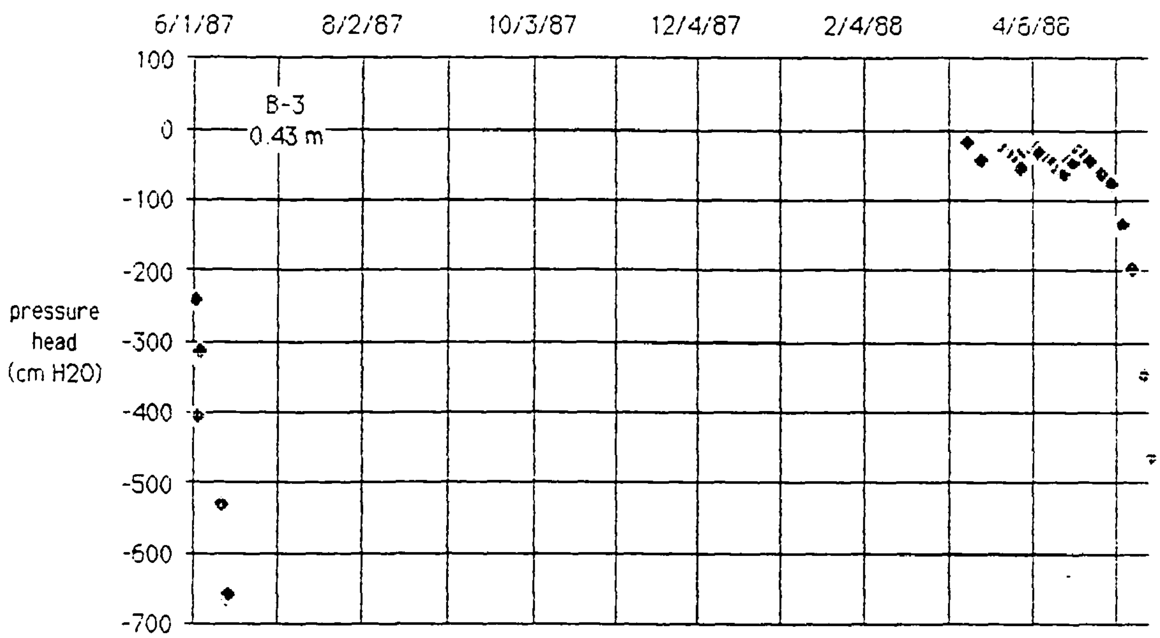
6/1/87
8/2/87
10/3/87
12/4/87
2/4/88
4/6/88
100
0
-100
-200
-300
-400
-500
-600
-700
pressure head (cm H2O)
B-3
0.43 m

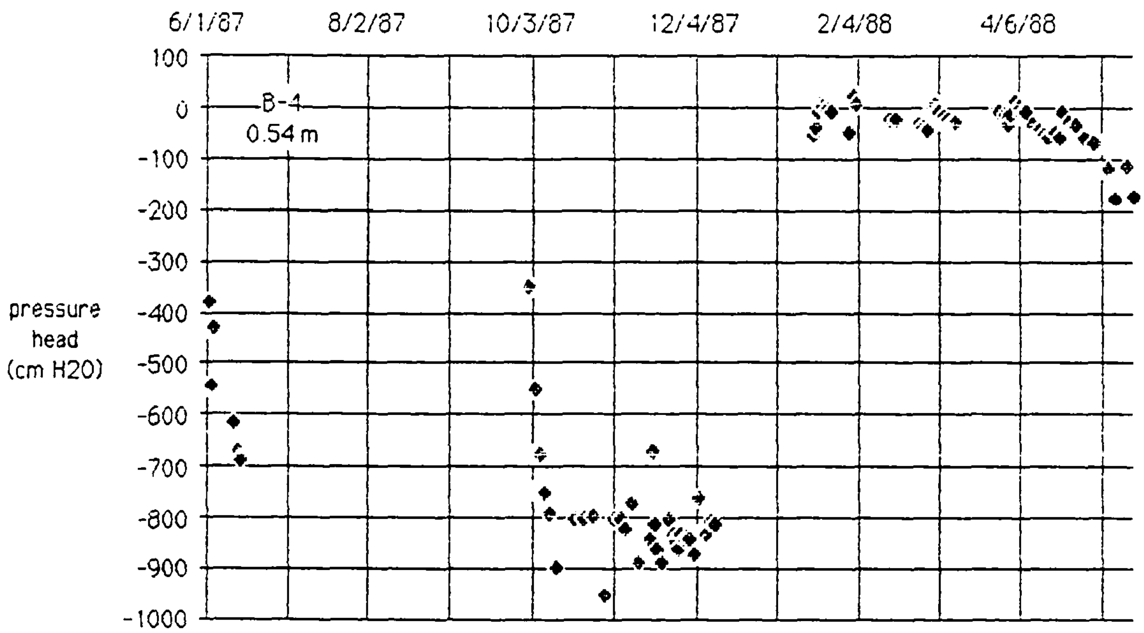
6/1/87
8/2/87
10/3/87
12/4/87
2/4/88
4/6/88
100
0
-100
-200
-300
-400
-500
-600
-700
-800
-900
-1000
pressure
head
(cm H20)
B-4
0.54 m

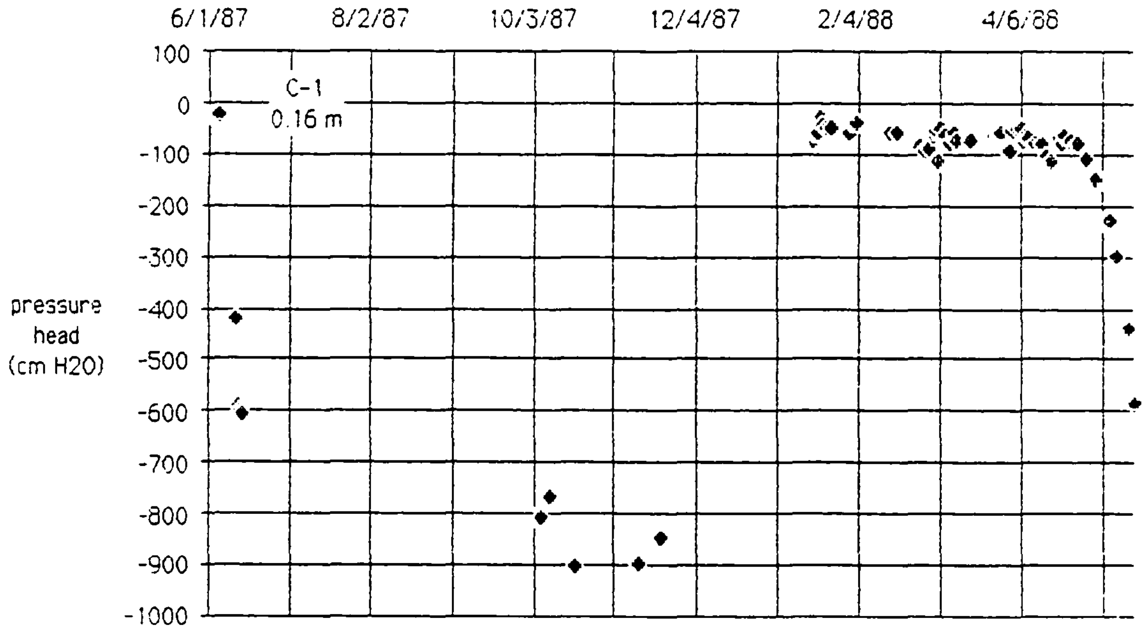
6/1/87
8/2/87
10/3/87
12/4/87
2/4/88
4/6/88
100
0
-100
-200
-300
-400
-500
-600
-700
-800
-900
-1000
pressure head (cm H20)
C-1
0.16 m

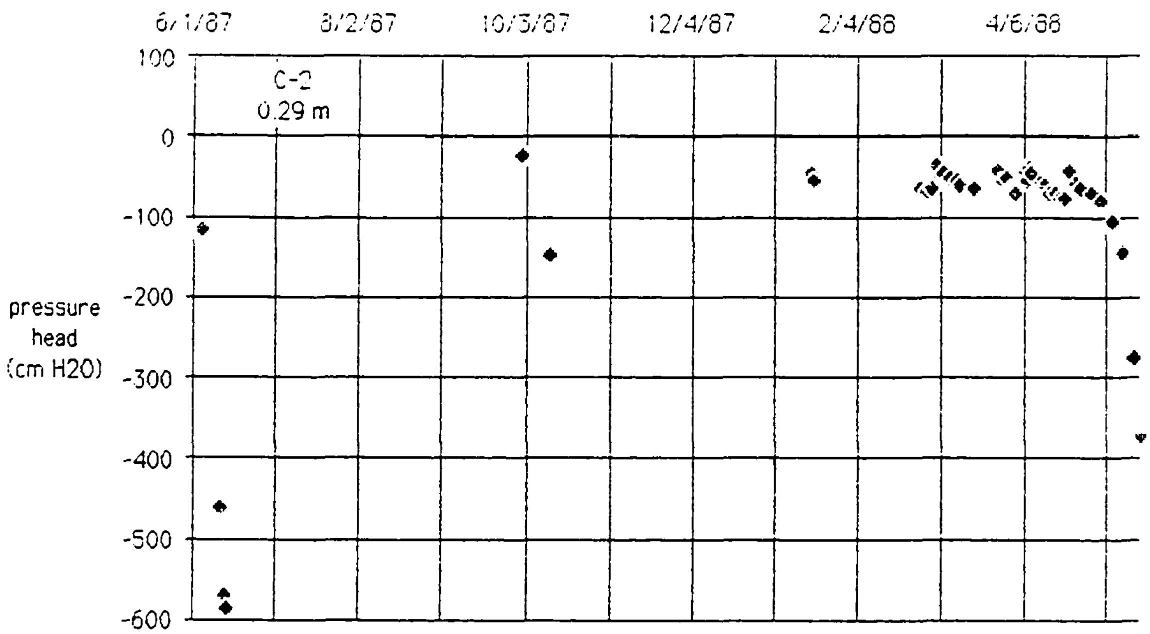
6/1/87
8/2/87
10/3/87
12/4/87
2/4/88
4/6/88
C-2
0.29 m
pressure
head
(cm H2O)
100
0
-100
-200
-300
-400
-500
-600

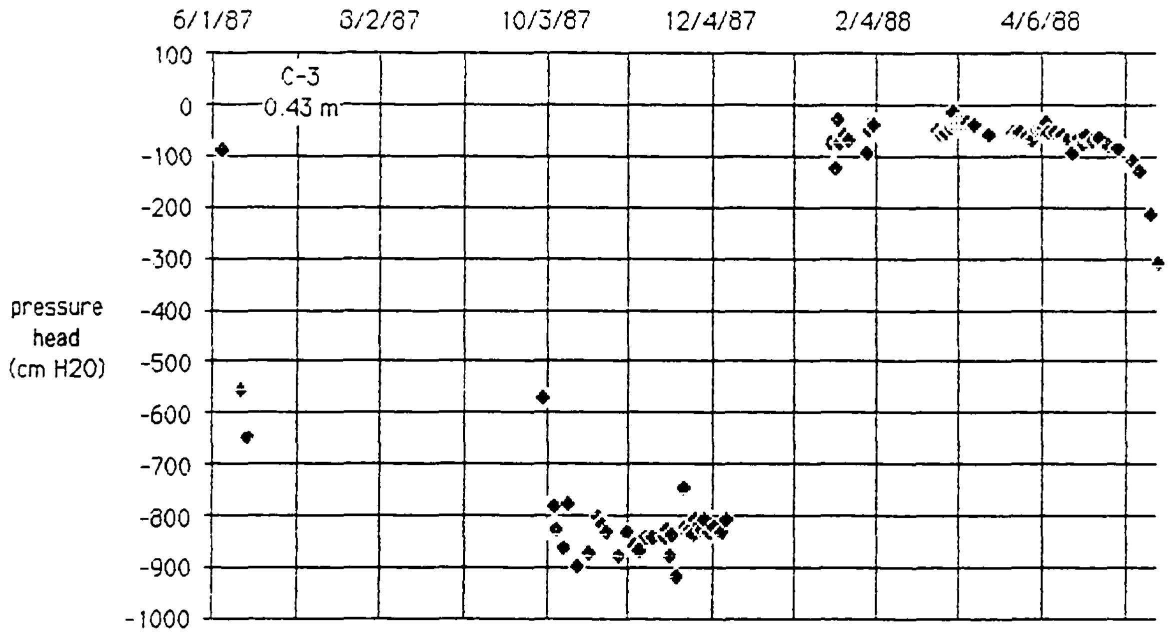

6/1/87
8/2/87
10/3/87
12/4/87
2/4/88
4/6/88
C-3
0.43 m
100
0
-100
-200
-300
-400
-500
-600
-700
-800
-900
-1000
pressure
head
(cm H20)

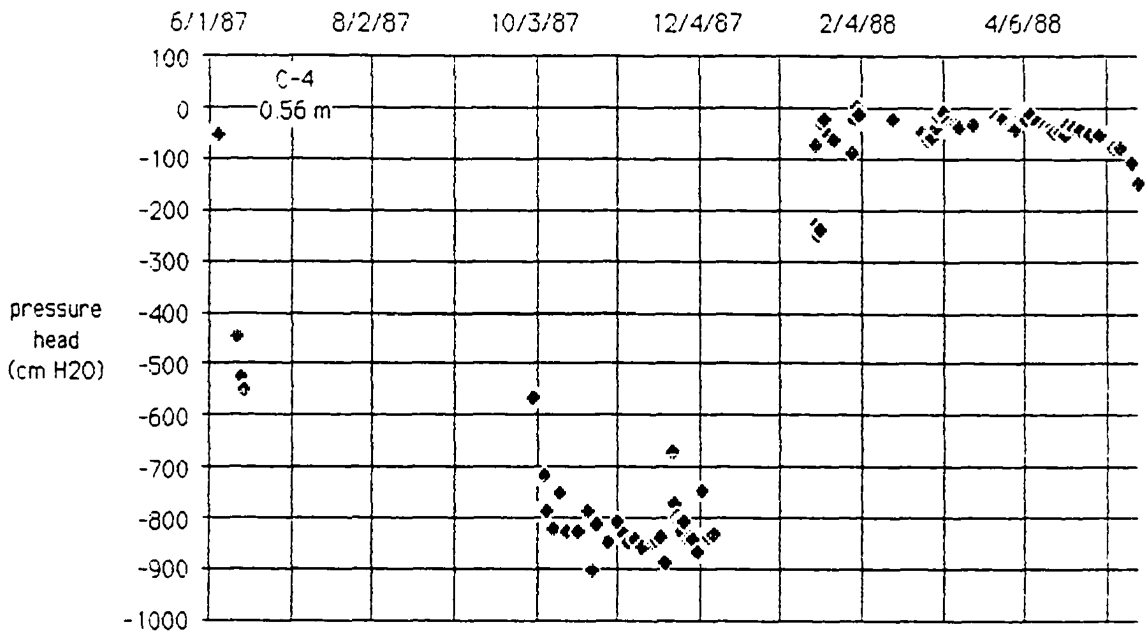
6/1/87
8/2/87
10/3/87
12/4/87
2/4/88
4/6/88
C-4
0.56 m
100
0
-100
-200
-300
-400
-500
-600
-700
-800
-900
-1000
pressure
head
(cm H2O)

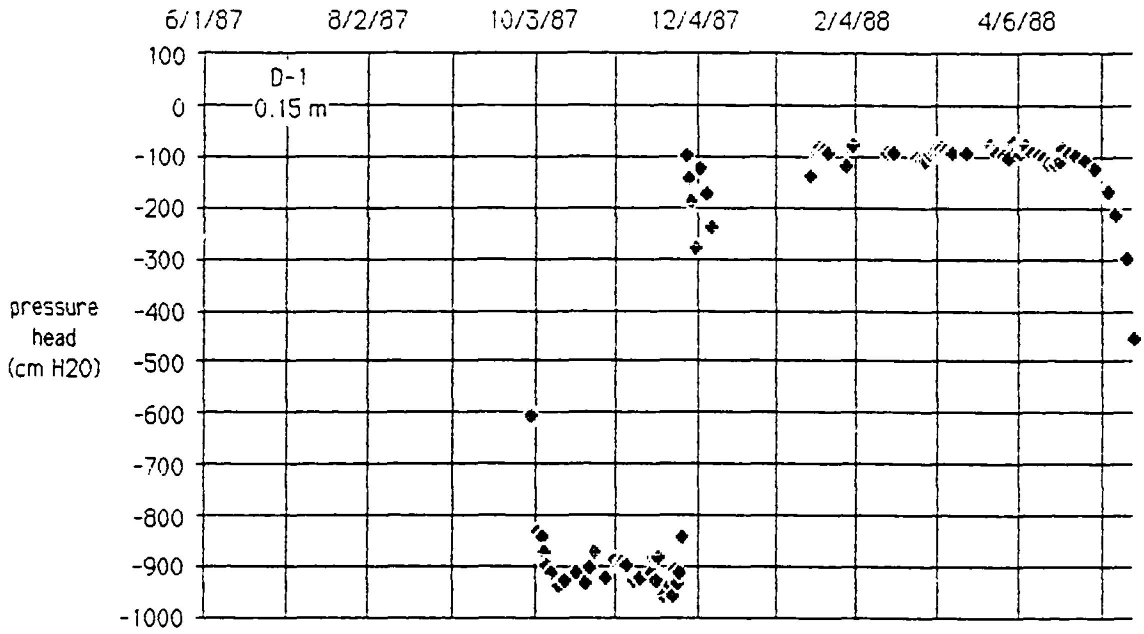
6/1/87
8/2/87
10/3/87
12/4/87
2/4/88
4/6/88
100
0
-100
-200
-300
-400
-500
-600
-700
-800
-900
-1000
pressure
head
(cm H20)
D-1
0.15 m

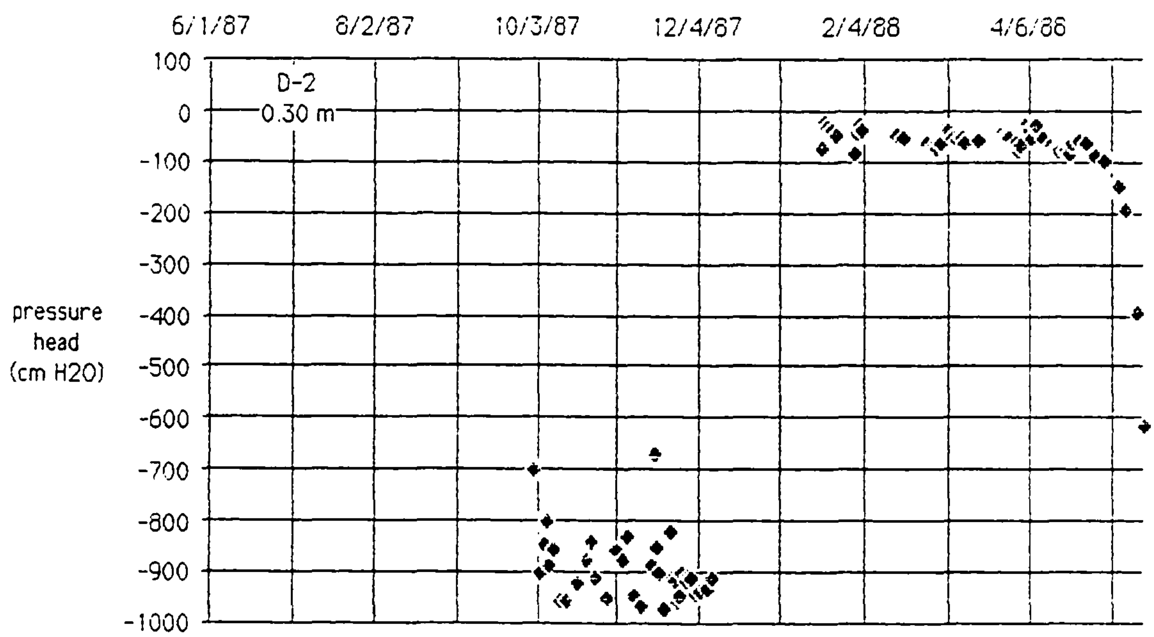

6/1/87
8/2/87
10/3/87
12/4/87
2/4/88
4/6/88
100
0
-100
-200
-300
-400
-500
-600
-700
-800
-900
-1000
pressure head (cm H2O)
D-2
0.30 m

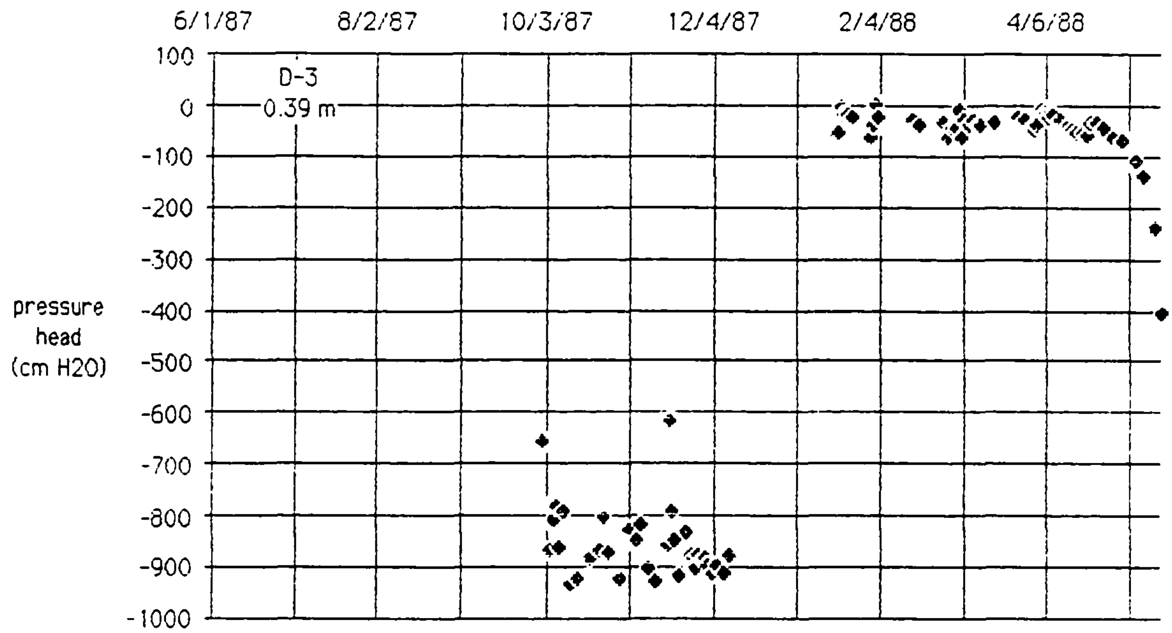
6/1/87
8/2/87
10/3/87
12/4/87
2/4/88
4/6/88
100
0
-100
-200
-300
-400
-500
-600
-700
-800
-900
-1000
pressure head (cm H2O)
D-3
0.39 m

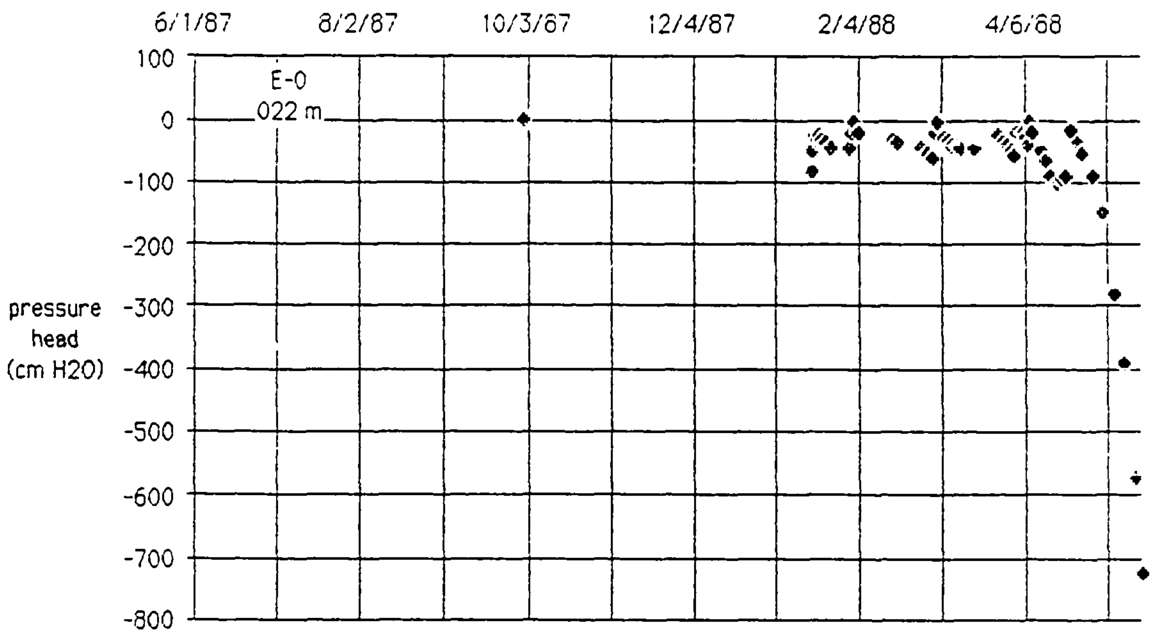
6/1/87
8/2/87
10/3/87
12/4/87
2/4/88
4/6/88
E-0
.022 m
pressure
head
(cm H2O)
100
0
-100
-200
-300
-400
-500
-600
-700
-800

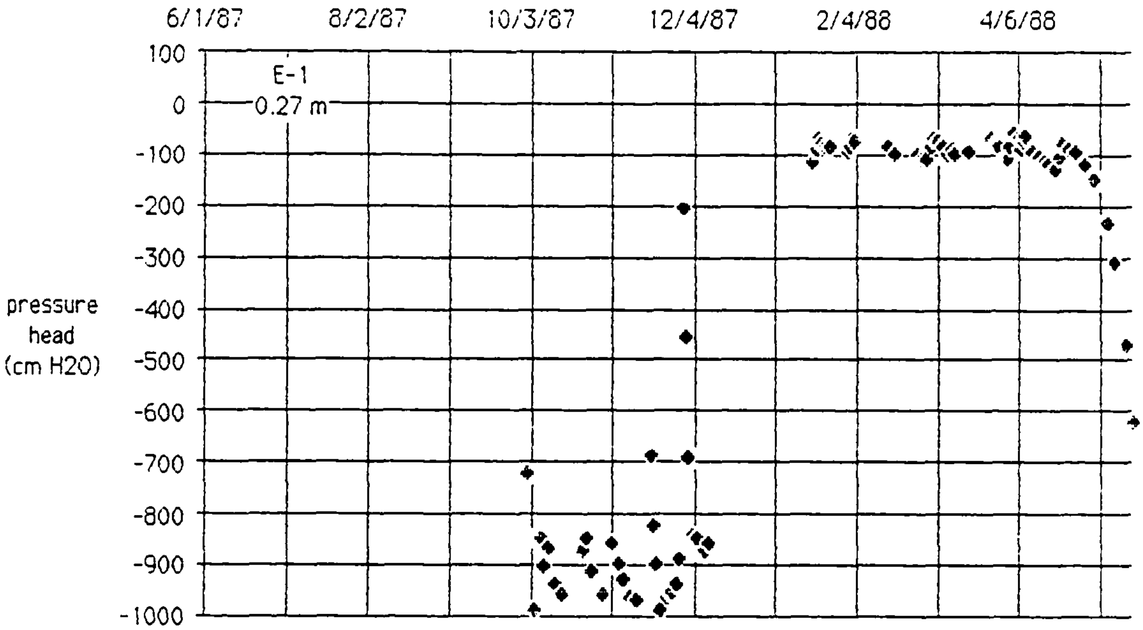
6/1/87
8/2/87
10/3/87
12/4/87
2/4/88
4/6/88
100
0
-100
-200
-300
-400
-500
-600
-700
-800
-900
-1000
E-1
0.27 m
pressure
head
(cm H20)

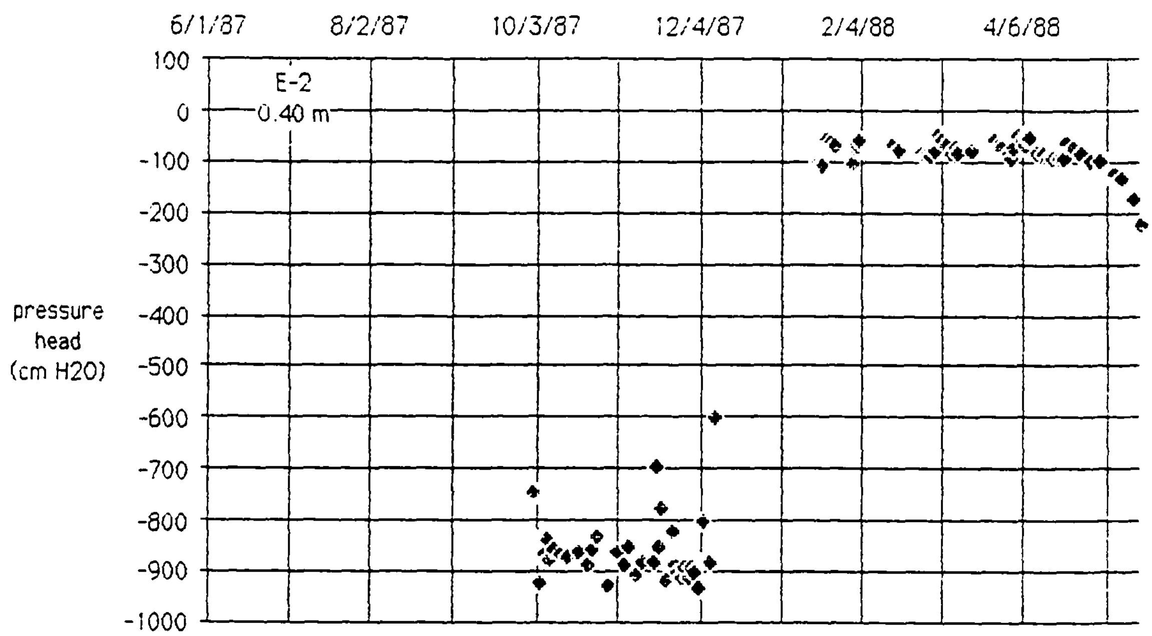
6/1/87
8/2/87
10/3/87
12/4/87
2/4/88
4/6/88
100
0
-100
-200
-300
-400
-500
-600
-700
-800
-900
-1000
pressure
head
(cm H2O)
E-2
0.40 m

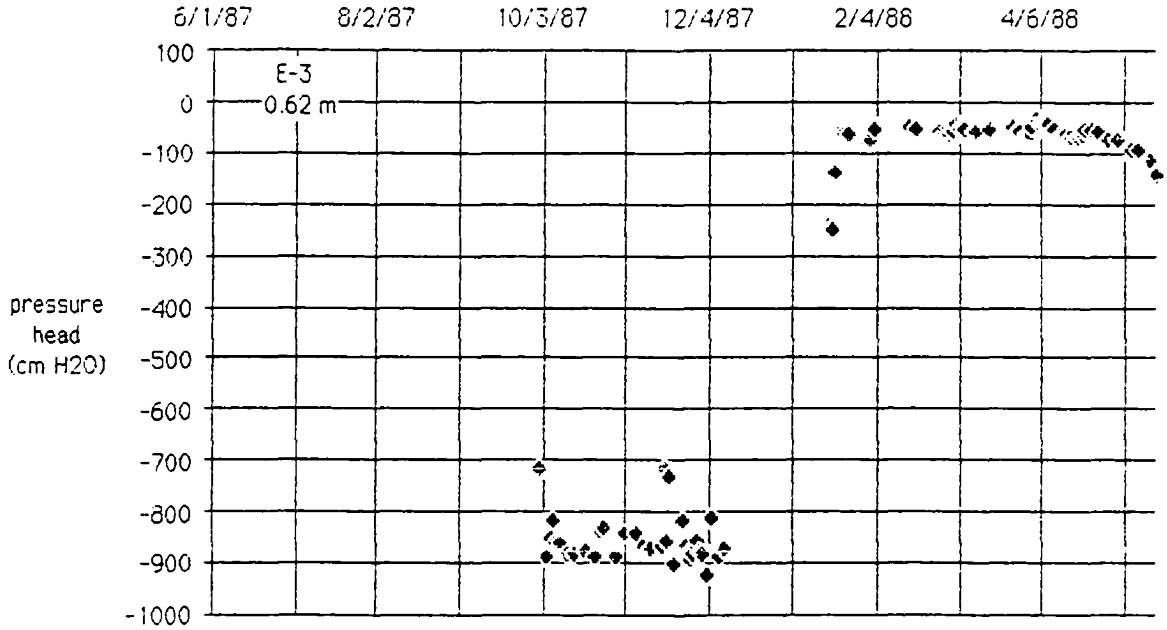
6/1/87
8/2/87
10/3/87
12/4/87
2/4/88
4/6/88
100
0
-100
-200
-300
-400
-500
-600
-700
-800
-900
-1000
pressure head (cm H2O)
E-3
0.62 m

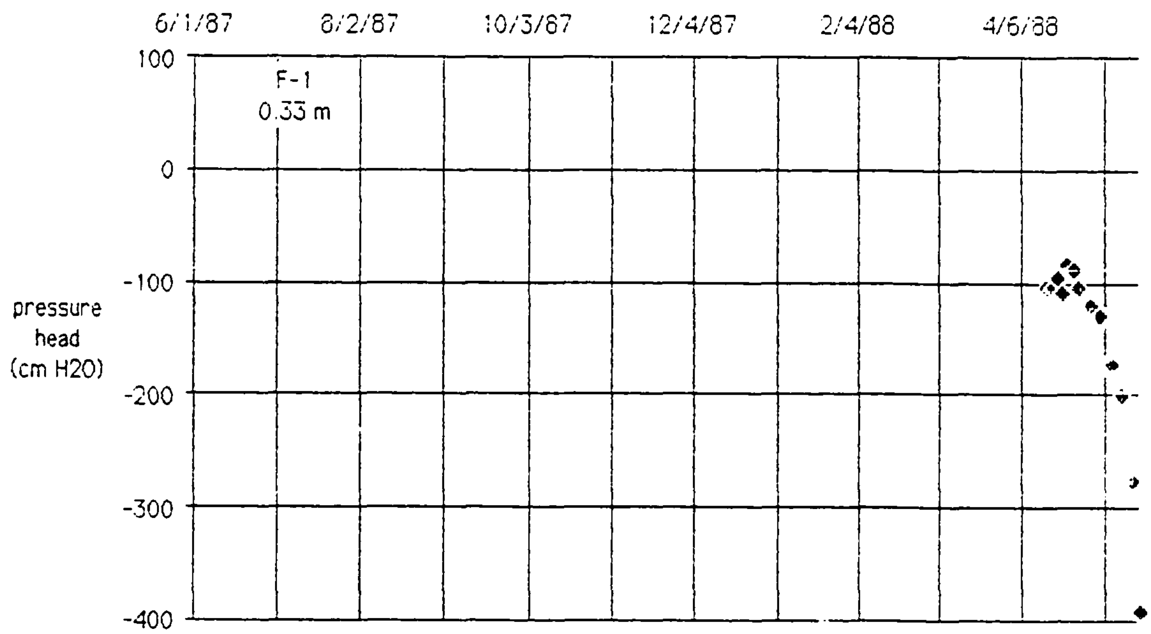
6/1/87
8/2/87
10/3/87
12/4/87
2/4/88
4/6/88
100
0
-100
-200
-300
-400
F-1
0.33 m
pressure
head
(cm H20)

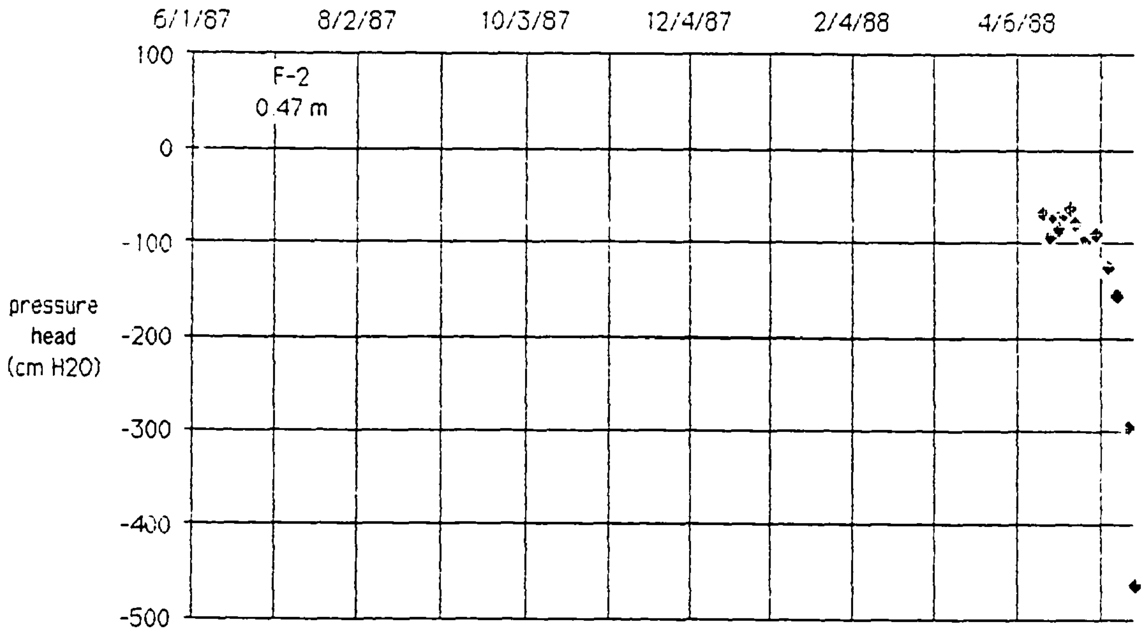
6/1/87
8/2/87
10/3/87
12/4/87
2/4/88
4/6/88
100
0
-100
-200
-300
-400
-500
pressure head (cm H2O)
F-2
0.47 m

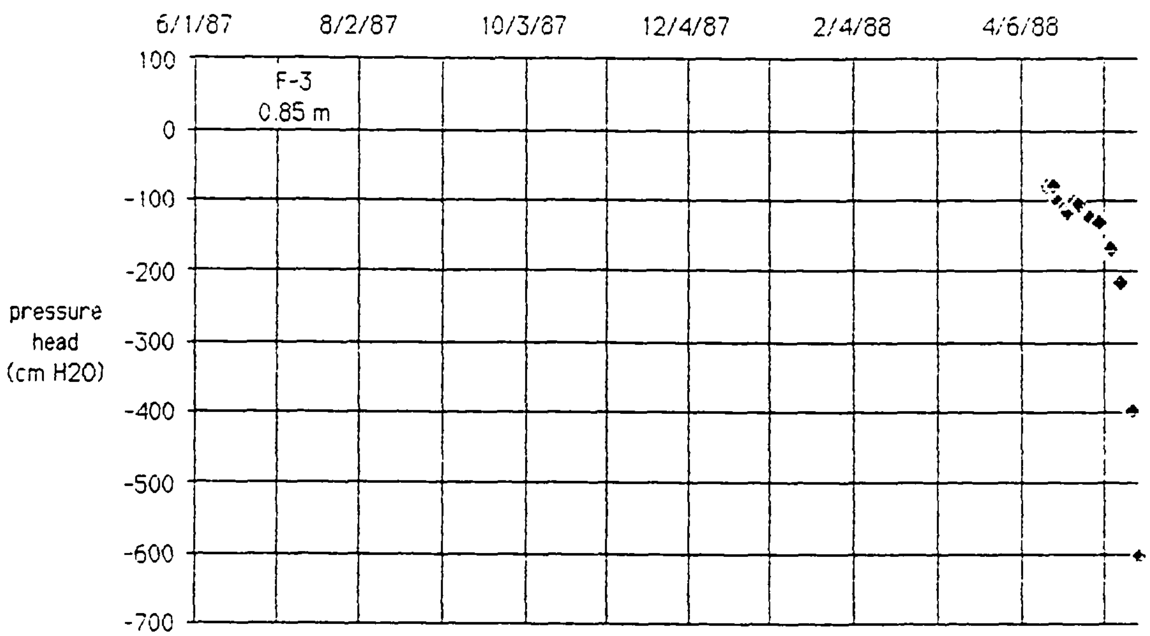
6/1/87
8/2/87
10/3/87
12/4/87
2/4/88
4/6/88
F-3
0.85 m
pressure head (cm H20)
100
0
-100
-200
-300
-400
-500
-600
-700

DAILY MEASURABLE PRECIPITATION
National Weather Service
Greater Cincinnati International Airport

date	precip. (m)
10/1/87	0.00E+00
10/2/87	0.00E+00
10/3/87	0.00E+00
10/4/87	0.00E+00
10/5/87	0.00E+00
10/6/87	1.45E-02
10/7/87	5.08E-04
10/8/87	0.00E+00
10/9/87	0.00E+00
10/10/87	8.38E-03
10/11/87	2.03E-03
10/12/87	0.00E+00
10/13/87	0.00E+00
10/14/87	0.00E+00
10/15/87	0.00E+00
10/16/87	0.00E+00
10/17/87	0.00E+00
10/18/87	0.00E+00
10/19/87	0.00E+00
10/20/87	0.00E+00
10/21/87	0.00E+00
10/22/87	0.00E+00
10/23/87	2.54E-04
10/24/87	3.30E-03
10/25/87	0.00E+00
10/26/87	0.00E+00
10/27/87	7.11E-03
10/28/87	0.00E+00
10/29/87	0.00E+00
10/30/87	0.00E+00
10/31/87	0.00E+00
11/1/87	0.00E+00
11/2/87	0.00E+00
11/3/87	0.00E+00
11/4/87	0.00E+00
11/5/87	0.00E+00
11/6/87	0.00E+00
11/7/87	1.27E-03
11/8/87	0.00E+00
11/9/87	1.27E-03
11/10/87	0.00E+00
11/11/87	0.00E+00
11/12/87	0.00E+00
11/13/87	0.00E+00
11/14/87	0.00E+00
11/15/87	0.00E+00
11/16/87	0.00E+00
11/17/87	3.81E-03
11/18/87	0.00E+00
11/19/87	0.00E+00
11/20/87	2.54E-04
11/21/87	0.00E+00
11/22/87	0.00E+00
11/23/87	1.27E-03
11/24/87	7.87E-03
11/25/87	0.00E+00
11/26/87	1.02E-02
11/27/87	0.00E+00
11/28/87	1.98E-02
11/29/87	0.00E+00
11/30/87	5.08E-04
12/1/87	1.78E-03
12/2/87	0.00E+00
12/3/87	3.30E-03
12/4/87	0.00E+00
12/5/87	0.00E+00
12/6/87	0.00E+00
12/7/87	0.00E+00
12/8/87	7.62E-04
12/9/87	2.03E-03
12/10/87	0.00E+00
12/11/87	2.03E-03
12/12/87	0.00E+00
12/13/87	0.00E+00
12/14/87	1.45E-02
12/15/87	7.11E-03
12/16/87	0.00E+00
12/17/87	0.00E+00
12/18/87	0.00E+00
12/19/87	4.83E-03
12/20/87	1.78E-03
12/21/87	0.00E+00
12/22/87	0.00E+00
12/23/87	0.00E+00
12/24/87	5.33E-03
12/25/87	2.03E-02
12/26/87	3.56E-03
12/27/87	1.52E-03
12/28/87	1.24E-02
12/29/87	5.08E-04

12/30/87	0.00E+00
12/31/87	2.54E-04
1/1/88	0.00E+00
1/2/88	0.00E+00
1/3/88	0.00E+00
1/4/88	0.00E+00
1/5/88	0.00E+00
1/6/88	0.00E+00
1/7/88	1.27E-03
1/8/88	2.54E-04
1/9/88	0.00E+00
1/10/88	0.00E+00
1/11/88	0.00E+00
1/12/88	0.00E+00
1/13/88	0.00E+00
1/14/88	0.00E+00
1/15/88	0.00E+00
1/16/88	0.00E+00
1/17/88	8.13E-03
1/18/88	2.54E-04
1/19/88	3.68E-02
1/20/88	5.08E-04
1/21/88	2.54E-04
1/22/88	5.08E-04
1/23/88	1.27E-03
1/24/88	0.00E+00
1/25/88	2.03E-03
1/26/88	1.27E-03
1/27/88	2.54E-04
1/28/88	0.00E+00
1/29/88	0.00E+00
1/30/88	0.00E+00
1/31/88	1.70E-02
2/1/88	4.90E-02
2/2/88	3.05E-02
2/3/88	8.38E-03
2/4/88	4.32E-03
2/5/88	2.54E-04
2/6/88	0.00E+00
2/7/88	0.00E+00
2/8/88	0.00E+00
2/9/88	0.00E+00
2/10/88	0.00E+00
2/11/88	9.65E-03
2/12/88	1.52E-03
2/13/88	0.00E+00
2/14/88	2.03E-03
2/15/88	2.29E-03
2/16/88	0.00E+00
2/17/88	0.00E+00
2/18/88	0.00E+00
2/19/88	1.04E-02
2/20/88	0.00E+00
2/21/88	0.00E+00
2/22/88	0.00E+00
2/23/88	7.11E-03
2/24/88	0.00E+00
2/25/88	0.00E+00
2/26/88	0.00E+00
2/27/88	0.00E+00
2/28/88	0.00E+00
2/29/88	0.00E+00
3/1/88	0.00E+00
3/2/88	6.10E-03
3/3/88	2.44E-02
3/4/88	1.04E-02
3/5/88	0.00E+00
3/6/88	0.00E+00
3/7/88	0.00E+00
3/8/88	0.00E+00
3/9/88	4.06E-03
3/10/88	0.00E+00
3/11/88	0.00E+00
3/12/88	9.40E-03
3/13/88	2.54E-04
3/14/88	5.08E-04
3/15/88	5.08E-04
3/16/88	0.00E+00
3/17/88	0.00E+00
3/18/88	4.32E-03
3/19/88	0.00E+00
3/20/88	0.00E+00
3/21/88	0.00E+00
3/22/88	0.00E+00
3/23/88	0.00E+00
3/24/88	0.00E+00
3/25/88	2.21E-02
3/26/88	5.08E-04
3/27/88	0.00E+00
3/28/88	0.00E+00
3/29/88	0.00E+00
3/30/88	5.08E-04
3/31/88	3.81E-03
4/1/88	5.33E-03
4/2/88	3.30E-03
4/3/88	3.33E-02

4/4/88	0.00E+00
4/5/88	0.00E+00
4/6/88	1.57E-02
4/7/88	5.33E-03
4/8/88	0.00E+00
4/9/88	0.00E+00
4/10/88	0.00E+00
4/11/88	0.00E+00
4/12/88	0.00E+00
4/13/88	0.00E+00
4/14/88	0.00E+00
4/15/88	0.00E+00
4/16/88	0.00E+00
4/17/88	0.00E+00
4/18/88	1.40E-02
4/19/88	0.00E+00
4/20/88	0.00E+00
4/21/88	1.73E-02
4/22/88	1.02E-03
4/23/88	2.54E-03
4/24/88	0.00E+00
4/25/88	0.00E+00
4/26/88	0.00E+00
4/27/88	7.62E-04
4/28/88	1.02E-03
4/29/88	0.00E+00
4/30/88	0.00E+00
5/1/88	0.00E+00
5/2/88	0.00E+00
5/3/88	0.00E+00
5/4/88	0.00E+00
5/5/88	0.00E+00
5/6/88	0.00E+00
5/7/88	0.00E+00
5/8/88	0.00E+00
5/9/88	8.38E-03
5/10/88	0.00E+00
5/11/88	0.00E+00
5/12/88	0.00E+00
5/13/88	2.03E-03
5/14/88	0.00E+00
5/15/88	0.00E+00
5/16/88	0.00E+00
5/17/88	0.00E+00
5/18/88	0.00E+00
5/19/88	0.00E+00
5/20/88	2.79E-03
5/21/88	0.00E+00
5/22/88	0.00E+00
5/23/88	3.28E-02
5/24/88	4.57E-03
5/25/88	0.00E+00
5/26/88	0.00E+00
5/27/88	0.00E+00
5/28/88	0.00E+00
5/29/88	0.00E+00
5/30/88	0.00E+00
5/31/88	0.00E+00

DATE & TIME	DRAIN DISCH. (m^3/s)		WATER LEVELS (m)							
		instr *	P-4	P-6	P-7	P-8	P-9	P-10	P-11	P-12
		casing top	-0.10	0.00	0.18	0.14	0.38	0.31	0.47	0.8
1/17/88 9:45	0.00E+00		-0.98	-1.27	NA	NA	NA	NA	NA	NA
1/17/88 16:15	0.00E+00		-1.10	-1.27	NA	NA	NA	NA	NA	NA
1/18/88 10:00	0.00E+00		-1.10	-1.27	NA	NA	NA	NA	NA	NA
1/19/88 9:30	0.00E+00		-1.10	-1.27	NA	NA	NA	NA	NA	NA
1/19/88 16:15	0.00E+00		-1.07	-1.13	NA	NA	NA	NA	NA	NA
1/20/88 10:15	0.00E+00		-0.78	-0.87	NA	NA	NA	NA	NA	NA
1/20/88 13:35	0.00E+00		-0.77	-0.93	NA	NA	NA	NA	NA	NA
1/20/88 14:10	0.00E+00		-0.81	-1.02	NA	NA	NA	NA	NA	NA
1/20/88 14:35	0.00E+00		-0.85	-0.98	NA	NA	NA	NA	NA	NA
1/20/88 15:05	0.00E+00		-0.81	-0.99	NA	NA	NA	NA	NA	NA
1/20/88 15:40	0.00E+00		-0.78	-0.99	NA	NA	NA	NA	NA	NA
1/20/88 16:10	0.00E+00		-0.80	-1.07	NA	NA	NA	NA	NA	NA
1/20/88 16:45	0.00E+00		-0.80	-1.02	NA	NA	NA	NA	NA	NA
1/21/88 9:45	0.00E+00		-0.85	-1.27	NA	NA	NA	NA	NA	NA
1/21/88 10:45	0.00E+00		-0.84	-1.27	NA	NA	NA	NA	NA	NA
1/22/88 9:15	0.00E+00		-0.90	-1.27	NA	NA	NA	NA	NA	NA
1/24/88 11:00	0.00E+00		-1.03	-1.27	NA	NA	NA	NA	NA	NA
1/31/88 11:45	0.00E+00		-1.10	-1.27	NA	NA	NA	NA	NA	NA
2/1/88 9:15	0.00E+00		-0.61	-0.63	NA	NA	NA	NA	NA	NA
2/1/88 16:40	0.00E+00		-0.47	-0.57	NA	NA	NA	NA	NA	NA
2/2/88 10:00	5.00E-05		-0.44	-0.52	NA	NA	NA	NA	NA	NA
2/2/88 17:00	2.50E-05		-0.63	-0.57	NA	NA	NA	NA	NA	NA
2/3/88 9:30	4.00E-05		-0.85	-1.04	NA	NA	NA	NA	NA	NA
2/15/88 9:30	4.17E-06		-0.73	-0.70	mab	mab	dry	dry	NA	NA
2/16/88 16:20	2.50E-06		-0.84	-1.27	dry	dry	dry	dry	NA	NA
2/18/88 8:50	1.67E-07		-0.89	-1.27	dry	dry	dry	dry	NA	NA
2/19/88 9:00	1.00E-05		-0.75	-0.84	dry	dry	dry	dry	NA	NA
2/27/88 15:15	1.67E-07		-0.88	-1.27	dry	dry	dry	dry	NA	NA
2/29/88 9:00	1.67E-07		-0.92	-1.27	dry	dry	dry	dry	NA	NA
3/2/88 9:40	0.00E+00		-0.93	-1.27	dry	dry	dry	dry	NA	NA
3/3/88 9:15	1.17E-05		-0.71	-0.65	dry	-0.85	wab	wab	NA	NA
3/3/88 16:45	5.00E-05		-0.60	-0.66	mab	-0.83	mab	-0.9	NA	NA
3/4/88 10:45	1.00E-04		-0.50	-0.55	dry	-0.84	-0.8	-0.83	NA	NA
3/5/88 16:40	6.67E-06		-0.85	-1.23	dry	mab	dry	mab	NA	NA
3/6/88 12:50	3.33E-06		-0.86	-1.27	dry	dry	dry	dry	NA	NA
3/8/88 9:30	1.67E-07		-0.88	-1.27	dry	dry	dry	dry	NA	NA
3/9/88 9:45	1.67E-07		-0.88	-1.27	dry	-0.84	mab	dry	NA	NA
3/11/88 11:30	1.67E-07		-0.88	-1.27	dry	-0.86	mab	dry	NA	NA
3/12/88 11:00	0.00E+00		-0.88	-1.27	dry	-0.83	dry	dry	NA	NA
3/16/88 16:50	1.67E-07		-0.88	-1.27	dry	-0.80	mab	mab	NA	NA
3/17/88 16:55	1.67E-07		-0.86	-1.27	dry	-0.78	mab	dry	NA	NA
3/26/88 12:45	3.00E-05		-0.86	-1.27	dry	-0.72	dry	dry	dry	mab
3/28/88 11:00	0.00E+00		-0.86	-1.27	dry	-0.77	dry	dry	dry	dry
3/29/88 16:40	0.00E+00		-0.87	-1.27	dry	-0.74	dry	dry	dry	dry
3/31/88 9:45	0.00E+00		-0.89	-1.27	dry	-0.79	dry	dry	dry	dry

4/1/88 11:30	0.00E+00	-0.90	-1.27	dry	-0.78	dry	dry	dry	dry
4/2/88 11:30	0.00E+00	-0.86	-1.27	dry	-0.78	dry	dry	dry	dry
4/4/88 12:00	2.00E-05	-0.80	-1.27	dry	-0.70	dry	-0.82	dry	-1.46
4/5/88 11:20	3.33E-06	-0.85	-1.27	dry	-0.70	dry	dry	dry	-1.46
4/6/88 10:25	2.00E-05	-0.69	-1.27	dry	-0.71	dry	dry	dry	-1.41
4/7/88 10:30	6.67E-05	-0.60	-0.83	dry	-0.70	-0.9	-0.86	dry	-1.34
4/8/88 9:45	1.00E-05	-0.85	-1.27	dry	-0.71	dry	dry	dry	-1.33
4/11/88 10:15	0.00E+00	-0.88	-1.27	dry	-0.72	dry	dry	dry	-1.36
4/13/88 11:40	0.00E+00	-0.88	-1.27	dry	-0.75	dry	dry	dry	dry
4/15/88 9:45	0.00E+00	-0.93	-1.27	dry	-0.77	dry	dry	dry	dry
4/17/88 11:45	0.00E+00	-0.97	-1.27	dry	-0.77	dry	dry	dry	-1.45
4/19/88 10:05	0.00E+00	-0.99	-1.27	dry	-0.77	dry	dry	dry	-1.46
4/21/88 9:45	0.00E+00	-0.98	-1.27	dry	-0.78	dry	dry	dry	dry
4/22/88 10:35	0.00E+00	-1.05	-1.27	dry	-0.76	dry	dry	dry	dry
4/25/88 9:25	0.00E+00	-1.06	-1.27	dry	-0.76	dry	dry	dry	dry
4/27/88 10:00	0.00E+00	-1.08	-1.27	dry	-0.77	dry	dry	dry	dry
5/1/88 9:50	0.00E+00	-1.10	-1.27	dry	-0.79	dry	dry	dry	dry
5/4/88 10:20	0.00E+00	-1.10	-1.27	-0.8	dry	dry	dry	dry	dry

APPENDIX B
TENSIOMETER DESIGN, INSTALLATION, AND CALIBRATION

DESIGN

The tensiometers (Figure B.1) used at the Delhi Pike slide were assembled using manometer tubes with porous stones, rubber stoppers, and gaskets (series 2300), and capillary tubing (MYT001) manufactured by the Soilmoisture Equipment Co., Santa Barabara, California. There are two reasons for this choice: First, it is inexpensive; total cost for an average tensiometer, including mercury, is approximately $20, roughly half that of commercially available instruments. Instruments, including several tensiometers and piezometers during this study, have been stolen during research projects at Delhi Pike, so this design cuts initial as well as replacement costs in the likely event of theft. Second, the glass mercury reservoirs used by Murdoch (1987) were attractive targets for vandalism, so I designed an instrument in which all of the mercury is contained in a shatterproof nylon capillary tube.

INSTALLATION

To install each tensiometer, I used a hand auger to drill a hole slightly larger than the tensiometer tube diameter and added finely-crumbled colluvial clay and de-aired (boiled) water to the hole to form a slurry, inserted the tensiometer tube, and twisted until it became firmly seated in the base of the hole to insure good hydraulic contact. Stones and roots, however, made it impossible to install tensiometers deeper than about 0.6 m. Finally, I tamped and mounded soil around the top of each tensiometer tube to prevent surface water from entering the hole. Each capillary tube was bent into a U-shape, attached it to a wooden dowel, which had been driven vertically into the soil, using plastic cable ties, wire, or strapping tape. Finally, the capillary tube was filled with with approximately 1.5 cm^3 of technical grade mercury using suction from a common plastic syringe, and the tensiometer tube filled with de-aired water.

Tensiometers of different lengths (0.30 m, 0.61 m, 0.91 m, and 1.22) were installed in groups A, B, and C, but only three tensiometers (0.30 m, 0.61 m, and 0.91 m) were installed in groups D and E. In January 1988, a fourth shallow shallow tensiometer was added to group E, and in April 1988 tensiometer group F, consisting of three instruments, was installed.

CALCULATION OF PRESSURE HEAD

Average pressure head over the contact area of the porous stone is given by the sum of the difference in mercury level across the manometer and the pressure head due to the water column within the tensiometer tube (Croney and others, 1952; Bear, 1979). If h_{tube} is the total tensiometer tube length from top to porous stone midpoint, h_{cap} is the length of capillary tube inside the tensiometer, h_{wl} is the water level beneath the tensiometer tube top, and the capillary tube enters the tensiometer 0.04 m from the top of the tensiometer tube, then the pressure head due to the water column can be written as

$$\psi_{tube} = (h_{tube} - h_{wl}) - (h_{cap} - h_{wl} + 0.04 \text{ m})$$

$$= h_{tube} - h_{cap} + 0.04 \text{ m}$$

and the total pressure head, ψ, is

$$\psi = G_{Hg}h_{Hg} + h_{tube} - h_{cap} + 0.04 \text{ m}$$

where G_{Hg} is the specific gravity of mercury (taken to be constant at 13.55) and h_{Hg} is the difference in mercury level across the manometer. For this study, h_{Hg} is negative when the height of mercury in the closed side of the manometer is higher than the height of the mercury in the atmospheric side of the manometer (as in Figure B.1). In theory the limit of such tensiometers should be limited to the vapor pressure of water at the operating temperature, but Croney and others (1952) suggest a practical upper limit of -0.70 m of Hg (-9.5 m H_2O).

The tensiometers used in this study have a portion of air-filled capillary tube, on the order of several tens of centimetres long, which will introduce some error (see Calibration Procedure below). Although Croney and others (1952) write that it is a simple matter to completely fill the capillary tube with water and then inject mercury to displace the water, this was virtually impossible in the field. Instead, I used a syringe to suck mercury into the capillary tube and left the remainder filled with air.

CALIBRATION PROCEDURE

I chose several new tensiometer tubes at random and calibrated them in the laboratory to determine tensiometer response time and the amount of error due to air in the capillary tube. Each of these tubes was assembled, mounted on a vertical support, and partly immersed in water roughly up to the midpoint of the porous stone. The top of the tensiometer tube was then sealed with a rubber stopper, pressurizing the tube. Declining mercury level differences in the capillary tube were measured during calibration periods of up to 2 hrs. in order to estimate the time required to respond to a perturbation. Figure B.2 shows that response to the perturbation was rapid in all cases, and that the tensiometers had essentially reached their equilibrium pressure heads within approximately 15 min.

Figure B.1 Schematic illustration of mercury manometer tensiometers used at Delhi Pike, including variables necessary for calculation of pressure head.

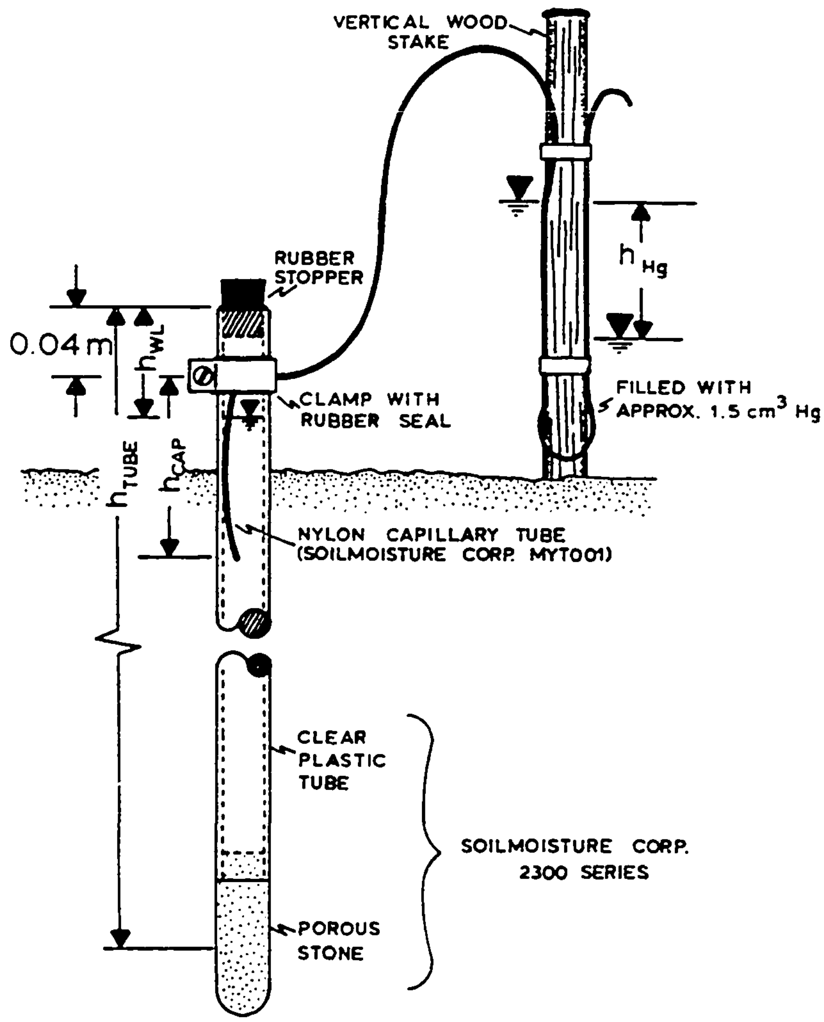
VERTICAL WOOD STAKE
RUBBER STOPPER
0.04 m
h_{WL}
h_{Hg}
CLAMP WITH RUBBER SEAL
FILLED WITH APPROX. 1.5 cm³ Hg
h_{TUBE}
h_{CAP}
NYLON CAPILLARY TUBE (SOILMOISTURE CORP. MYT001)
CLEAR PLASTIC TUBE
SOILMOISTURE CORP. 2300 SERIES
POROUS STONE

Figure B.2 Calibration curves for tensiometers showing decrease in pressure head perturbation with time and equilibrium pressure head, theoretically equal to zero.

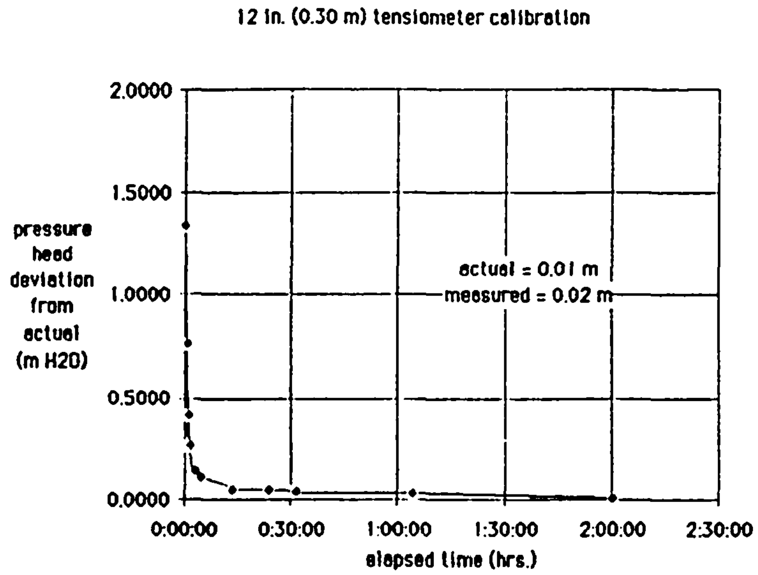
12 in. (0.30 m) tensiometer calibration
2.0000
1.5000
1.0000
0.5000
0.0000
pressure head deviation from actual (m H2O)
actual = 0.01 m
measured = 0.02 m
0:00:00
0:30:00
1:00:00
1:30:00
2:00:00
2:30:00
elapsed time (hrs.)

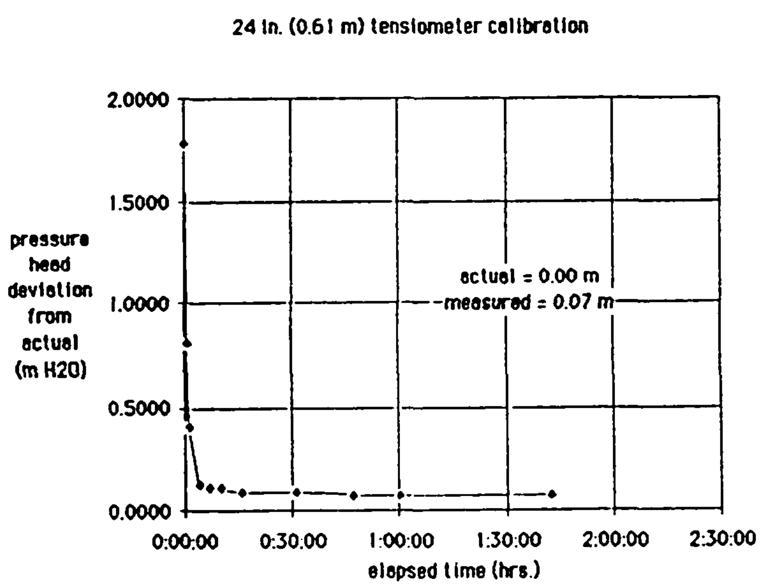
24 in. (0.61 m) tensiometer calibration
2.0000
1.5000
1.0000
0.5000
0.0000
pressure head deviation from actual (m H2O)
actual = 0.00 m
measured = 0.07 m
0:00:00
0:30:00
1:00:00
1:30:00
2:00:00
2:30:00
elapsed time (hrs.)

36 In. (0.91 m) tensiometer calibration

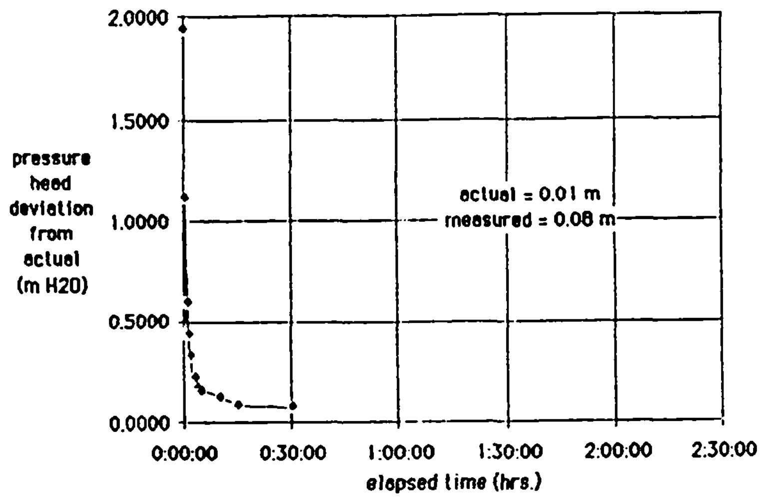

36 In. (0.91 m) tensiometer calibration, trial #2

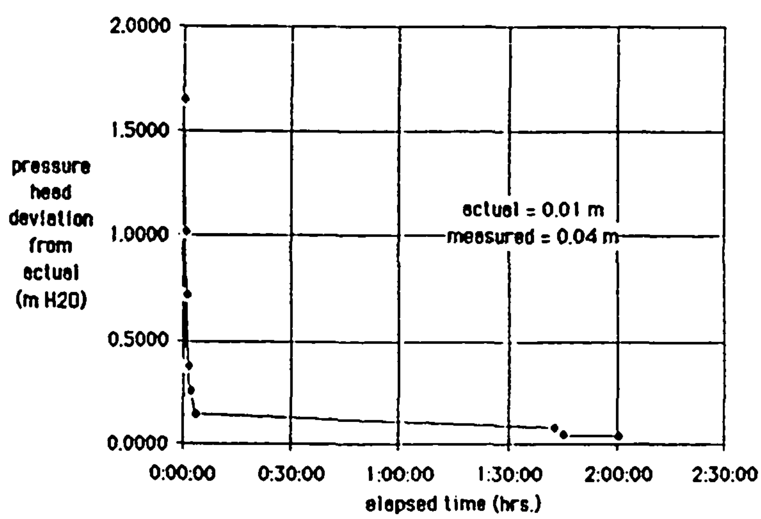

Table B.1 Tensiometer Calibration and Errors

tube length (m)	actual ψ (m)	measured ψ (m)	error (m)
0.305	0.01	0.02	0.01
0.610	0.00	0.07	0.07
0.914	0.01	0.08	0.07
0.914	0.01	0.04	0.03

Actual pressure head was slightly positive in all cases because the tubes were pushed into the water when the rubber stopper was inserted to pressurize the instruments, but equilibrium pressure head was slightly negative for the 0.30 m and 0.61 m tubes, and slightly positive for the two 0.91 m tubes. A second 0.91 m tube was tested because the results of the first 0.91 m test were different than had been expected from the 0.30 m and 0.61 m calibrations. Results for all three tube lengths, summarized above in Table B.1, show that instrumental error is on the order of 10^{-2} m for pressure heads near 0 m. It was difficult to measure mercury levels in the field more accurately than about $\pm 10^{-3}$ m, which corresponds to a pressure head error of about $\pm 10^{-2}$ m, so the inaccuracy of the instruments should not markedly affect the quality of data used in this study, and is more than compensated for by the economy and durability of the design.

APPENDIX C
FINITE DIFFERENCE COMPUTER PROGRAM FOR SOLUTION OF THE MODIFIED DUPUIT HILLSIDE FLOW EQUATION

```
program downhill_flow_rchge;

(*****************************************************************************

  Direct Thomas algorithm solution to the one-dimensional,fully saturated
  nonlinear equation for hillside flow with time-variant recharge. Uses
  explicit (time-lagging) linearization in the alternate Douglas & Jones
  predictor-corrector formulation. Initial heads and constants are read in
  from an ASCII disk file, and results are written to a second ASCII disk
  file compatible with Microsoft Excel (i.e. entries separated by chr(9)
  tabs).  Default maximum 50 spatial and 200 temporal grid nodes.

  written in Macintosh Turbo Pascal v. 1.00a

  Bill Haneberg
  John L. Rich Geomechanics Laboratory
  "Your source for high quality, low cost geomechanics research."
  Department of Geology
  University of Cincinnati
  Cincinnati, Ohio 45221-0013

  working version of 1/21/88

 *****************************************************************************)

uses sane;                         { Standard Apple Numeric Environment }

var

  disk : text;                 { defines output device }
  p,                           { effective porosity }
  k,                           { saturated hydraulic conductivity }
  pdivk,                       { porosity / hydraulic conductivity }
  h,                           { soil thickness normal to slope }
  time,                        { elapsed time }
  slope,                       { slope angle in degrees }
  deta,                        { spatial grid increment }
  dt : extended;               { temporal grid increment }
  a,b,c,                       { Thomas algorithm matrices }
  x,f : array[1..50] of extended; {    "        "        "    }
  heads :                      { array of total heads }
      array[1..2,1..50] of extended;
  rain :                       { array of rainfall values }
      array[1..200] of extended;
  neta, nt,                    { number of spatial & temporal nodes }
  eta,s,t : integer;           { loop counters }
  texttype,
  textcreator :                { system file-creating parameters }
      packed array [1..4] of char;

(*****************************************************************************)

procedure dataread;
```

```
{
  Prompts for initial data file name, opens initial data file, reads in
  data, and closes initial data file.
}

var
  infile, name : string;

begin
  writeln;
  write('name of initial data file to be read:  ');
  readln(infile);
  writeln;
  writeln;
  reset(disk,infile);
  readln(disk,name);
  writeln('reading initial data file ',name,'...');
  writeln;
  readln(disk,p);
  readln(disk,k);
  readln(disk,h);
  readln(disk,neta);
  readln(disk,deta);
  readln(disk,nt);
  readln(disk,dt);
  readln(disk,slope);
  for eta := 1 to neta do
    readln(disk,heads[1,eta]);
  for t := 1 to nt do                        { set all rain equal to zero }
    rain[t] := 0.;
  t := 0;
  while not seekeof(disk) do                 { read in only non-zero rainfall }
    begin
      t := t + 1;
      readln(disk,rain[t]);
    end;
  t := 0;
  writeln;
  writeln('                                  ... finished reading initial data file. ');
  writeln;
  writeln;
  close(disk);
end;

{****************************************************************************}

procedure fileopen;

{
  Opens disk text file for data output.  Remember to declare the variable
  disk : text as a global variable, and to close it at end of program!
}

var
```

```
  texttype,
  textcreator : packed array [1..4] of char;
  filename : string;

begin

  writeln;
  write('name for output disk file? ');
  readln(filename);
  writeln;

  rewrite(disk,filename);
  writeln(disk,'text file name: ',filename);
  writeln;
  writeln('==========================================================================');
  writeln;
  writeln(disk);
  writeln(disk,'p = ',chr(9),p,chr(9));
  writeln(disk,'k = ',chr(9),k,chr(9));
  writeln(disk,'dx = ',chr(9),deta,chr(9));
  writeln(disk,'dt = ',chr(9),dt,chr(9));
  writeln(disk,'beta = ',chr(9),slope,chr(9));

  write(disk,chr(9));              { tab req'd to separate columns in Excel }
  write(disk,chr(9));

  for eta := 1 to neta do
      write(disk,(eta-1)*deta:1:3, chr(9));

  writeln(disk);

  end;

(*****************************************************************************)


procedure filewrite;

{
  Writes one line of data to a disk opened in procedure fileopen.
  This modification writes residual heads (present-original) to disk.
}

begin

  write(disk,(time/3.6e03):3:3,chr(9));

  if t = 0 then
      write(disk,0.0,chr(9))
    else
      write(disk,rain[t],chr(9));

  for eta := 1 to neta do
    write(disk,(heads[1,eta]):3:4,chr(9));
```

```
  writeln(disk);

end;

{****************************************************************************}

procedure initialization;

{
  Reads in initial heads and initializes assorted variables, opens and
  writes t = 0 data to output disk file.
}

begin

  writeln;
  writeln;
  writeln('========================================================================');
  writeln;

  dataread;                  { read in raw data }

  fileopen;                  { open data output file }

  time := 0.;                { miscellaneous initilization }

  slope := slope/57.29577951; { convert degrees to radians }

  pdivk := p/k;              { combined constant }

  for eta := 1 to neta do
    heads[2,eta] := heads[1,eta];

  filewrite;                 { put initial heads on disk}

end;

{****************************************************************************}

procedure predictor;

{
  Fills a,b,c, and f arrays with Douglas-Jones predictor values to be
  used in procedure thomas. Notation after Wang and Anderson, 1982,
  Introduction to Groundwater Modeling.
}

begin

  for eta := 3 to neta-2 do                { fill array interiors }

    begin
      a[eta-1] := 1.;
      b[eta-1] := -2.*(1. + p*sqr(deta)/k/dt/heads[1,eta]/cos(slope));
```

```
      c[eta-1] := 1.;
      f[eta-1] := -2.*p*sqr(deta)/k/dt/cos(slope);
      f[eta-1] := f[eta-1] - sqr(heads[1,eta+1]-heads[1,eta-1])/4./heads[1,eta];
      f[eta-1] := f[eta-1] + deta*tan(slope)*(heads[1,eta+1]-heads[1,eta-1])/heads[1,eta]/2.;
      f[eta-1] := f[eta-1] - rain[t]*sqr(deta)/k/heads[1,eta]/cos(slope);
    end;

                                     { fixed-head uphill boundary }

     a[1] := 0.;
     b[1] := -2.*(1. + p*sqr(deta)/k/dt/heads[1,2]/cos(slope));
     c[1] := 1.;
     f[1] := -2.*p*sqr(deta)/k/dt/cos(slope);
     f[1] := f[1] - sqr(heads[1,3]-heads[1,1])/4./heads[1,2];
     f[1] := f[1] + deta*tan(slope)*(heads[1,3]-heads[1,1])/heads[1,2]/2.;
     f[1] := f[1] - heads[1,1];
     f[1] := f[1] - rain[t]*sqr(deta)/k/heads[1,2]/cos(slope);


                                     { fixed-head downhill boundary }

     a[neta-2] := 1.;
     b[neta-2] := -2.*(1. + p*sqr(deta)/k/dt/heads[1,neta-1]/cos(slope));
     c[neta-2] := 0.;
     f[neta-2] := -2.*p*sqr(deta)/k/dt/cos(slope);
     f[neta-2] := f[neta-2] - sqr(heads[1,neta]-heads[1,neta-2])/4./heads[1,neta-1];
     f[neta-2] := f[neta-2] + deta*tan(slope)*(heads[1,neta]-heads[1,neta-2])/heads[1,neta-1]/
2.;
     f[neta-2] := f[neta-2] - heads[1,neta];
     f[neta-2] := f[neta-2] - rain[t]*sqr(deta)/k/heads[1,neta-1]/cos(slope);

   end;

 (**********************************************************************)

 procedure corrector;

 {
   Fills a,b,c, and f arrays with Douglas-Jones corrector values to be
   used in procedure thomas. Notation after Wang and Anderson, 1982,
   Introduction to Groundwater Modeling.
 }
 begin

   for eta := 3 to neta-2 do                { fill array interiors }

     begin
       a[eta-1] := 1.;
       b[eta-1] := -2.*(1. + p*sqr(deta)/k/dt/heads[2,eta]/cos(slope));
       c[eta-1] := 1.;
       f[eta-1] := -2.*p*sqr(deta)/k/dt/heads[2,eta]/cos(slope)*heads[1,eta];
       f[eta-1] := f[eta-1] - sqr(heads[2,eta+1]-heads[2,eta-1])/2./heads[2,eta];
       f[eta-1] := f[eta-1] + deta*tan(slope)*(heads[2,eta+1]-heads[2,eta-1])/heads[2,eta];
       f[eta-1] := f[eta-1] - heads[1,eta-1] + 2.*heads[1,eta] - heads[1,eta+1];
       f[eta-1] := f[eta-1] - 2.*rain[t]*sqr(deta)/k/heads[2,eta]/cos(slope);
     end;
```

```
                                        { fixed-head uphill boundary }

    a[1] := 0.;
    b[1] := -2.*(1. + p*sqr(deta)/k/dt/heads[2,2]/cos(slope));
    c[1] := 1.;
    f[1] := -2.*p*sqr(deta)*heads[1,2]/k/dt/cos(slope)/heads[2,2];
    f[1] := f[1] - sqr(heads[2,3]-heads[2,1])/2./heads[2,2];
    f[1] := f[1] + deta*tan(slope)*(heads[2,3]-heads[2,1])/heads[2,2];
    f[1] := f[1] - heads[1,1] + 2.*heads[1,2] - heads[1,3] - heads[2,1];
    f[1] := f[1] - 2.*rain[t]*sqr(deta)/k/heads[2,2]/cos(slope);

                                        { fixed-head downhill boundary }

    a[neta-2] := 1.;
    b[neta-2] := -2.*(1. + p*sqr(deta)/k/dt/heads[2,neta-1]/cos(slope));
    c[neta-2] := 0.;
    f[neta-2] := -2.*p*sqr(deta)*heads[1,neta-1]/k/dt/cos(slope)/heads[2,neta-1];
    f[neta-2] := f[neta-2] - sqr(heads[2,neta-2]-heads[2,neta])/2./heads[2,neta-1];
    f[neta-2] := f[neta-2] + deta*tan(slope)*(heads[2,neta-2]-heads[2,neta])/heads[2,neta-1];
    f[neta-2] := f[neta-2] - heads[1,neta] + 2.*heads[1,neta-1] - heads[1,neta-2];
    f[neta-2] := f[neta-2] - heads[2,neta];
    f[neta-2] := f[neta-2] - 2.*rain[t]*sqr(deta)/k/heads[2,neta-1]/cos(slope);

  end;

{*****************************************************************************}

procedure thomas;

{
  Thomas algorithm for solution of systems of linear equations with
  tridiagonal coefficient matrices.  Adapted from FORTRAN subroutine
  TRIDIA of Wang and Anderson, 1982, Introduction to Groundwater Modeling.
}

var
  j, nu : integer;
  alpha,
  beta,
  gamma : array[1..100] of extended;

begin
  alpha[1] := b[1];
  beta[1] := c[1]/alpha[1];
  gamma[1] := f[1]/alpha[1];

  for eta := 2 to neta-2 do

    begin
      alpha[eta] := b[eta]-a[eta]*beta[eta-1];
      beta[eta] := c[eta]/alpha[eta];
      gamma[eta] := (f[eta]-a[eta]*gamma[eta-1])/alpha[eta];
    end;
```

```
  x[neta-2] := gamma[neta-2]:
  nu := neta-2;

  for eta := 1 to nu do

    begin
      j := nu-eta;
      x[j] := gamma[j]-beta[j]*x[j+1]:
    end:

 end;

{****************************************************************************;

begin                                  { main program }

  initialization;

      time := 0.;

  for t := 1 to nt do                    { main time loop }

    begin

      time := time+dt:                   { simulation time in hours }

      gotoxy(30,21):
      write('predicting...'):

      predictor;

      thomas;
                                            { make sure water level doesn't
                                          exceed soil thickness }
      for eta := 2 to neta-1 do
       if x[eta-1] >  h
        then heads[2,eta] :=  h
          else if heads[2,eta] < 0. then heads[1,eta] := 1e-06
            else heads[2,eta] := x[eta-1];

      heads[2,1] := heads[1,1];
      heads[2,neta] := heads[1,neta];

      gotoxy(30,21);
      write('correcting...');

      corrector;

      thomas;
                                        { make sure water level doesn't
                                          exceed soil thickness }
     for eta := 2 to neta-1 do
       if x[eta-1] > h
        then heads[1,eta] := h
          else if heads[1,eta] < 0. then heads[1,eta] := 1e-06
            else heads[1,eta] := x[eta-1];
```

```
      heads[1,1] := heads[2,1];
      heads[1,neta] := heads[2,neta];

      gotoxy(30,23);
      write('time = ',(time/3.6e03):5:2,' hrs.');
      gotoxy(30,24);
      write('rain = ',rain[t],' m/s');


      writeln;

      filewrite;

    end;                                  { end of main time loop }

  close(disk);                            { close ouput file }

  writeln;
  writeln('                                 end of job');
  writeln;
  writeln('                             press RETURN to exit');
  writeln;
  readln;

  end.                                    { end main program }
```

APPENDIX D
NUMERICAL SIMULATION OF ONE-DIMENSIONAL VERTICAL INFILTRATION AND EVAPORATION

PHYSICS OF INCOMPRESSIBLE UNSATURATED FLOW

Flow of incompressible water through an unsaturated porous, non-reactive, non-expansive, incompressible soil is generally described by the so-called Richards equation

$$\frac{\partial \Theta}{\partial t} = \nabla \cdot (K \nabla \Phi) \tag{D.1}$$

(e.g., Bear, 1979), where Θ is volumetric water content, $K = K(\psi)$ is hydraulic conductivity and a function of pressure head, Φ is total head, and $\nabla = \partial / \partial x_i$ is the usual differential operator. Defining total head as the sum of elevation head and pressure head (z axis positive downward), $\Phi = (\psi - z)$, and multiplying the left side of (D.1) by $(\partial\psi/\partial\psi)$, the governing equation for vertical unsaturated flow becomes

$$C \frac{\partial \psi}{\partial t} = \frac{\partial}{\partial z}\left[K \left(\frac{\partial \psi}{\partial z} - 1 \right) \right] \tag{D.2}$$

where the derivative

$$C \equiv \frac{\partial \Theta}{\partial \psi} \tag{D.3}$$

is known as specific storage capacity. The variables ψ, Θ, and K are all share highly nonlinear relationships. Soil moisture characteristic curves for Kope colluvium exist only for pressure heads greater than about -1 m (Murdoch, 1987), which is far above pressure head values measured during summer and autumn, so an exponential relationship between hydraulic conductivity and pressure head of the form

$$K = K_{sat}\, e^{\{\alpha(\psi - \psi_{crit})\}} \tag{D.4}$$

is assumed, where α is a constant with units of [length^{-1}], K_{sat} is saturated hydraulic conductivity, and ψ_{crit} is the lower limit of tension saturation, which is sometimes called the air entry pressure. Water content and pressure head are further assumed to be related by

$$\Theta = \Theta_{sat}\ e^{(\psi\ -\ \psi_{crit})} \qquad \text{(D.5)}$$

where Θ_{sat} is saturated volumetric water content. The derivative (D.3) is evaluated as

$$C = \frac{\Theta_{sat}}{e^{\psi_{crit}}}\ e^{\psi} \qquad \text{(D.6)}$$

which can be substituted back into (D.2) to arrive at a soluble form of the governing equation. Equations (D.4) and (D.6) specify that both hydraulic conductivity and water content are equal to saturated values at $\psi = \psi_{crit}$ and approach zero as ψ approaches negative infinity.

NUMERICAL SOLUTION

Finite Difference Approximation

There are few analytic solutions to (D.2), so infiltration problems are virtually always solved numerically. Havercamp and others (1977) evaluated six different finite difference formulations of (D.2) for unsaturated conditions only, and suggest that trade-offs between numerical error and computation time make implicit discretization schemes preferable. In addition, Havercamp and Vauclin (1981) show that the local form of the Richards equation is more stable than the decomposed form, in which all the derivatives in (D.2) are expanded. Based upon these comparisons, an explicit linearization and implicit discretization scheme was chosen for the finite difference approximation

$$\frac{C(\psi_i^j-\psi_i^{j-1})}{\delta t}$$

$$= \frac{1}{\delta z}\left[\left(\frac{\psi_{i+1}^j - \psi_i^j}{\delta z} - 1\right)\left(\frac{K_{i+1}^{j-1} + K_i^{j-1}}{2}\right) - \left(\frac{\psi_i^j - \psi_{i-1}^j}{\delta z} - 1\right)\left(\frac{K_i^{j-1} + K_{i-1}^{j-1}}{2}\right)\right] \tag{D.7}$$

where superscripts represent time indices and subscripts represent spatial indices, to reduce computing time while maintaining acceptable mass balance accuracy. As with all fully implicit discretizations, (D.7) is unconditionally stable but only first order accurate in time (Anderson and others, 1984; Ferziger, 1981). Explicit linearization, however, uses pressure head values from the previous (j-1)$^{\text{th}}$ time step to estimate hydraulic conductivity at the current j$^{\text{th}}$ time step, so time increments must be kept small, particularly while gradients are changing rapidly. Rearrangement of (D.7) gives a system of linearized equations of the form

$$\left(K_{i-1}^{j-1} + K_i^{j-1}\right)\psi_{i-1}^j - \left(K_{i-1}^{j-1} + 2K_i^{j-1} + K_{i+1}^{j-1} + \frac{2\,C\,\delta z^2}{\delta t}\right)\psi_i^j + \left(K_{i+1}^{j-1} + K_i^{j-1}\right)\psi_{i+1}^j$$

$$= \delta z\left(K_{i+1}^{j-1} - K_{i-1}^{j-1}\right) - \left(\frac{2\,C\,\delta z^2}{\delta t}\right)\psi_i^{j-1} \tag{D.8}$$

with a tridiagonal coefficient matrix, which is be solved using a standard algorithm (e.g., Wang and Anderson, 1982; Remson and others, 1971; Anderson and others, 1984; Ferziger, 1981).

Boundary and Initial Conditions

Boundary conditions are treated by combining the hydrologic model of Freeze (1969) and the mathematical formalism of Mls (1987). The lower boundary is the simpler of the two, and is assumed to be saturated with some constant rate of flux, Q, in or out of the bottom boundary. Positive Q represents flow out of the problem domain, whereas negative Q represents flow into the problem domain. The upper boundary can have either specified rate of flux, R, or, when the upper boundary node becomes saturated, a specified pressure head of zero. Positive R represents flow into the problem domain (infiltration), whereas negative R represents flow out of the problem domain (evaporation). Deciding when to switch from specified flux to fixed is largely an arbitrary decision that can be argued, but this model assumes that all rainfall can infiltrate until $R > K_{sat}$, at which point the ground becomes saturated and excess rainfall runs off. For simplicity, rainfall rate is used for the upper boundary flux in the model. If the $R \leq K(\psi)$ at the upper boundary, then a flux boundary condition is used. If $K(\psi) < R < K_{sat}$ at the upper boundary, then $K(\psi)$ is set equal to R so that no ponding occurs. Finally, if the $R > K_{sat}$, then R is set equal to K_{sat}. An alternative boundary treatment, which might be more useful when modeling field data, would be to use a fixed head boundary with boundary pressure heads at each time increment given by a time series.

Flux across the upper boundary is given by Darcy's law

$$R = -K\left(\frac{\partial\psi}{\partial z} - 1\right) \tag{D.9}$$

where R is the rate of volumetric recharge per unit of surface area normal to the z-axis [L/T], The flux equation, (D.9), can be re-arranged to solve for the derivative

$$\frac{\partial\psi}{\partial z} = -\frac{R}{K} + 1 \tag{D.10}$$

A central difference approximation of (D.10), where spatial node 1 is imaginary and spatial node 2 lies on the flux boundary, is, after rearranging to solve for ψ_1^j,

$$\psi_1^j = \psi_3^j - 2\delta z\left(1 - R^j/K_2^{j-1}\right) \tag{D.11}$$

As before, the i subscripts are spatial indices and the j superscripts are temporal indices. To formulate the flux boundary finite difference approximation, (D.11) is substituted into (D.8), which is in turn rearranged to arrive at

$$-\left(K_1^{j-1} + 2K_2^{j-1} + K_3^{j-1} + \frac{2\,C\,\delta z^2}{\delta t}\right)\psi_2^j + \left(K_1^{j-1} + 2K_2^{j-1} + K_3^{j-1}\right)\psi_3^j$$

$$= \delta z\left(K_3^{j-1} - K_1^{j-1}\right) + 2\,\delta z\left(1 - R^j/K_2^{j-1}\right) - \left(\frac{2\,C\,\delta z^2}{\delta t}\right)\psi_2^{j-1} \tag{D.12}$$

When the upper boundary node becomes saturated and its pressure head is fixed, however, the number of linearized equations to be solve decreases by one, and the upper boundary finite difference approximation is

$$-\left(K_2^{j-1} + 2K_3^{j-1} + K_4^{j-1} + \frac{2\,C\,\delta z^2}{\delta t}\right)\psi_3^j + \left(K_3^{j-1} + K_4^{j-1}\right)\psi_3^j$$

$$= \delta z\left(K_4^{j-1} - K_2^{j-1}\right) - \left(\frac{2\,C\,\delta z^2}{\delta t}\right)\psi_3^{j-1} \tag{D.13}$$

Note that in (D.13) the boundary node expression is expanded around node 3 rather than node 2.

Some mass flux, Q, is allowed across the lower boundary, which Freeze (1969) relates to the regional water table. Thus the lower boundary finite difference approximation is

$$-\left(K^{j-1}_{nz-2} + 2\,K^{j-1}_{nz-1} + K^{j-1}_{nz}\right)\psi^{j}_{nz-2} + \left(K^{j-1}_{nz-2} + 2K^{j-1}_{nz-1} + K^{j-1}_{nz} + \frac{2\,C\,\delta z^2}{\delta t}\right)\psi^{j}_{nz-1}$$

$$= \delta z\left(K^{j-1}_{nz} - K^{j-1}_{nz-2}\right) - 2\,\delta z\left(1 - Q^{j}/K^{j-1}_{nz-2}\right) + \left(\frac{2\,C\,\delta z^2}{\delta t}\right)\psi^{j-1}_{nz-1} \qquad \text{(D.14)}$$

INPUT VARIABLES

Values of $K_{sat} = 1.3\times10^{-5}$ m/s (see Chapeter 1) and $\Theta_{sat} = 0.45$ from Murdoch (1987) are assumed on the basis of field and laboratory results. Murdoch's data also imply a zone of tension saturation from about -0.1 m $\leq \psi \leq$ 0.0 m, so ψ_{crit} = -0.1 m, and α = 10 m^{-1} was also assumed. Spatial grid increments of 0.02 m and temporal grid increments of 36 to 3600s were used in simulations of infiltration into a 1 m thick, homogeneous soil underlain by both an impermeable base (Q = 0) and a recharging leaky base ($Q \ll K_{sat}$).

COMPUTER PROGRAM

The finite difference model developed in the preceding pages was solved with the accompanying computer program written in Borland Turbo Pascal, v. 1.00a, on an Apple Macintosh 512KE microcomputer. The code is in standard Pascal except for ASCII file handling, an array-checking compiler directive, and the inclusion of ROM toolbox units for floating point arithmetic (SANE) and operating system interface (QUICKDRAW, MEMTYPES, OSINTF). The latter three units are used only to access the system clock, which can be excluded without substantially changing the program. Default array values of 60 spatial nodes and 1000 temporal nodes are used because of memory limitations.

Data are read from an ASCII disk file specified by the user, with values separated by carriage returns. The order of values is:

input file name (infile)
lower limit of tension saturation (phicrit)
saturated hydraulic conductivity (ksat)
lower node constant influx or outflux (q)

alpha (alph)
saturated volumetric water content (thetasat)
number of spatial grid nodes (nz)
number of temporal grid nodes (nt)
spatial grid increment (dz)
temporal grid increment (dt)
number of time increments between output file disk writes (dtwrite)
initial pressure heads (psi[1..nz] from ground surface down)
surface influx/outflux (r[1..nt])

Examination of the procedure *dataread* should further clarify input data file structure. Results are likewise written to an ASCII disk file, but this time with each entry separated by a CHR(9) tab and each line separated by a carriage return so that the data can be read by the Microsoft Excel or other graphics programs for editing and plotting.

```
program specified_flux_infiltration;

{*****************************************************************************

   Matrix solution of the localized expansion of the Richards equation
  for vertical infiltration. Upper boundary is specified flux, lower
  boundary is a water table with specified recharge. Upper boundary
  becomes fixed head if rainfall exceeds saturated hydraulic conductivity,
  otherwise surface conductivity is set equal to rainfall rate so that
  ponding cannot occur. Lower boundary has unit pressure head gradient
  if recharge/discharge term is zero. Vertical coordinate system is positive
  downward.

  Initial heads and constants are read in from an ASCII disk file with
  entries separated by carraige returns, and results are written to a
  second ASCII disk file compatible with Microsoft Excel (i.e. entries
  separated by chr(9) tabs).

  Default values are 60 spatial and 1200 temporal grid nodes.

  All variables are defined as global except in procedure thomas.

  written in Macintosh Turbo Pascal v. 1.00a

  Bill Haneberg
  John L. Rich Geomechanics Laboratory
  "Where Science goes for a good time"
  Department of Geology
  University of Cincinnati
  Cincinnati, Ohio 45221-0013

  version of 7/21/88

 *****************************************************************************}

{$R+}                            { array range checking checking }

uses                             { misc. Turbo Pascal compiler directives }
  sane,                          { see Borland Intl. documentation for }
  memtypes,                      { toolbox interface unit explanations }
  quickdraw,
  osintf;

type
  little_vector = array[1..60] of extended;
  big_vector = array[1..1200] of extended;

var
  saturated : boolean;           { depends on upper boundary condition }
  clock : datetimerec;           { Macintosh system clock record }
  t1,t2 : longint;               { dummy time variables }
  disk : text;                   { defines output device }
  ksat,                          { saturated hydraulic conductivity }
  q,                             { flux to water table; see Freeze, 1969 }
  alph,                          { power law constant }
  coeff,                         { specific storage capacity }
  stor,                          { combined storage constant }
  thetasat,                      { saturated volumetric water content }
  rain,                          { dummy variable for surface flux }
  time,                          { elapsed time }
  psicrit,                       { lower limit of tension saturation }
  maxdiff,                       { max. matrix inversion error }
  dz,                            { spatial grid increment }
  dt : extended;                 { temporal grid increment }
```

```
  k,                                  { actual hydraulic conductivity array }
  a,b,c,                              { Thomas algorithm column vectors }
  x,f,                                {      "          "        "    }
  psi :little_vector;                 { vector containing pressure heads }
  r : big_vector;                     { infiltration-evaporation rate vector }
  nz, nt,                             { number of spatial & temporal nodes }
  dtwrite,                            { # of time increments between disk writes }
  numeq,                              { number of equations to be solved }
  z,s,t : integer;                    { loop counters }
  texttype,
  textcreator : packed array [1..4] of char;
                                      { system file-creating parameters }

{************************************************************************}

procedure dataread;

{
  Prompts for initial data file name, opens initial data file, reads in
  data, and closes initial data file.
}

var
  infile, name : string;

begin
  writeln;
  write('name of initial data file to be read: ');
  readln(infile);
  writeln;
  writeln;
  reset(disk,infile);
  readln(disk,name);
  writeln('reading initial data file ',name,'... ');
  writeln;
  readln(disk,psicrit);
  readln(disk,ksat);
  readln(disk,q);
  readln(disk,alph);
  readln(disk,thetasat);
  readln(disk,nz);
  readln(disk,nt);
  readln(disk,dz);
  readln(disk,dt);
  readln(disk,dtwrite);

  for z :=  1 to nz do
    readln(disk,psi[z]);

  for t := 1 to nt do
    r[t] := 0.;
  t := 0;
  while not seekeof(disk) do                    { read in recharge until eof }
    begin
      t := t + 1;
      readln(disk,r[t]);
    end;

  t := 0;
  writeln;
  writeln('                                     ... finished reading initial data file. ');
  writeln;
  close(disk);
end;

{************************************************************************}
```

```
procedure fileopen;

{
  Opens disk text file for data output.  Remember to declare the variable
  disk : text as a global variable, and to close it at end of program!
}

var

  texttype,
  textcreator : packed array [1..4] of char;
  filename : string;

begin

  write('name for output disk file? ');
  readln(filename);
  writeln;

  rewrite(disk,filename);
  writeln(disk,'text file name: ',filename);
  writeln;
  writeln('=================================================================================');
  writeln;
  writeln(disk);
  writeln(disk,'ksat = ',chr(9),ksat,chr(9));
  writeln(disk,'q = ',chr(9),q,chr(9));
  writeln(disk,'alpha = ',chr(9),alph,chr(9));
  writeln(disk,'psicrit = ',chr(9),psicrit,chr(9));
  writeln(disk,'thetasat = ',chr(9),thetasat,chr(9));
  writeln(disk,'dz = ',chr(9),dz,chr(9));

  write(disk,chr(9));                      { insert two blank fields }
  write(disk,chr(9));

  for z := 1 to nz-2 do
      write(disk,(z-1)*dz:1:3, chr(9));

  writeln(disk);

  end;

(*****************************************************************************)


procedure filewrite;

{
  Writes one line of data to a disk opened in procedure fileopen.
}

begin

  write(disk,(time/3.6e03):3:3,chr(9));

  if t > 0 then
      write(disk,r[t],chr(9))
    else
      write(disk,r[1]-r[1],chr(9));

  for z := 2 to nz-1 do
    write(disk,(psi[z]):3:6,chr(9));

  writeln(disk);
```

```
end;

{*************************************************************************}

procedure initialization;

{
  Reads in initial heads and initializes assorted variables, opens and
  writes t = 0 data to output disk file.
}

begin

  writeln;
  writeln;
  writeln('===============================================================================');
  writeln;

  dataread;                              { read in raw data }
  fileopen;                              { open data output file }
  time := 0.;                            { set the simulation clock }
  psi[1] := psi[3]+2.*(psi[2]-psi[3]);   { set upper node }
  filewrite;                             { out initial heads on disk}
  clearscreen;

end;

{*************************************************************************}

procedure conduct;

{
  Fills hydraulic conductivity array k[1..nz] using values of psi
  from previous time step.
 }

begin

  for z := 2 to nz-1 do
    if psi[z] > psicrit then k[z] := ksat
      else  k[z] := ksat*exp(alph*(psi[z] + psicrit));

 end;

{*************************************************************************}

procedure fluxmatrix;

{
  Fills a,b,c, and f arrays to be used in procedure thomas for specified
  flux upper boundary. Notation after Wang and Anderson, 1982, Introduction
  to Groundwater Modeling.
}

begin

  saturated := false;

  numeq := nz-2;                         { how many equations to solve? }

  for z := 3 to nz-2 do                  { fill array interiors }

    begin

      if psi[z] < psicrit then           { tension saturated? }
```

```
        begin
          coeff := thetasat*exp(psi[z])/exp(psicrit);
          stor := 2.*coeff*sqr(dz)/dt;
        end
      else
        stor := 0.;

      a[z-1] := k[z-1] + k[z];
      b[z-1] := -(k[z-1] + 2.*k[z] + k[z+1] + stor);
      c[z-1] := k[z+1] + k[z];
      f[z-1] := dz*(k[z+1]-k[z-1]) - stor*psi[z];

    end;

                                             { upper flux boundary }

    if psi[2] < psicrit then
      begin
        coeff := thetasat*exp(psi[2])/exp(psicrit);
        stor := 2.*coeff*sqr(dz)/dt;
      end
    else
      stor := 0.;

    a[1] := 0.;
    b[1] := -(k[3] + 2.*k[2] + k[1] + stor);
    c[1] := k[3] + 2.*k[2] + k[1];
    f[1] := dz*(k[3]-k[1]) + 2.*dz*(1 - r[t]/k[2])*(k[1]+k[2]) - stor*psi[2];

                                             { lower flux boundary }


    if psi[nz-1] < psicrit then
      begin
        coeff := thetasat*exp(psi[nz-1])/exp(psicrit);
        stor := 2.*coeff*sqr(dz)/dt;
      end
    else
      stor := 0.;

      a[nz-2] := k[nz-2] + 2.*k[nz-1] + k[nz];
      b[nz-2] := -(k[nz-2] + 2.*k[nz-1] + k[nz] + stor);
      c[nz-2] := 0.;
      f[nz-2] := dz*(k[nz]-k[nz-2])-2.*dz*(k[nz-1]+k[nz])*(1 + q/k[nz-1]);
      f[nz-2] := f[nz-2] - stor*psi[nz-1];

  end;
{*****************************************************************************}

procedure satmatrix;

{
  Fills a,b,c, and f arrays to be used in procedure thomas for a saturated
  upper boundary. Notation after Wang and Anderson, 1982, Introduction to
  Groundwater Modeling.
}


begin

  saturated := true;
  numeq := nz-3;                        { how many equations to solve? }

  for z := 4 to nz-2 do                 { fill array interiors }

    begin
```

```
      if psi[z] < psicrit then              { tension saturated? }
        begin
          coeff := thetasat*exp(psi[z])/exp(psicrit);
          stor := 2.*coeff*sqr(dz)/dt;
        end
      else
        stor := 0.;

      a[z-2] := k[z-1] + k[z];
      b[z-2] := -(k[z-1] + 2.*k[z] + k[z+1] + stor);
      c[z-2] := k[z+1] + k[z];
      f[z-2] := dz*(k[z+1]-k[z-1]) - stor*psi[z];

    end;
                                            { upper flux boundary }

    if psi[3] < psicrit then
      begin
        coeff := thetasat*exp(psi[3])/exp(psicrit);
        stor := 2.*coeff*sqr(dz)/dt;
      end
    else
      stor := 0.;

    a[1] := 0.;
    b[1] := -(k[4] + 2.*k[3] + ksat + stor);
    c[1] := k[3] + k[4];
    f[1] := dz*(k[4]-ksat) - stor*psi[3];

                                            { lower flux boundary }


    if psi[nz-1] < psicrit then             { tension saturated? }
      begin
        coeff := thetasat*exp(psi[nz-1])/exp(psicrit);
        stor := 2.*coeff*sqr(dz)/dt;
      end
    else
      stor := 0.;

      a[nz-3] := k[nz-2] + 2.*k[nz-1] + k[nz];
      b[nz-3] := -(k[nz-2] + 2.*k[nz-1] + k[nz] + stor);
      c[nz-3] := 0.;
      f[nz-3] := dz*(k[nz]-k[nz-2])-2.*dz*(k[nz-1]+k[nz])*(1 - q/k[nz-1]);
      f[nz-3] := f[nz-3] - stor*psi[nz-1];

 end;
(****************************************************************************)

procedure boundaryheads;

{
  Calculates pressure head at imaginary nodes by extrapolating specified
  gradients from interior nodes.  These values are then used to calculate
  conductivity and the storage coefficient in the next time step.  Time
  steps must be kept small ( 1 min or less) to use this explicit
  linearization method.
}

begin
                                                        { upper boundary }
  psi[1] := psi[3]-2.*dz*(1-r[t]/ksat);

  if psi[1] > psicrit then k[1] := ksat
```

```
    else k[1] := ksat*exp(alph*(psi[1] + psicrit));

                                                        { lower boundary }
  psi[nz] := psi[nz-2] + 2.*dz*(1 - q/ksat);

  if psi[nz] > psicrit then k[nz] := ksat
    else  k[nz] := ksat*exp(alph*(psi[nz] + psicrit));

end;

(****************************************************************************)

procedure thomas (var thoma,thomb,thomc,thomf,thomx:little_vector;
                  how_many_eqs:integer);

{
  Thomas algorithm for solution of systems of linear equations with
  tridiagonal coefficient matrices.  Adapted from FORTRAN subroutine
  TRIDIA of Wang and Anderson, 1982, Introduction to Groundwater Modeling.
}

var
  i, nu : integer;
  alpha,
  beta,
  gamma : array[1..100] of extended;

begin

  alpha[1] := thomb[1];
  beta[1] := thomc[1]/alpha[1];
  gamma[1] := thomf[1]/alpha[1];

  for z := 2 to how_many_eqs do

    begin
      alpha[z] := thomb[z]-thoma[z]*beta[z-1];
      beta[z] := thomc[z]/alpha[z];
      gamma[z] := (thomf[z]-thoma[z]*gamma[z-1])/alpha[z];
    end;

  thomx[how_many_eqs] := gamma[how_many_eqs];
  nu := how_many_eqs-1;

  for z := 1 to nu do

    begin
      j := how_many_eqs-z;
      thomx[j] := gamma[j]-beta[j]*thomx[j+1];
    end;

 end;
(****************************************************************************)

procedure swapvalues;

{
  Swaps newly-calculated values from procedure tridia with old values.
}

var
  low : integer;
```

```
begin

  if saturated then low := 3
    else low := 2;

  for z := low to nz-1 do
    psi[z] := x[z - low + 1];

 end;

{*****************************************************************************}

procedure display;

{
  Displays real time, simulation time, error, and whatever else might
  seem worthwhile at the time.
}

var
  temp : longint;

begin

  if t = 1 then temp := t1
    else temp := t2;

  getdatetime(t2);                          { t2 is real time in seconds }

  gotoxy(20,10);
  write('increment real time:',(t2-temp):3,  s');

  gotoxy(20,11);
  write('elapsed real time:', (t2-t1):5,' s');

  gotoxy(20,12);
  write('simulation time: ',(time/3.6e03):3:2,' hrs.');

  gotoxy(20,13);
  write('infiltration rate: ',r[t],' m/s );

  gotoxy(20,14);
  write('surface hydraulic conductivity: ',k[2],' m/s');

  gotoxy(20,17);
  write('surface pressure head: ',psi[2]:2:4,  m  ');

  gotoxy(20,19);
  write('basal pressure head: ',psi[nz-1]:2:4,' m  ');

end;

{*****************************************************************************}

procedure checktime;

{
  Checks to see if current time is the specified multiple of time increments
  (dtwrite).  If so, data from current time are written to disk.  If not,
  move on to next time increment.
}

var
  timefactor : extended;

begin
```

```
  timefactor := t/dtwrite;
  if (timefactor - trunc(timefactor)) = 0.
    then filewrite;
end;

(*************************************************************************)

procedure cleanup;

{
  Closes disk file, prints end of job statement.
}

begin
  close(disk);                    { close ouput file }
  writeln;
  writeln;
  writeln('                                end of job');
  writeln;
  writeln('                       press RETURN to exit');
  writeln;
  readln;
end;

(*************************************************************************)

procedure checksaturation;

{
  Adjusts upper boundary to prevent ponding and calls appropriate
  matrix-filling procedure. If infiltration rate exceeds saturated
  conductivity, then the rate is set equal to conductivity and satmatrix
  is called. If infiltration rate exceeds actual surface conductivity but
  is below saturated conductivity, then surface conductivity is set equal
  to infiltration rate and fluxmatrix is called.  If infiltration rate is
  less than actual conductivity, then fluxmatrix is called.
}

begin

  if r[t] > ksat then                { saturated ground surface }
    begin
      r[t] := ksat;
      k[2] := ksat;
      psi[2] := 0.;
      satmatrix
    end;

  if r[t] > k[2] then                { unsaturated ground surface }
    begin                            { with no ponding }
      k[2] := r[t];
      fluxmatrix
    end
    else
      fluxmatrix;

end;

(*************************************************************************)
(*************************************************************************)

begin                           { main program }

  getdatetime(t1);              { starting real time }
  initialization;
```

```
  for t := 1 to nt do              { main time loop }

    begin
      time := time+dt;             { simulation time in seconds }
      conduct;                     { fill hydraulic conductivity matrix }
      boundaryheads;               { calculate head at imaginary nodes }
      checksaturation;             { decide which upper boundary condition }
      thomas(a,b,c,f,x,numeq);     { solve for pressure heads }
      swapvalues;                  { put x values into psi vector }
      display;                     { show important stuff }
      checktime;                   { and put them on the disk }
    end;                           { end of main time loop }

  cleanup;                         { close down everything and go home }

end.                               { end main program }

{****************************************************************************}
{****************************************************************************}
```

APPENDIX E
PERTURBATION SOLUTION OF THE LINEARIZED STEADY-STATE HILLSIDE FLOW EQUATION

GENERAL SOLUTION

Under steady state conditions the governing equation for modified Dupuit flow, equation (1.3), reduces to the nonhomogeneous, nonlinear ordinary differential equation

$$-\frac{R}{K}=\left[\frac{d^2h}{d\xi^2}\,h+\left(\frac{dh}{d\xi}\right)^2\right]\cos\beta-\frac{dh}{d\xi}\sin\beta \tag{E.1}$$

Now (E.1) can be linearized by assuming that water level, h, consists of two parts: an average component that remains constant along slope and a smaller perturbed component that varies along slope

$$h(\xi)=\bar{h}+\tilde{h}(\xi) \tag{E.2}$$

in which $\tilde{h} \ll \bar{h}$, so that substitution of (E.2) into (E.1) yields

$$-\frac{R}{K}=\left[\frac{\partial^2\tilde{h}}{\partial\xi^2}(\bar{h}+\tilde{h})+\left(\frac{\partial\tilde{h}}{\partial\xi}\right)^2\right]\cos\beta-\frac{\partial\tilde{h}}{\partial\xi}\sin\beta \tag{E.3}$$

The assumption that $\tilde{h} \ll \bar{h}$ allows all terms involving products of $\tilde{h}$ to vanish, so to first order in $\tilde{h}$ equation (E.3) becomes

$$-\frac{R}{K\,\bar{h}\cos\beta}=\frac{d^2\tilde{h}}{d\xi^2}-\frac{d\tilde{h}}{d\xi}\frac{\tan\beta}{\bar{h}} \tag{E.4}$$

which is a second order linear ordinary differential equation that can be solved using the method of undetermined coefficients (e.g. O'Neil, 1983; Boyce and DiPrima, 1977). For its homogeneous portion, (E.4) has the characteristic equation

$$m^2 + bm = 0 \quad \text{where} \quad b = \frac{-\tan\beta}{\bar{h}} \tag{E.5}$$

with eigenvalues

$$m_1 = -b$$
$$m_2 = 0 \tag{E.6 a,b}$$

For two real and distinct eigenvalues, a general solution to the homogeneous portion of (E.4) is

$$\tilde{h} = c_1 \exp(m_1\xi) + c_2 \exp(m_2\xi) \tag{E.7}$$

or, substituting (E.6 a,b) into (E.7),

$$\tilde{h} = c_1 \exp(-b\xi) + c_2 \tag{E.8}$$

The particular solution to the nonhomogeneous part of (E.4), $\tilde{h}_p$, must be differentiated at least once to arrive at the nonhomogeneous portion, so guess that $\tilde{h}_p$ is a first degree polynomial of the form

$$\tilde{h}_p = c_3\,\xi + c_4 \tag{E.9}$$

Now differentiate (E.9) and substitute the results into (E.4) to get

$$c_3 \frac{\tan\beta}{\bar{h}} = \frac{R}{K\,\bar{h}\cos\beta} \tag{E.10}$$

with $c_4 = 0$, and finally solve for the non-zero coefficient term

$$c_3 = \frac{R}{K\sin\beta} \tag{E.11}$$

The general solution to (E.4) is a linear combination of (E.8) and (E.11), hence

$$\tilde{h} = c_1 \exp(-b\xi) + c_2 + c_3 \xi \tag{E.12}$$

PARTICULAR SOLUTION

Constants c_1 and c_2 are found by evaluating the general solution (E.12) at both ends of the problem domain, $\xi = 0$ and $\xi = L$, where L is the length of the porous slab. This Appendix considers only the boundary conditions $\tilde{h} = 0$ at $\xi = 0$ and $\xi = L$, although there is no mathematical reason why other boundary conditions could not be evaluated. First evaluate (E.12) at $\xi = 0$ and solve for c_1 to get

$$c_1 = - c_2 \tag{E.13}$$

and substitute (E.13) into (E.12), this time evaluated at $\xi = L$, to arrive at

$$0 = - c_2 \exp(-bL) + c_2 + \frac{R}{K \sin \beta} \xi \tag{E.14}$$

Solving (E.14) for c_2

$$c_2 = - \frac{RL}{[1 - \exp(-bL)] K \sin \beta} \tag{E.15}$$

which gives, after substituting (E.13), (E.15), and (E.11) into (E.12) and rearranging,

$$\tilde{h} = \frac{R}{K \sin \beta}\left[\xi - L \frac{1 - \exp(-b\xi)}{1 - \exp(-bL)}\right] \tag{E.16}$$

which can be checked by differentiating with respect to ξ and substituting the results back into (E.4).

VERIFICATION OF THE NUMERICAL SOLUTION

Equation (E.16) can now be used to verify the numerical model developed in Chapter 1 by comparing the closed form solution of (E.4) with the results of the computer program for large values of t. To obtain a steady state numerical solution, the program *downhill_flow_rchge*, listed in Appendix C, was modified to handle constant, rather than time variant, recharge and also to write results to disk only after the last time increment. The computational parts of the program, however, remained unchanged. As shown in Figure E.1, which illustrates analytical and numerical solutions for values of $p = 0.025$, $R/K = 0.00024$, $\beta = 22^{o}$, and $t = 300$ hrs., agreement between analytical and numerical results is excellent for values of $\delta\xi = 5.0$ and 2.5 m, but large errors occur for $\delta\xi = 10.0$ m. Maximum error for $\delta\xi = 2.5$ m was 0.15%. The value of $R/K = 0.0024$ was obtained by averaging 1 m of rainfall, the average annual precipitation in Cincinnati, over 1 year and then dividing the result by $K = 1.3\times10^{-5}$ m/s.

Figure E.1 Comparison of steady state phreatic surface profiles generated with equation (E.16) and a modification of the computer program listed in Appendix C.

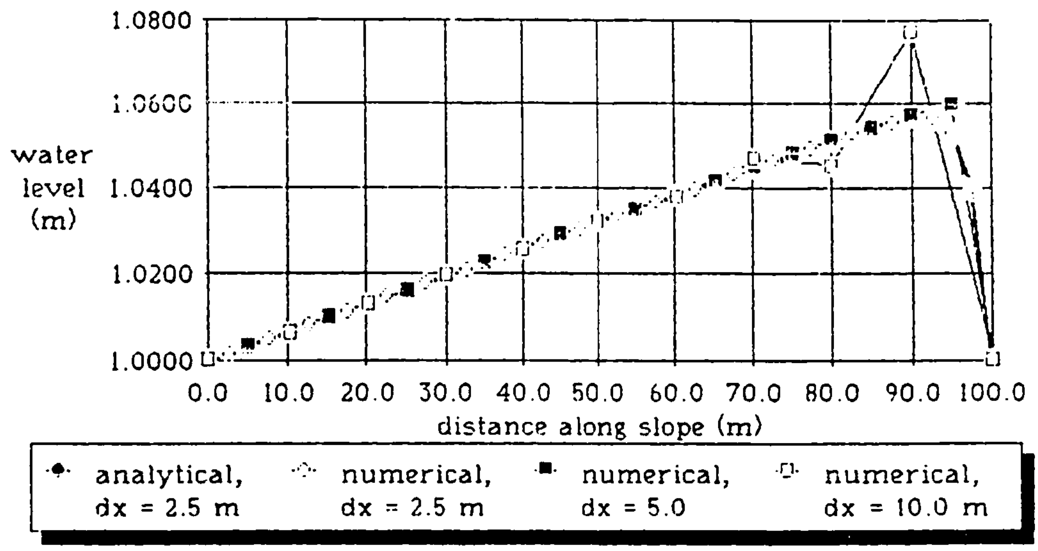

1.0800
1.0600
water level (m)
1.0400
1.0200
1.0000
0.0
10.0
20.0
30.0
40.0
50.0
60.0
70.0
80.0
90.0
100.0
distance along slope (m)
analytical, dx = 2.5 m
numerical, dx = 2.5 m
numerical, dx = 5.0
numerical, dx = 10.0 m

APPENDIX F
FACTOR OF SAFETY AGAINST SLIDING FOR A VARIABLY-SATURATED INFINITE SLOPE

LIMIT EQUILIBRIUM EQUATION

In this Appendix the standard infinite slope analysis is modified to take variable soil moisture profiles into account. Limit equilibrium slope stability analyses estimate a factor of safety against sliding by dividing the gravitational driving force into the resisting force due to soil shear strength. Variables used, along with a free-body diagram of a representative slope element, are schematically illustrated in Figure F.1. The approach taken here departs from standard infinite slope analyses by calculating the weight of a variably-saturated soil column as

$$\mathbf{W} = H\,\gamma_m + \gamma_w \int_0^H \theta(z)\,dz \tag{F.1}$$

where γ_m is the unit weight of the dry soil matrix, γ_w is the unit weight of water, and $\theta(z)$ is the volumetric water content, which is a function of both space and time during infiltration. For simplicity infiltration is assumed to be vertical only, so that water content is constant parallel to the slope. The gravitational driving force resolved parallel to the slip surface, **S**, is thus given by

$$\mathbf{S} = \mathbf{W} \sin\beta$$

$$= \left[H\,\gamma_m + \gamma_w \int_0^H \theta(z)\,dz \right] \sin\beta \tag{F.2}$$

Figure F.1 Schematic illustration of variables used in the variably-saturated infinite slope analysis. Pressure head increases hydrostatically volumetric water content is constant beneath water table (i.e. $\psi = 0$ isobar), but are functions of z above the water table. Bold face vectors denote forces acting on a representative slice of unit width.

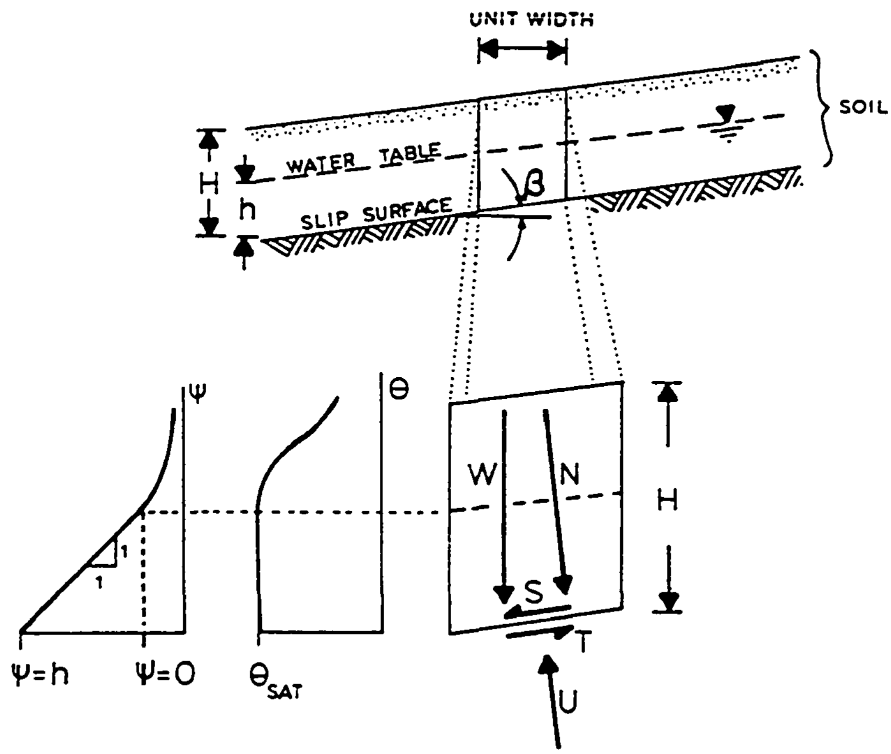
UNIT WIDTH
SOIL
H
h
WATER TABLE
SLIP SURFACE
β
Ψ
Θ
1
1
Ψ=h
Ψ=0
Θ_SAT
W
N
S
T
U
H

Shearing resistance is controlled by soil shear strength, τ, which is in general assumed to be of the form

$$\tau = c + \sigma_{eff} \tan \phi \tag{F.3}$$

along the failure surface, where c is cohesive strength (see below), σ_{eff} is effective normal stress, and ϕ is the angle of internal friction. Although the principle of effective stress in saturated media has been long established (Terzaghi, 1923), there is some debate in the literature concerning effective stress in partially-saturated media. For example, Fredlund (1987) fits curves to laboratory triaxial test data and proposes an unsaturated shear strength law that specializes to

$$\tau = c + \sigma_n \tan \phi - u_w \tan \phi^b \tag{F.4}$$

for atmospheric pore air pressure, where σ_n is total normal stress, u_w is pore water pressure, and ϕ^b is the slope of a plot of pore pressure *vs.* shear strength with constant normal stress. According to the laboratory data summarized by Fredlund, ϕ^b ranges from 5° to 15° less than ϕ for the soils tested. McTigue and others (1983), in contrast, propose an effective stress law that implies shear strength of the form

$$\tau = c + \left(\sigma_n + \frac{\theta}{n} u_w\right) \tan \phi \tag{F.5}$$

for one dimension and atmospheric air pressure, where θ is volumetric water content and n is porosity. Fredlund's law is backed by experimental data, but it lacks a sound theoretical foundation; the law proposed by McTigue and others, on the other hand, is theoretically rigorous but has no empirical substantiation. However, it is reasonable to assume that volumetric water content is fairly close to saturation when thin colluvium hillsides near

Cincinnati are in danger of failing, so the error introduced by assuming that a classical shear strength criterion of the form

$$\tau = c + (\sigma_n - u_w) \tan \phi \tag{F.6}$$

applies to slightly unsaturated soil will be negligible. Shearing resistance in natural clays undergoing progressive failure is controlled by residual shear strength (Skempton, 1964, 1985), in which zero cohesive strength is assumed, giving a failure criterion of the form

$$\tau = (\sigma_n - u_w) \tan \phi_r \tag{F.7}$$

where ϕ_r is the residual angle of internal friction. Integrating along the failure surface beneath a representative element of unit width gives the resisting force, **T**

$$\mathbf{T} = (\mathbf{N} - \mathbf{U}) \tan \phi_r \tag{F.8}$$

where **N** is soil weight resolved normal to the failure surface and **U** is the buoyant normal force counteracting **N**. These are given by

$$\mathbf{N} = \mathbf{W} \cos \beta$$

$$= \left[H\, \gamma_m + \gamma_w \int_0^H \theta(z)\, dz \right] \cos \beta \tag{F.9}$$

and

$$\mathbf{U} = \psi\, \gamma_w \cos \beta \tag{F.10}$$

hence

$$\mathbf{T} = \left[H\, \gamma_m + \gamma_w \int_0^H \theta(z)\, dz - \psi\, \gamma_w \right] \cos \beta \tan \phi_r \tag{F.11}$$

Division of (F.2) into (F.11) yields the factor of safety for a partially saturated infinite slope

$$
\begin{aligned}
F &= T/S \\
&= \frac{(N - U)}{S} \tan \phi_r \\
&= \frac{\left[H\,\gamma_m + \gamma_w \int_0^H \theta(z)\,dz - \psi\,\gamma_w \right] \tan \phi_r}{\left[H\,\gamma_m + \gamma_w \int_0^H \theta(z)\,dz \right] \tan \beta}
\end{aligned}
\tag{F.12}
$$

SPECIAL CASES

Cases of $\psi = 0$ and $\psi = H$

Equation (F.12) can be specialized to recover two commonly-used simplifications. For a hillside in which the water table coincides with the failure surface, $\psi = 0$ and after substitution (F.12) simplifies to

$$
F = \frac{\tan \phi_r}{\tan \beta} \tag{F.13}
$$

For a hillside saturated to the ground surface, $\psi = H$ and $\theta(z) = n$, so

$$
F = \left(1 - \frac{\psi_w}{\psi_m + n\,\psi_w} \right) \frac{\tan \phi_r}{\tan \beta} \tag{F.14}
$$

Inspection shows that the sum $\psi_m + n\psi_w$ is equal to the saturated unit weight of the soil, ψ_{sat}, and (F.14) becomes

$$F = \left(1 - \frac{\psi_w}{\psi_{sat}}\right) \frac{\tan \phi_r}{\tan \beta} \tag{F.15}$$

Finally, because the unit weight of water is roughly half the saturated unit weight of most soils, equation (F.15) can be further simplified to

$$F = \frac{\tan \phi_r}{2 \tan \beta} \tag{F.16}$$

Case of Constant θ

Field data from the Delhi Pike landslide complex suggest that it is a reasonable first approximation to assume that **θ** is constant with depth, and under this condition (F.12) can be simplified to

$$F = \frac{\left[\psi_m + \psi_w \left(\theta - \frac{\psi}{H}\right)\right] \tan \phi_r}{\left(\psi_m + \psi_w\right) \tan \beta} \tag{F.17}$$

The problem remains complicated, however, because in unsaturated porous media $\theta = f(\psi)$ and (F.13) is nonlinear in ψ However, laboratory measurements of water content *vs.* pressure head in colluvium samples from Delhi Pike (Murdoch, 1987) suggest that, if hysteresis is ignored for simplicity, water content may be approximated as

$$\theta = n \exp\left\{\alpha(\psi - \psi_{sat})\right\} \tag{F.18}$$

for $\psi < \psi_{sat}$ and

$$\theta = n \tag{F.19}$$

for for $\psi \geq \psi_{sat}$, where n is porosity, ψ_{sat} is the lower limit of tension saturation, and α is a constant. Thus for constant θ, F can be calculated by substituting either (F.18) or (F.19) as appropriate into (F.17).

SENSITIVITY ANALYSIS

Changes in F in response to changes in the values of variables can be examined using a relatively simple form of sensitivity analysis (USDA Forest Service, 1987). Average values for each of the variables in (F.12) are assumed and used to estimate a baseline factor of safety against sliding, F_{avg}. Then, for a generic variable x, the value of each variable is changed by small increments within reasonable bounds while the remaining values are held constant, and the percent change in factor of safety 100 $(F - F_{avg})/F_{avg}$ is plotted against the normalized percent change in that variable 200 $(x - x_{avg})/(x_{max} - x_{min})$. The latter range is chosen so that all of the independent variables can be plotted on the same axis over the range of -100% to +100%.

The accompanying BASIC computer program *SENSITIVITY.BAS* evaluates the sensitivity of the infinite slope stability equation for $\theta(z)$ = constant over specified ranges β, ϕ_r, γ_m, and ψ. Results for typical Cincinnati thin colluvium hillside values are shown in Figure F.2, and show that the stability equation is very sensitive to changes in ψ, but almost equally insensitive to changes in β, ϕ_r, and γ_m. Because β, ϕ_r, and γ_m might be assumed to be relatively constant through time, the sensitivity analysis suggests that basal pressure head, ψ, is the critical value controlling stability.

EVALUATION OF CRITICAL BASAL PRESSURE

The factor of safety equation (F.8) can be set equal to unity re-arranged to solve for the critical basal pressure head at failure

Figure F.2 Sensitivity of the factor of safety equation for constant θ and variable β, ϕ_r, γ_m, H, and ψ. Variable ranges, which were chosen as representative of thin colluvium hillsides in the Cincinnati area, are $1 \leq H \leq 2$ m, $1000 \leq \gamma_m \leq 2000$ kg m^{-3}, $20° \leq \beta \leq 28°$, $20° \leq \phi_r \leq 25°$, and $0 \leq \psi \leq 2$ m H_2O. Other constant are $n = 0.45$, $\alpha = 5$, $\psi_{crit} = -0.1$ m H_2O, $\gamma_w = 981$ kg m^{-3}, and $F_{avg} = 0.43$.

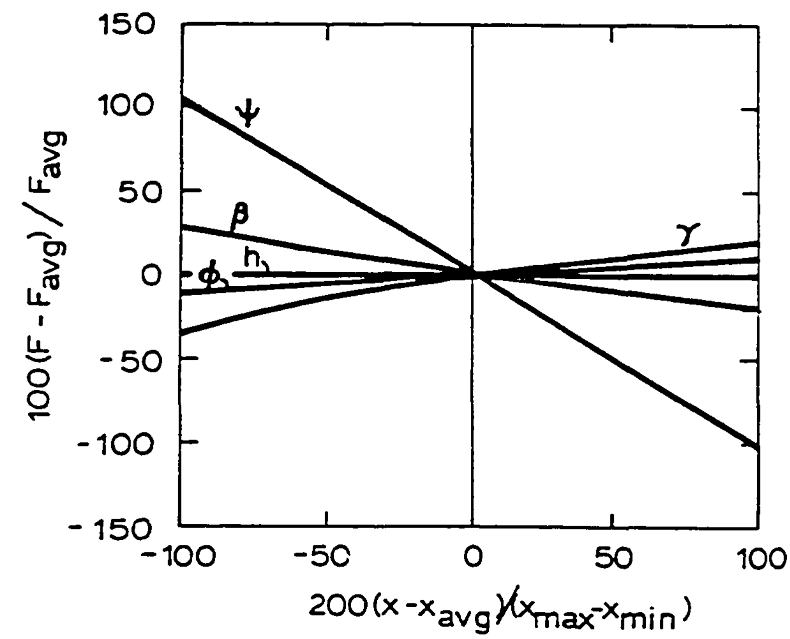

150
100
50
0
-50
-100
-150
-100
-50
0
50
100
$100(F - F_{avg})/F_{avg}$
$200(x - x_{avg})/(x_{max} - x_{min})$
ψ
β
γ
ϕ
h

$$\psi_{crit} = -\left(\frac{\tan \beta}{\tan \phi_r} - 1\right)\left(H \frac{\gamma_m}{\gamma_w} - \int_0^H \theta(z)\, dz\right) \tag{F.20}$$

Again assuming that θ is constant with depth

$$\psi_{crit} = -H\left(\frac{\tan \beta}{\tan \phi_r} - 1\right)\left(\frac{\gamma_m}{\gamma_w} - \theta\right) \tag{F.21}$$

Critical basal pressure head at failure can then be estimated by iterating either (F.18) or (F.19), as appropriate, and (F.21) to convergence as shown in the accompanying BASIC program *PSICRIT.BAS*. Figure F.3 shows that ψ_{crit} clusters around zero for typical values of β and ϕ_r, so in general Cincinnati area thin colluvium hillsides should be stable as long as $\psi < -1$ m H_2O along potential failure surfaces. This estimate agrees with many observations that these hillsides fail during winter and spring months, when the colluvium is moist and susceptible to rapid water level fluctuations.

Figure F.3 Critical basal pressure head at failure for variably-saturated infinite slope, calculated using typical values for thin colluvium hillsides in Cincinnati.

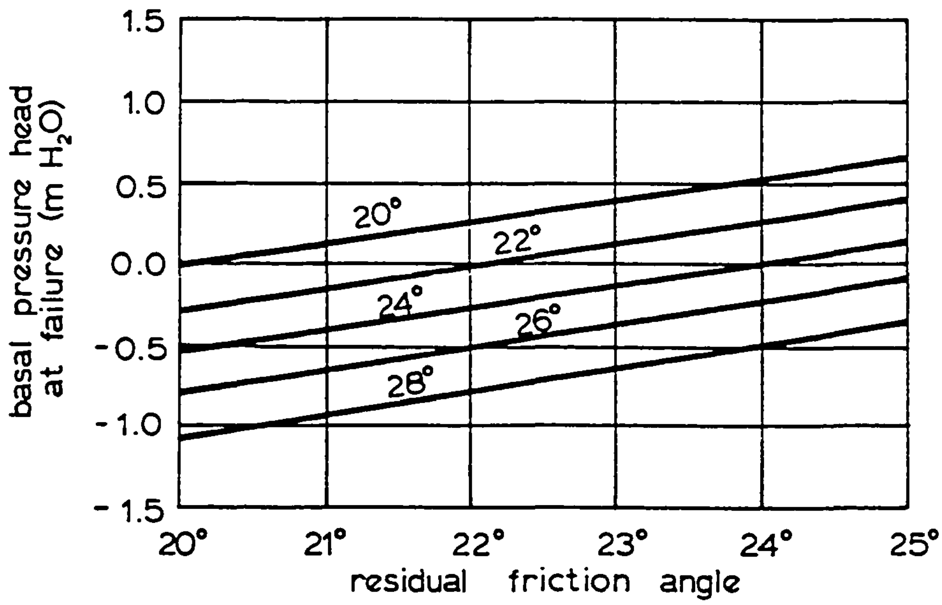
basal pressure head at failure (m H_2O)
1.5
1.0
0.5
0.0
-0.5
-1.0
-1.5
20°
22°
24°
26°
28°
20°
21°
22°
23°
24°
25°
residual friction angle

```
'   SENSITIVITY.BAS

'   Program to evaluate sensitivity of factor of safety equation for an
'   unsaturated or saturated infinite slope with water content as function
'   of pressure head. Output is written to an ASCII disk file compatible with
'   Microsoft Excel.

'   William C. Haneberg
'   John L. Rich Geomechanics Laboratory
'   Department of Geology
'   University of Cincinnati
'   Cincinnati, OH 45221-0013

'   written in Macintosh BASIC, v. 3.0

'   version of September 1988

'                       VARIABLES

'   hiphi = maximum angle of friction
'   lophi = minimum angle of friction
'   avgphi = average angle of friction
'   himatrix = maximum matrix unit weight
'   lomatrix = minimum matrix unit weight
'   avgmatrix = average matrix unit weight
'   hithick = maximum soil thickness
'   lothick = minimum soil thickness
'   avgthick = average soil thickness
'   hipsi = maximum basal pressure head
'   lopsi = minimum basal pressure head
'   avgpsi = average basal pressure head
'   hibeta = maximum slope angle
'   lobeta = minimum slope angle
'   avgbeta = average slope angle
'   theta = volumetric water content = f(psi)
'   poros = porosity (= saturated volumetric water content)
'   alpha = constant term in pressure-water content eqn.
'   psicrit = lower limit of tension saturation
'   water = unit weight of water
'   degstorads = degree to radian conversion factor = 57.29...
'   F = factor of safety against sliding
'   Favg = baseline factor of safety using average values

'   TYPICAL VALUES FOR CINCINNATI COLLUVIUM HILLSIDES

degstorads = 57.29577951#
poros = .45
alpha = 5
psicrit = -.1
water = 981
himatrix = 2000
lomatrix = 1000
hibeta = 30
lobeta = 20
```

```
PRINT

PRINT "delta phi";CHR$(9);"delta F"
FOR angle = lophi TO hiphi STEP .5
   phi = angle/degstorads
   GOSUB calculate
   deltaF = 100*(F-Favg)/Favg
   deltaphi = 200*(phi-avgphi)/(hiphi/degstorads-lophi/degstorads)
   PRINT deltaphi;CHR$(9);deltaF
NEXT
phi = avgphi
PRINT

PRINT "delta beta";CHR$(9);"delta F"
FOR angle = lobeta TO hibeta
   beta = angle/degstorads
   GOSUB calculate
   deltaF = 100*(F-Favg)/Favg
   deltabeta = 200*(beta-avgbeta)/(hibeta/degstorads-lobeta/degstorads)
   PRINT deltabeta;CHR$(9);deltaF
NEXT
beta = avgbeta
PRINT

PRINT "delta thick";CHR$(9);"delta F"
FOR thick = lothick TO hithick STEP .25
   GOSUB calculate
   deltaF = 100*(F-Favg)/Favg
   deltathick = 200*(thick-avgthick)/(hithick-lothick)
   PRINT deltathick;CHR$(9);deltaF
NEXT
thick = avgthick
PRINT

PRINT "delta matrix";CHR$(9);"delta F"
FOR matrix = lomatrix TO himatrix STEP 100
   GOSUB calculate
   deltaF = 100*(F-Favg)/Favg
   deltamatrix = 200*(matrix-avgmatrix)/(himatrix-lomatrix)
   PRINT deltamatrix;CHR$(9);deltaF
NEXT
matrix = avgmatrix
PRINT

CLOSE #1

END


'   SUBROUTINE TO CALCULATE FACTOR OF SAFETY

calculate:
   IF psi < psicrit THEN theta = poros*EXP(alpha*(psi-psicrit))
   IF psi => psicrit THEN theta = poros
```

```
   F = (matrix + water*(theta-psi))/(matrix+water*theta)
   F = F*TAN(phi)/TAN(beta)
RETURN
```

```
'   PSICRIT.BAS

'   Program to calculate critical basal pressure head for stability of an
'   unsaturated or saturated infinite slope with water content as function
'   of pressure head. Results are written to an ASCII disk file compatible
'   with Microsoft Excel.

'   William C. Haneberg
'   John L. Rich Geomechanics Laboratory
'   Department of Geology
'   University of Cincinnati
'   Cincinnati, OH 45221-0013

'   written in Macintosh BASIC, v. 3.0

'   version of August 1988

'                          VARIABLES
'
'   tolerance = maximum allowable error
'   difference = error in given iteration
'   oldvalue = dummy variable
'   thickness = thickness of soil [L]
'   theta = actual volumetric water content
'   thetasat = saturated volumetric water content
'   alpha = constant term in pressure-water content eqn.
'   hcrit = lower limit of tension saturation [L]
'   matrix = unit weight of soil matrix [WEIGHT/L^3]
'   water = unit weight of water [WEIGHT/L^3]
'   phi = residual angle of internal friction [DEGREES]
'   lophi, hiphi = upper and lower limites of residual friction angle
'   beta = slope angle [DEGREES]
'   lobeta, hibeta = upper and lower limits of slope angle
'   height = pressure head at failure
'   degstorads = degree to radian conversion factor = 57.29...
'   count = iteration counter
'   slope = index variable for phi
'   strength = index variable for beta

'   TYPICAL VALUES FOR CINCINNATI COLLUVIUM

tolerance = .0000001
initialheight = -1!
difference =1000
thickness = 1.5
thetasat = .45
alpha = 5
hcrit = -.1
matrix = 1525
water = 981
lophi = 20
hiphi = 25
lobeta = 20
hibeta = 30
```

```
lophi = 20
hiphi = 25
lobeta = 20
hibeta = 30
hithick = 2
lothick = .5
hipsi = 2
lopsi = -2

'   GET OUPUT FILE NAME AND OPEN DISK FILE FOR OUTPUT

outfile$=FILES$(0,"enter output file name")
IF outfile$ = "" THEN END
OPEN outfile$ FOR OUTPUT AS *1

PRINT"SENSITIVITY ANALYSIS OF PARTIALLY-SATURATED INFINITE SLOPE"
PRINT
PRINT"delta(variable) is normalized to +/- 100% of half-range about the
average"
PRINT
PRINT*1,"porosity =",CHR$(9),poros
PRINT*1,"alpha = ",CHR$(9),alpha
PRINT*1,"psi crit = ",CHR$(9),psicrit
PRINT*1, "unit wt. water =",CHR$(9),water
PRINT*1,"unit wt. matrix = ",CHR$(9),lomatrix,CHR$(9),"to",CHR$(9),himatrix
PRINT*1,"beta = ",CHR$(9),lobeta,CHR$(9),"to",CHR$(9),hibeta
PRINT*1,"phi = ",CHR$(9),lophi,CHR$(9),"to",CHR$(9),hiphi
PRINT*1,"psi = ",CHR$(9),lopsi,CHR$(9),"to",CHR$(9),hipsi
PRINT*1,"soil thickness = ",CHR$(9),lothick,CHR$(9),"to",CHR$(9),hithick

'   CALCULATE AVERAGE VALUES

avgmatrix = (himatrix+lomatrix)/2!: matrix = avgmatrix
avgthick = (hithick+lothick)/2!: thick = avgthick
avgphi = (hiphi+lophi)/2!/degstorads: phi = avgphi
avgbeta = (hibeta+lobeta)/2!/degstorads: beta = avgbeta
avgpsi = (hipsi+lopsi)/2!: psi = avgpsi

GOSUB calculate
Favg = F
PRINT*1,"Favg =",CHR$(9),Favg
PRINT

'   CALCULATE CHANGE IN F AS CONTROLLED BY CHANGES IN EACH CONTROL
'   PARAMETER (PSI/H, BETA, PHI, MATRIX)

PRINT "delta psi";CHR$(9);"delta F"
FOR psi = lopsi TO hipsi STEP .25
   GOSUB calculate
   deltaF = 100*(F-Favg)/Favg
   deltapsi = 200*(psi-avgpsi)/(hipsi-lopsi)
   PRINT deltapsi;CHR$(9);deltaF
NEXT
psi = avgpsi
```

```
degstorads = 57.29577951#
count = 0

outfile$=FILES$(0,"enter output ASCII file name:")
IF outfile$ = "" THEN END

OPEN outfile$ FOR OUTPUT AS #1

PRINT #1,
PRINT #1,"CRITICAL BASAL PRESSURE HEAD FOR FAILURE OF INFINITE SLOPE"
PRINT #1,
PRINT #1,"soil thickness = ";thickness
PRINT #1,"saturated water content = ";thetasat
PRINT #1,"alpha = ";alpha
PRINT #1,"lower limit tension saturation = ";hcrit
PRINT #1,"matrix unit weight = ";matrix
PRINT #1,"water unit weight = ";water
PRINT #1,"iteration tolerance = ";tolerance
PRINT #1,
PRINT #1,
PRINT #1, "phi";CHR$(9);"psi crit"
FOR slope = lobeta TO hibeta
     beta = slope/degstorads
     PRINT #1, CHR$(9);"beta =";slope;" degrees"
   FOR strength = lophi TO hiphi STEP .5
       height = initialheight
       difference = 1000
       phi = strength/degstorads
       WHILE difference > tolerance
           count = count + 1
           oldvalue = height
           IF height > hcrit THEN theta = thetasat
           IF height <= hcrit THEN theta = thetasat*EXP(alpha*(height-hcrit))
           height = -thickness*(matrix + theta*water)*(TAN(beta)/TAN(phi) -
1!)/water
           difference = ABS(height - oldvalue)
       WEND
       PRINT #1, phi*degstorads;CHR$(9);height
  NEXT
  PRINT #1,
NEXT
CLOSE #1
END
```

APPENDIX G
JANBU SLOPE STABILITY ANALYSIS AND ESTIMATE OF DRAIN SPACING

JANBU COMPUTER PROGRAM

The accompanying FORTRAN-77 (with 8x extensions) computer program uses Janbu's (1973) method of slices to estimate the stability of slopes with irregularly-shaped shear surfaces. This program is limited to homogeneous soil with no external loading, although the generalized procedure of slices is capable of treating layered and inhomogeneous soils, distributed and point loads applied at the ground surface, and earthquake loads. Also, because the program was designed to analyze the stability of natural hillsides, cohesionless residual shear strength is assumed. Soil and water weights for each slice are calculated by integrating the volume of each slice beneath the ground, phreatic, and slip surfaces using the trapezoid rule (see subroutine trapzd), and subtracting the appropriate integrals from each other. The line of action of the horizontal interslice force, E, at the i^{th} interface is assumed to act at a height $h_i = (g_i - s_i)/3$, where g_i and s_i are the heights of the ground and slip surfaces at the i^{th} interface, and at an angle that is the average of the slip surface slopes of the two adjacent slices. The iterative procedure used to solve for interslice shear and horizontal normal forces was taken directly from Janbu (1973, p. 69).

Required data are read into the program from a user-specified ASCII disk file in the following order:

initial guess at factor of safety [real]
unit weight of soil [real]
unit weight of water [real]
angle of internal friction [real]
iteration tolerance [real]
number of slices [integer]

x(1), ground(1), water(1), slip(1) [real]

.

.

.

x(slices+1), ground(slices+1), water(slices+1), slip(slices+1) [real]

where x(n) is a vector containing the horizontal coordinates of each interface between slices, ground(n) is a vector containing the vertical coordinates of the ground surface, water(n) is a vector containing the vertical coordinates of the phreatic surface, and slip(n) is a vector containing the vertical coordinates of the potential slip surface.

APPLICATION TO DELHI PIKE

The Janbu analysis program described above was used to evaluate the accuracy of the infinite slope simplification developed in Appendix E and used in Chapter 3 of this dissertation. Data from a trench at Delhi Pike, excavated by R.W.Fleming (personal communication), were used to determine ground and slip surfaces and to divide the hillside into 21 slices (Figure G.1). Soil weight was estimated using values of 70% fine grained matrix with a unit weight of 19,600 N/m^3 and 30% limestone blocks with a unit weight of

Table G.1 Comparison of Janbu and Infinite Slope Analyses

phreatic surface	@ slip surface	@ ground surface
soil unit weight	22.0x10^3 N/m^3	22.0x10^3 N/m^3
water unit weight	9.8x10^3 N/m^3	9.8x10^3 N/m^3
residual friction angle	22°	22°
average slope angle	18°	18°
F_{janbu}	1.25	0.64
$F_{infinite}$	1.24	0.62
error(infinite)	-0.8%	-3.1%

Figure G.1 Approximation of hillside geometry at Delhi Pike used in Janbu stability analysis.

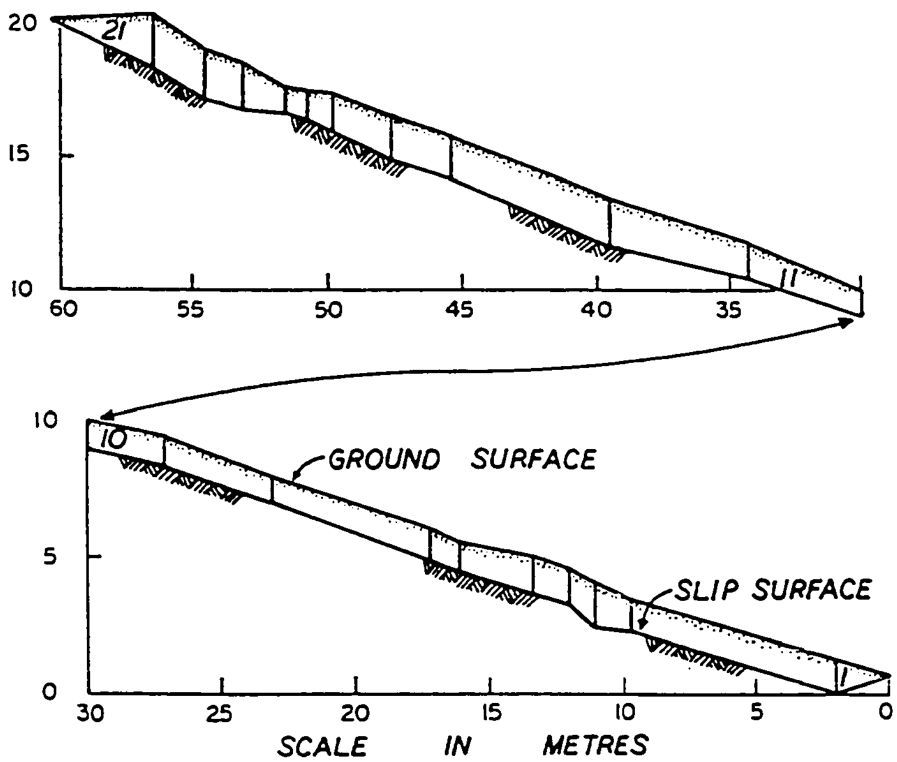
20
21
15
10
60
55
50
45
40
35
11
10
10
GROUND SURFACE
5
SLIP SURFACE
1
0
30
25
20
15
10
5
0
SCALE IN METRES

26,600 N/m^3, and a residual angle of internal friction of 22° was assumed on the basis of direct shear test data. Both matrix unit weight and residual friction angles were selected using laboratory data provided by R.W. Fleming (personal communication). Factors of safety against sliding, F, calculated using both the Janbu and the infinite slope methods for completely saturated and completely unsaturated hillsides at Delhi Pike are shown above in Table G.1. As expected, the Janbu method predicts higher factors of safety because it takes interslice forces into account; however, this difference is negligible because changes in slip surface geometry that produce non-zero differences in interslice forces (dE and dT in Janbu's notation) across each slice are minimal, and for practical purposes the hillside is an infinite slope.

ESTIMATE OF DRAIN SPACING

If a steady-state phreatic surface were to exist (see Chapters 2 and 3 for a discussion of this possibility), how closely would drains have to be spaced to maintain acceptable water levels throughout the entire hillside at Delhi Pike? The infinite slope analysis validated above can be combined with the method of Schmid and Luthin (1964) to give a first approximation of drain spacing necessary to stabilize thin colluvium hillsides such as those at Delhi Pike under two sets of conditions: the most extreme case of steady-state recharge equal to saturated hydraulic conductivity and the a extreme case of steady-state recharge equal to the 100 yr. rainfall distributed over 24 hrs.

Most Extreme Case

For steady-state recharge equal to hydraulic conductivity

$$R/K = 1 \times 10^0 \qquad \text{(G.1)}$$

where R is recharge and K is saturated hydraulic conductivity of the soil, and

$$\alpha = 0.32 \tag{G.2}$$

where α is the slope of the impermeable substrate. Using (G.1) and (G.2), Figure 2 of Schmid and Luthin gives a value of

$$L/H = 2\times10^{0} \tag{G.3}$$

where L is distance between drains and H is critical water level that must not be exceeded.

For hillsides such as those at Delhi Pike assume typical values of

$\phi_r = 22^{o}$	(residual friction angle)
$\beta = \arctan\alpha = 18^{o}$	(slope angle)
$D = 1.5$ m	(soil thickness)
$\gamma_{soil} = 2.0\text{x}104\ N/m^3$	(saturated soil unit weight)
$\gamma_{water} = 9.8\text{x}103\ N/m^3$	(water unit weight)

and solve the standard infinite slope stability equation for water level, H, at F = 1

$$H = -D\,\frac{\gamma_{soil}}{\gamma_{water}}\left(\frac{\sin\beta}{\tan\phi_r} - \cos\beta\right) \tag{G.4}$$

Now substitution of the typical values into (G.4) yields

$$H \approx 6\text{x}10^{-1}\ m \tag{G.5}$$

and subsequent substitution of (G.5) into (G.3) gives minimum drain spacing necessary to maintain stability

$$L \approx 1\text{x}10^{-0}\ m \tag{G.6}$$

Less Extreme Case

It is unlikely that R = K can be maintained over long periods of time, so for a less extreme situation assume that R is equal to the 100 yr. maximum daily rainfall infiltrates over a period of 24 hrs. From Chow and others (1988), the 100 yr. rainfall for the Cincinnati area is 0.15 m/24 hrs., or 1.7×10^{-6} m/s, and from Chapter 1, $K = 1.3 \times 10^{-5}$ m/s, so

$$R/K = 1.3 \times 10^{-1} \tag{G.7}$$

and from Schmid and Luthin (1964, Figure 2)

$$L/H = 5 \times 10^{0} \tag{G.8}$$

so, recalling $H \approx 6 \times 10^{-1}$ m from (G.5) critical drain spacing is

$$L \approx 3 \times 10^{0} \text{ m} \tag{G.9}$$

for the less extreme case.

Even if recharge is reduced by another order of magnitude, $R/K = 1.5 \times 10^{-2}$, $L/H = 2.5 \times 10^{1}$ and $H \approx 1.5 \times 10^{1}$ m. With the value of K assumed here, however, this low rate of recharge corresponds to daily rainfall of 0.07 to 0.08 m. For comparison, the maximum daily rainfall during spring 1988 was about 0.05 m, which suggests that $R/K \approx 10^{-2}$ is too low for design purposes and a more conservative estimate of drain spacing would be on the order of $10^{0} < L < 10^{1}$ m.

```
      program janbu

C     -----------------------------------------------------------------

C     Stability analysis for homogeneous soil slopes as described in
C     N. Janbu, 1973, Slope stability calculations, IN R.C. Hirschfeld
C     & S.J. Poulos, eds., Embankment-Dam Engineering:Wiley-Interscience.

C     This program does not treat distributed surface loads, point
C     surface loads, or applied horizontal loads, but may be extended
C     to do so; see Janbu (1973) for explanation.

C     Input data are read from a user-specified ASCII file, and results
C     are written to a second ASCII disk file. Default vector size of 25
C     can accomondate up to 24 slices.

C     Originally written and run in Microsoft FORTRAN-77 with 8x
C     extensions (do while...repeat, do..end do, if..then..end if)
C     on an Apple Macintosh 512KE. If it won't work on your computer,
C     that's not my problem.

C     William C. Haneberg
C     John L. Rich Geomechanics Laboratory
C     Department of Geology
C     University of Cincinnati
C     Cincinnati, OH 45221-0013

C     September 1988

C     -----------------------------------------------------------------

C          variable list...

C     x        vector of x-coordinates
C     slip     vector of z-coordinates for slip surface
C     water    vector of z-coordinates for phreatic surface
C     ground   vector of z-coordinates for ground surface
C     beta     vector of slip surface slopes for each slice
C     tanalpha average slope between two adjacent slices
C     e        vector of interslice horizontal forces
C     t        vector of interslice vertical forces
C     h        vector of line of action heights for e
C     dw       vector of soil weight for each slice
C     du       vector of water weight for each slice
C     de       vector of interslice horiz. force derivatives
C     dt       vector of interslice vertical force derivatives
C     n        vector of n-factors for each slice
C     area1    area of slice beneath ground surface
C     area2    area of slice beneath phreatic surface
C     area3    area of slice beneath slip surface
C     oldf0    factor of safety without interslice forces
C     oldfT    factor of safety for with interslice forces
C     new      dummy factor of safety variable during iterations
C     wetwt    moist unit weight of soil
C     watwt    unit weight of water
C     phi      residual angle of internal friction
```

```
C   toler     maximum allowable error per iteration
C   differ    error per iteration
C   relerr    relative error between oldf0 and oldf1
C   drive     driving forces for a given slice
C   resist    resisting forces for a given slice
C   dsum      sum of driving forces for all slices
C   rsum      sum of resisting forces for all slices
C   degrad    degree to radian conversion factor (a constant)
C   i         vector index
C   count     loop counter
C   slices    number of slices

C   ------------------------------------------------------------------

C        declare all variables...

    implicit none

    real*4 slip(25),water(25),ground(25),dw(25),du(25),n(25),x(25)
    real*4 e(25),t(25),h(25),de(25),dt(25),beta(25),drive(25)
    real*4 resist(25)
    real*4 area1,area2,area3,tanalpha,dsum,rsum,desum,dtsum
    real*4 oldf0, oldf1,wetwt,watwt,toler,length,depth,crack,phi
    real*4 factor,new,differ,degrad,relerr
    integer*2 slices,i,count
    character*25 infile,outfile

C   ------------------------------------------------------------------

C        print greeting, get name of input and output ASCII files...

    write(9,120)
120   format(16X,'JANBU STABILITY ANALYSIS FOR HOMOGENEOUS SLOPES')
    print*
    print*
    write(*,121)
121   format(30X,'William C. Haneberg')
    write(*,122)
122   format(22X,'John L. Rich Geomechanics Laboratory')
    write(*,123)
123   format(30X,'Department of Geology')
    write(*,124)
124   format(28X,'University of Cincinnati')
    write(*,125)
125   format(28X,'Cincinnati, OH 45221-0013')
    print*
    write(*,126)
126   format(29X,'version of October 1988 )
    print*
    print*
    write(*,127)
127   format(19X,'file names must be less than 25 characters')
    print*
    write(*,128)
128   format('Name of ASCII input file? ')
    read*, infile
```

```
      print*
      write(*,129)
  129 format('Name of ASCII output file? ')
      read*, outfile
      print*

c     ---------------------------------------------------------------

c          read in data from ASCII disk file...

      open(unit=1,file=infile,status='old',action='read')

      print *,'reading data file ',infile
      print*

      read (1,100) oldf0
  100 format(f4.2)
      read (1,101) wetwt
  101 format(f6.0)
      read (1,102) watwt
  102 format(f6.0)
      read (1,103) phi
  103 format(f5.3)
      read (1,104) toler
  104 format(f5.3)
      read (1,105) crack
  105 format(f6.0)
      read (1,106) slices
  106 format(i3)

      do (i=1,slices+1)
        read (1,107) x(i),ground(i),water(i),slip(i)
  107   format(4(f8.3))
      end do

      close(unit=1)

c     ---------------------------------------------------------------

c          calculate things that stay constant through iterations...

      degrad = 57.29577950
      phi = phi/degrad

c          soil weight, water weight, and slope for each slice;
c          passive earth pressure is assumed to calculate line
c          of action height, h(i), for each interface.

      do (i=1,slices)

        call trapzd(x(i),x(i+1),ground(i),ground(i+1),area1)
        call trapzd(x(i),x(i+1),water(i),water(i+1),area2)
        call trapzd(x(i),x(i+1),slip(i),slip(i+1),area3)

        dw(i) = (area1-area3)*wetwt
        du(i) = (area2-area3)*watwt
```

```
        h(i) = (ground(i)-slip(i))/3.

        beta(i)=atan((slip(i+1)-slip(i))/(x(i+1)-x(i)))

      end do

C     -------------------------------------------------------------------

C          iterate factor of safety to convergence for T = 0, E = 0

      differ = 1e06
      count = 0

      do while (differ .gt. toler)

        differ = 0.0e-09
        count = count + 1
        dsum = 0.
        rsum = 0.

C          calculate resisting and driving forces for each slice, and
C          then sum them over all of the slices...

        do (i=1,slices)
          n(i) = cos(beta(i))**2*(1+tan(beta(i))*tan(phi)/oldf0)
          resist(i) = (dw(i)-du(i))*tan(phi)/n(i)
          rsum = rsum + resist(i)
          drive(i) = dw(i)*tan(beta(i))
          dsum = dsum + drive(i)
        end do

        new = rsum/dsum
        differ = abs(new-oldf0)
        oldf0 = new

      repeat

      write(9,130) oldf0,count
130     format('F = ',f5.2,' after ',i2,' iterations',
     X  ' with no interslice forces')
      print*

C     -------------------------------------------------------------------

C          and now use F for T = 0 as a basis for
C          iterating F for T > 0 and E > 0

      oldfT = oldf0
      differ = 1e06
      count = 0

      do while (differ .gt. toler)

        differ = 0.0e-09
        count = count + 1
```

```
      dsum = 0.
      rsum = 0.

C        first, calculate interslice forces and derivatives--
C        see Janbu (1973, p. 69) for details...

      do (i=1,slices)
        de(i) = drive(i) - resist(i)/oldfT
        desum = desum + de(i)
      end do

      e(1) = 0.
      t(1) = 0.

      e(slices+1) = 0.
      t(slices+1) = 0.

      do (i=2,slices)
        tanalpha = (slip(i+1)-slip(i-1))/(x(i+1)-x(i-1))
        e(i) = e(i-1)+de(i-1)
        t(i) = -e(i)*tanalpha
        t(i) = t(i) + h(i)*(e(i+1)+e(i-1))/(x(i+1)-x(i-1))
      end do

      do (i=1,slices)
        dt(i) = t(i+1) - t(i)
        dtsum = dtsum + dt(i)
      end do

C        now, use these new dT values to calculate resisting and
C        driving forces for each slice, and sum them over all of
C        the slices...

      do (i=1,slices)
        n(i) = cos(beta(i))**2*(1+tan(beta(i))*tan(phi)/oldfT)
        resist(i) = (dw(i)+dt(i)-du(i))*tan(phi)/n(i)
        rsum = rsum + resist(i)
        drive(i) = (dw(i)+dt(i))*tan(beta(i))
        dsum = dsum + drive(i)
      end do

      new = rsum/dsum
      differ = abs(new-oldfT)
      oldfT = new

    repeat

    write(*,131) oldfT,count
131   format('F = ',f5.2,' after ',i2,' iterations',
     X  ' with interslice forces')
    print*
    print*

C   ------------------------------------------------------------------

C        write results to disk file...
```

```
C       this version saves a minimal amount of data,
C       but can be expanded to save interslice forces,
C       slice weights, and so forth...

      phi = phi*degrad
      relerr = 100.*abs((oldf0-oldfT)/oldfT)

      open(unit=2,file=outfile,status='new',action='write')

      write (2,110) infile
110   format ('input data file: ',a25)
      write (2,111) wetwt
111   format('soil unit wt.: ',f6.0)
      write(2,112) watwt
112   format('water unit wt.: ',f6.0)
      write(2,113) phi
113   format('residual phi: ',f5.2)
      write (2,116) toler
116   format('iteration tolerance: ',f5.3)
      write(2,117) oldf0
117   format('F = ',f6.3,' with no interslice forces')
      write(2,118) oldfT
118   format('F = ',f6.3,' with interslice forces')
        write(2,119) relerr
119   format('relative error: ',f5.2,'%')

      close(unit=2)

      print*
      print*,'data written to disk file ',outfile
      print*
      print*,'press RETURN to exit'
      pause

      end

C     ------------------------------------------------------------------

C       use values y1 and y2 to integrate between x1 and x2
C       with the trapezoid rule...

      subroutine trapzd(x1,x2,y1,y2,area)
        real*4 dx
        dx = abs(x2 - x1)
        area = dx*(y2 + y1/2.)
      return
      end

C     ------------------------------------------------------------------
```